On the Solution of the Pellet- and Reactor Model for the Steam Methane Reforming Process Using the Methods of Weighted Residuals

Stian Tangen

Preface

When choosing the subject for the Masters thesis, it was natural for me to choose reactor modeling. This is both due to an personal interest for the subject, but also since it is important subject for the industries.

I would also like to use this preface to give a thanks to my supervisor Hugo A. Jakobsen and my co-supervisor Jannike Solsvik for their support and guidance during this thesis.

I declare that this is an independent work according to the exam regulations of the Norwegian University of Science and Technology

_____   _____
Stian Tangen   Date

Abstract

The purpose of the thesis is to prove that the mole based formulation of a pellet model simulating the steam methane reforming reaction is identical to the novel mass based formulation. To prove this, the numerical methods of orthogonal collocation and least squares will be used. These numerical methods will also be examined to ensure that no numerical differences occur because of the numerical method used.

The different formulations were proven identical for the Maxwell-Stefan and the dusty gas diffusion models. This was not obtainable for the relatively simpler Wilke and Wilke-Bosanquet models. It was also proven that the numerical methods of orthogonal collocation and least squares yield identical results both for diffusion dominated and convective dominated problems. However, the orthogonal collocation method was superior in the terms of simulation speed for diffusion dominated problems, whereas the least squares method is superior for convective dominated problems.

A novel under-relaxation method was also developed during the thesis. By application of this method to the pellet models a reduction in simulation times by approximately 75% was seen.

Sammendrag

Hovedformålet med oppgaven er å bevise at pelletmodellene på de forskjellige formuleringene, mol- og massebasis, gir identiske resultater. For å bevise at formuleringene gir identiske resultater ble det brukt to forskjellige numeriske metoder, ortogonal kollokasjon og minste kvadraters metode. Disse numeriske metodene er også testet opp mot hverandre for å sikre at ingen numeriske forskjeller inntrer på grunn av valgt numerisk metode.

De forskjellige formuleringene ble bevist identiske for Maxwell-Stefan- og Dusty gas-diffusjon. Dette var ikke mulig å oppnå med de simplere diffusjonsmodellene Wilke og Wilke-Bosanquet. Det ble også bevist at de numeriske metodene oppnår identiske resultater for både diffusjonsdominerte og konveksjonsdominerte problemer. Det kom tydelig fram at ortogonal kollokasjon er betydelig raskere for diffusjonsdominerte problemer, mens minste kvadraters metode er langt raskere for konveksjonsdominerte problemer.

En hittil ukjent underrelaksasjonsmetode er også presentert i denne oppgaven. Ved bruk av underrelaksasjonsmetoden på pelletmodellene ble det sett en reduksjon i simuleringstid med ca. 75%.

Contents

List of Figures

List of Tables

Nomenclature

ΔH Heat of reaction $[kJ/mol]$

ϵ_p Particle porosity $[-]$

λ Conductivity $[W/mK]$

μ Dynamic viscosity $[kg/ms]$

∇ Divergence operator $[-]$

ω_i Mass fraction $[-]$

$\overline{M}$ Average molecular weight$[kg/kmol]$

∂ Partial derivative operator $[-]$

ρ Density $[kg/m^3]$

τ_p Tortuosity factor $[-]$

ξ Radial coordinate $[m]$

B Permeability $[m^2]$

c Concentration $[kmol/m^3]$

Cp Specific heat capacity $[J/kgK]$

Cp' Specific heat capacity $[J/kmoleK]$

D_p Pellet diameter $[m]$

D_{disp} Dispersion coefficient $[m^2/s]$

D_{ij} Binary diffusion coefficient for species i and j $[m^2/s]$

D_{iK} Knudsen diffusion coefficient for species i $[m^2/s]$

D_{pore} Pellet pore diameter $[m]$

h Heat transfer coefficient $[W/m^2K]$

J Mole based transport flux $[kmol/sm^2]$

j Mass based transport flux $[kg/sm^2]$

k_{cat} Conductivity of catalyst $[W/mK]$

k_i Mass transfer coefficient $[m/s]$

M_i Molecular weight for species i $[kg/kmol]$

p Pressure $[bar]$

Q External heat transfer $[J/m^3s]$

q Heat conductivity flux $[J/m^2s]$

R	Gas constant $[J/kmol K]$
R	Reaction mass source term $[kg/m^3 s]$
R	Reaction mole source term $[kmol/m^3 s]$
r	Reaction rate $[kmol/kgs]$
T	Temperature $[K]$
t	Time [s]
u	Mole averaged velocity $[m/s]$
v	Mass averaged velocity $[m/s]$
x_i	Mole fraction $[-]$

Subscripts

ξ	Radial direction
c	Corrective
cat	Catalyst
i, j	Indicate species type
p	Pellet

Superscripts

$*$	Dimensionless variable
b	Bulk
e	Effective
ref	Reference value

Abbreviations

LHS	Left hand side
RHS	Right hand side
OC	Orthogonal collocation
LSM	Least squares method
SMR	Steam methane reforming

1 Introduction

The purpose of this thesis is to prove that the governing equations on mole and mass basis yield identical results. This has been examined before by Solsvik and Jakobsen[2] for both the methanol and for the steam methane reforming(SMR) process in pellet models. They found a difference between the mass and mole based models. This was however most noticeable for the aggressive SMR reaction and the differences were assumed to have been caused by numerical problems.

Since the most noticeable difference was seen for the SMR process, this thesis will focus on that reaction. To prove that the governing equations on the different forms are identical, a set of model equations for the pellet will be derived, also the SMR process will be examined using four different diffusion models. Starting out with the most simple models only considering reaction and diffusion for both models and stepwise making the models more rigorous in order to indicate the potential error introduced by each assumption, this will be done until fully rigorous models are achieved.

Since the error was speculated to be of a numerical kind, two different numerical methods will be considered: the spectral methods of orthogonal collocation and least squares. This is done to see if any numerical differences can be seen for the different numerical methods. These numerical methods will also be further trialled with the intend to prove that the least squares method is more stable in simulating problems dominated by convective flow[3]. This is also done by using the SMR reaction. However here the reaction will take place in a pseudo homogeneous reactor where convective flow dominates rather than a diffusion dominated pellet model.

An extreme test will also be conducted for both of the numerical methods, solving the pure convective advection equation where no diffusion is present. Since diffusion is well know to stabilize numerical solvers and reduce occurring oscillations, the lack of this element is expected to yield problems for the solvers. However the least squares method is expected to yield better results than the orthogonal collocation method.

Both of the numerical methods will also be implemented as spectral element methods in order to examine the computational savings this introduces. For futher computational savings a novel under-relaxation method is also presented.

2 Theory

2.1 Steam methane reforming

In the models the steam methane reforming process is considered. Steam methane reforming is an important process for Norway in order to produce synthesis gas from natural gas. This reaction will be considered for both the pellet and the pseudo homogeneous reactor model.

The reaction is usually operated at high temperatures and pressure. In addition a nickel/alumina catalyst is needed in order to accelerate the reactions. With the use of a catalyst the reaction is quite rapid and the reaction is usually diffusion limited creating steep gradients in the pellet/reactor. The reaction kinetics considered in this thesis are the model presented by Xu and Froment[4].

$$CH_4 + H_2O \rightleftharpoons CO + 3H_2, \quad \Delta H_{298} = 206.2 \text{kJ/mol} \tag{1}$$

$$CH_4 + 2H_2O \rightleftharpoons CO_2 + 4H_2, \quad \Delta H_{298} = 164.7 \text{kJ/mol} \tag{2}$$

$$CO + H_2O \rightleftharpoons CO_2 + H_2, \quad \Delta H_{298} = -41.5 \text{kJ/mol} \tag{3}$$
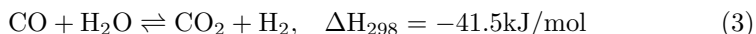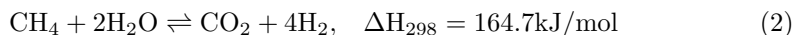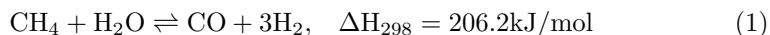
These are the most crucial reactions with the two reforming reactions being the two first and the water-gas shift reaction being the last. The process is in total endothermic and requires energy throughout production. Also the reaction produces moles giving that an increase in pressure or velocity is expected through the reactor. Less gradients are expected for velocity and pressure in the pellet model as the hydrogen easily diffuses out of the pellet preventing pressure increase.

2.1.1   Reactor/pellet operating conditions

Since the thesis will investigate the differences obtained by Solsvik and Jakobsen[2] when simulating the SMR reaction, the operating conditions presented in that article will be used here. These are shown in table 1. The operating conditions will be used for both the pellet and the reactor model.

Table 1: Reactor operating conditions used in the simulation of the SMR reaction

Description	Value	Description	Value
$D_p(m)$	0.0173	D_{pore}(nm)	40
$\epsilon_p(-)$	0.528	$\tau_p(-)$	3.5
p^b(bar)	29	T^b(K)	800
v^b(m/s)	1.89	ρ_{cat}(kg/m^3)	2300
k_{cat}(W/m K)	25	Cp_{cat}(J/kg K)	1000
$x^b_{CO}(-)$	6.3581E-005	k^b_{CO}(m/s)	0.065
$x^b_{CO_2}(-)$	0.0080931	$k^b_{CO_2}$(m/s)	0.055
$x^b_{H_2}(-)$	0.025567	$k^b_{H_2}$(m/s)	0.148
$x^b_{H_2O}(-)$	0.71335	$k^b_{H_2O}$(m/s)	0.16
$x^b_{CH_4}(-)$	0.21218	$k^b_{CH_4}$(m/s)	0.079
$x^b_{N_2}(-)$	0.040755	$k^b_{N_2}$(m/s)	0.067
$h(W/m^2K)$	1236	T_{wall}(K)	1100

2.2   Model equations

The model equations presented here will mainly be for the pellet model. The reactor model is presented in chapter 9.

The equations needed for a transient pellet model considering changing temperature, fluxes, species fraction, velocity, pressure and total concentration or density are presented. However they will only be presented in their original state and the derivation of the model equations used in the thesis are presented in appendix A. This is done in order to shorten the derivation of the model equations for each case, since the general equations will then only need to be simplified in order to account for the different assumptions in each case. The mass based derivation can be found in chapter A.1 and the mole based in chapter A.3 in the appendix. In the appendix also the different terms in the governing equations are explained. The model equations derived in the appendix are gathered in table 3 and 4 for convenience.

The equations presented in this chapter, are reduced to spherical coordinates in the appendix A, and total symmetry around the center of the particle is assumed. This effectively reduces the models to one dimension. To obtain the most accurate solution the model equations solved in the numerical system will also need to be approximately in the same order, to reduce the numerical loss in the process. This is obtained by transforming the equations to a dimensionless form with the use of the correlations given in table A.9, so that all components range between $|0 - 1|$.

2.2.1 Temperature and heat flux

To obtain an equation for temperature evolution through the pellet, the governing temperature equation(mass: eq.4, mole: eq.5) is considered. This equation gives the heat flux q which then can be used to obtain the temperature with the use of Fourier's law(6).

Temperature equations, mass and mole based respectively:

$$((1-\epsilon)\rho_p Cp_p + \epsilon\rho \sum_{i=1}^{n} \omega_i Cp_i)\frac{\partial T}{\partial t} + \rho \sum_{i=1}^{n} \omega_i Cp_i v \, \nabla \cdot T = -\nabla \cdot q + (-\triangle H_R)R + Q \tag{4}$$

$$((1-\epsilon)\rho_p Cp_p + \epsilon\rho \sum_{i=1}^{n} x_i Cp_i')\frac{\partial T}{\partial t} + c \sum_{i=1}^{n} x_i Cp_i' v \nabla \cdot T = -\nabla \cdot q + (-\Delta H_R)R + Q \tag{5}$$

Fourier's Law:

$$q = -\lambda\nabla \cdot T \tag{6}$$

Reaction term:

$$(-\Delta H_R)R = (1-\epsilon_{cat})\rho_{cat} \sum(-\Delta H_{ri})r_i \tag{7}$$

2.2.2 Species fractions and species transport fluxes

The change in species transport flux is obtained from the governing species balance(mass: eq.8, mole: eq.9). The species balance will only be solved for N-1 components and the last component will be obtained by using the corresponding constitutive law(mass: eq.13, mole: eq.15). In the equations the species fractions used in combination with the total concentration/density instead of component specific concentration or density which is normally seen.

Species balance equations, mass and mole based:

$$\frac{\partial}{\partial t}(\rho\omega_i) + \nabla \cdot (\rho\omega_i v) = -\nabla \cdot (j_i) + R_i \tag{8}$$

$$\frac{\partial}{\partial t}(cx_i) + \nabla \cdot (cx_i u) = -\nabla \cdot (J_i) + R_i' \tag{9}$$

Reaction term:

$$R_i = (1-\epsilon_{cat})\rho_{cat} r_i \tag{10}$$

$$R_i' = (1-\epsilon_{cat})M_i\rho_{cat} r_i \tag{11}$$

$$\tag{12}$$

Constitutive laws, mass and mole based:

$$\sum_{i=1}^{n} j_i = 0 \qquad (13)$$

$$\sum_{i=1}^{n} \omega_i = 1 \qquad (14)$$

$$\sum_{i=1}^{n} J_i = 0 \qquad (15)$$

$$\sum_{i=1}^{n} x_i = 1 \qquad (16)$$

Since the transport fluxes have been obtained with the use of the species balance equation, a multi component diffusion model can then be applied to obtain the species fractions. The diffusion models considered in this thesis will be the Wilke model[5] and the more rigorous Maxwell-Stefan model[6, 7], which are considering bulk diffusion. We will also consider some more advanced models considering both bulk and Knudsen diffusion, the Wilke model combined with the Bosanquet formula[8] and the rigorous dusty gas model[9, 10].

All the diffusion models can be found in the table 2 for both the mass and mole based equations. As for the species balance, the diffusion models will only be used to solve N-1 components, the last is solved with the constitutive law 14 for the mass based and 16 for the mole based model.

The binary diffusivities needed in the diffusion models are obtained with the equation[11]:

$$D_{ij} = \frac{0.00266 T^{3/2}}{p M_{ij}^{1/2} \sigma_{ij}^2 \Omega_D} \qquad (17)$$

The Knudsen diffusivites are obtained with the equation[12]:

$$\frac{1}{D_{iK}} = \frac{1}{D_{ij}} + \frac{1}{D_k} \qquad (18)$$

where D_{iK} is the diffusion coefficient in a single cylindrical pore, D_{ij} is the bulk diffusion coefficient and D_k is the Knudsen diffusion coefficient given by:

$$D_k \approx 48.5 d_p \frac{T}{M}^{0.5} \qquad (19)$$

To fully recreate the pellet model used by Solsvik and Jakobsen[2], the same parallel pore model[13] will be used in this thesis to describe the pore size distribution within the pellet.

$$D_{ij}^e = \frac{\epsilon}{\tau} D_{ij} \qquad (20)$$

$$D_{iK}^e = \frac{\epsilon}{\tau} D_{iK} \qquad (21)$$

Table 2: Diffusion models

Mass based diffusion models:

Wilke diffusion model:

$$j_i = -\rho D_{im} \nabla \omega_i \qquad D_{im} = \frac{1 - \omega_i}{\overline{M} \sum_{\substack{j=1 \\ j \neq i}}^{n} \frac{\omega_j}{M_j D_{ij}}} \tag{22}$$

Wilke–Bosanquet diffusion model:

$$j_i = -\rho D_{i,eff} \nabla \omega_i \qquad \frac{1}{D_{i,eff}} = \frac{1}{D_{im}} + \frac{1}{D_{iK}} \tag{23}$$

Maxwell-Stefan diffusion model:

$$j_i = \frac{-\rho \omega_i \nabla ln(\overline{M}) - \rho \nabla \omega_i + \overline{M} \omega_i \sum_{\substack{j=1 \\ j \neq i}}^{n} \frac{j_j}{M_j D_{ij}}}{\overline{M} \sum_{\substack{j=1 \\ j \neq i}}^{i} \frac{\omega_j}{M_j D_{ij}}} \tag{24}$$

Dusty gas diffusion model:

$$j_i = \frac{M^2 \sum_{\substack{j=1 \\ j \neq i}}^{n} \frac{\omega_i j_j}{M_j \tilde{D}_{ij}} - \frac{v \rho_i M}{\tilde{D}_{iK}} - \rho(\omega_i \nabla M + M \nabla \omega_i)}{M^2 \sum_{\substack{j=1 \\ j \neq i}}^{n} \frac{\omega_j}{M_j \tilde{D}_D ij} + \frac{M}{D_{iK}}} \tag{25}$$

Mole based diffusion models:

Wilke diffusion model:

$$J_i = -c D'_{im} \nabla \cdot x_i \qquad D'_{im} = \frac{1 - x_i}{\sum_{\substack{j=1 \\ j \neq i}}^{n} \frac{x_j}{D_{ij}}} \tag{26}$$

Wilke–Bosanquet diffusion model:

$$J_i = -c D'_{i,eff} \nabla \cdot x_i i \qquad \frac{1}{D'_{i,eff}} = \frac{1}{D'_{im}} + \frac{1}{D_{iK}} \tag{27}$$

Maxwell-Stefan diffusion model:

$$J_i = \frac{-c x_i + \sum_{\substack{j=1 \\ j \neq i}}^{n} \frac{j_j x_i}{D_{ij}}}{\sum_{\substack{j=1 \\ j \neq i}}^{i} \frac{x_j}{D_{ij}}} \tag{28}$$

Dusty gas diffusion model:

$$J_i = \frac{\sum_{\substack{j=1 \\ j \neq i}}^{n} \frac{j_j x_i}{D_{ij}} - \frac{c_i u}{D_{iK}} - c \nabla x_i}{\sum_{\substack{j=1 \\ j \neq i}}^{i} \frac{x_j}{D_{ij}} + \frac{1}{D_{iK}}} \tag{29}$$

2.2.3 Velocity

The mass and mole averaged velocity is mainly obtained from the governing continuity equations(mass: eq. 30 , mole: eq. 31), but a comparison is also made with the velocities obtained from the flux conversion equations 32 and 33[14]. The equation 33 is also important for the mole based model where the mass averaged velocity is needed.

Continuity equations, mass and mole based:

$$\frac{\partial \rho}{\partial t} + \nabla \cdot (\rho v) = 0 \tag{30}$$

$$\frac{\partial c}{\partial t} + \nabla \cdot (cu) = \sum_{i=1}^{n} R_i' \tag{31}$$

Alternate velocity equations:

$$u - v = \sum_{i=1}^{N} \frac{j_i \overline{M}}{\rho M_i} \tag{32}$$

$$v - u = \sum_{i=1}^{N} \frac{J_i M_i}{c_i \overline{M}} \tag{33}$$

2.2.4 Pressure

By obtaining the mass averaged velocity it is possible to produce the pressure change through the system by the use of Darcy's law[15] equation 34.

$$v = -\frac{B}{\mu}\frac{\partial p}{\partial \xi} \qquad B = \frac{\epsilon}{\tau}\frac{d_0^2}{32} \tag{34}$$

2.2.5 Total concentration or density

Total concentration or density is obtained from the ideal gas law or modified ideal gas law, eq A.36 and A.37 respectively. The modified version is multiplied with average mole weight to obtain the total density. The concentration equations is used for the mole based model and the density equation for the mass based.

$$\frac{p}{RT} = c \tag{35}$$

$$\frac{p\overline{M}}{RT} = \rho \tag{36}$$

2.3 Summaries of the basis equations, mole and mass based

The basis equations derived in the theory appendix A, which are used as a basis for all the pellet models are presented in table 3 and 4.

Table 3: Mass based model equations on dimensionless form

Species mass balance:

$$\frac{\partial}{\partial t^*}(\rho^*\omega_i) + \frac{1}{\xi^{*2}}\frac{\partial}{\partial \xi^*}(\xi^{*2}\rho^*\omega_i v_\xi^*) = -\frac{1}{\xi^{*2}}\frac{\partial}{\partial \xi^*}(\xi^{*2}j_i^*) + R_i\frac{\xi_{ref}^2}{D_{ref}\rho_{ref}} \tag{37}$$

The basic dimensionless temperature equation:

$$((1-\epsilon)\rho_p Cp_p + \epsilon\rho^*\rho_{ref}\sum_{i=1}^{n}\omega_i Cp_i)\frac{\partial T^*}{\partial t^*} =$$

$$-\rho^*\rho_{ref}v_r^*\sum_{i=1}^{n}\omega_i Cp_i\frac{\partial T^*}{\partial \xi^*} - \frac{(\frac{2q^*}{\xi^*}+\frac{\partial q^*}{\partial \xi^*})\lambda}{D_{ref}} + \frac{\xi_{ref}^2(-\triangle H_R)R}{D_{ref}T_{ref}} \tag{38}$$

The basic dimensionless continuity equation:

$$\frac{\partial \rho^*}{\partial t^*} + \frac{1}{\xi^{*2}}\frac{\partial}{\partial \xi^*}(\xi^{*2}\rho^* v^*) = 0 \tag{39}$$

Wilke diffusion model:

$$j_i^* = -\rho^*\frac{D_{im}}{D_{ref}}\frac{\partial \omega_i}{\partial \xi^*} \qquad D_{im} = \frac{1-\omega_i}{\overline{M}\sum_{\substack{j=1\\j\neq i}}^{n}\frac{\omega_j}{M_j D_{ij}}} \tag{40}$$

Wilke–Bosanquet diffusion model:

$$j_i^* = -\rho^*\frac{D_{i,eff}}{D_{ref}}\frac{\partial \omega_i}{\partial \xi^*} \qquad \frac{1}{D_{i,eff}} = \frac{1}{D_{im}} + \frac{1}{D_{iK}} \tag{41}$$

Maxwell-Stefan diffusion model:

$$j_i^* = \frac{\frac{-\rho^*\omega_i}{D_{ref}}\frac{1}{\overline{M}}\frac{\partial \overline{M}}{\partial \xi^*} - \frac{\rho^*}{D_{ref}}\frac{\partial \omega_i}{\partial \xi^*} + \overline{M}\omega_i\sum_{\substack{j=1\\j\neq i}}^{n}\frac{j_j^*}{M_j D_{ij}}}{\overline{M}\sum_{\substack{j=1\\j\neq i}}^{i}\frac{\omega_j}{M_j D_{ij}}} \tag{42}$$

Dusty gas diffusion model:

$$j_i^* = \frac{\overline{M}^2\sum_{\substack{j=1\\j\neq i}}^{n}\frac{\omega_i j_j^*}{M_j \tilde{D}_{ij}} - \frac{v^*\omega_i\overline{M}}{\tilde{D}_{iK}} - \frac{\omega_i\rho^*}{D_{ref}}\frac{\partial \overline{M}}{\partial \xi^*} - \frac{\rho^*\overline{M}}{D_{ref}}\frac{\partial \omega_i}{\partial \xi^*}}{\overline{M}^2\sum_{\substack{j=1\\j\neq i}}^{n}\frac{\omega_j}{M_j \tilde{D}_{D}ij} + \frac{\overline{M}}{D_{iK}}} \tag{43}$$

Table 4: Mole based model equations on dimensionless form

Species mole balance:

$$\frac{\partial}{\partial t^*}(c^* x_i) + \frac{1}{\xi^{*2}} \frac{\partial}{\partial \xi^*}(\xi^{*2} c^* x_i u_\xi^*) = -\frac{1}{\xi^{*2}} \frac{\partial}{\partial \xi^*}(\xi^{*2} J_i^*) + R_i' \frac{\xi_{ref}^2}{D_{ref} c_{ref}} \tag{44}$$

The basic dimensionless temperature equation:

$$((1-\epsilon)\rho_p Cp_p + \epsilon c^* c_{ref} \sum_{i=1}^n x_i Cp_i') \frac{\partial T^*}{\partial t^*} =$$
$$-c^* c_{ref} v_r^* \sum_{i=1}^n x_i Cp_i' \frac{\partial T^*}{\partial \xi^*} - \frac{(\frac{2q^*}{\xi^*} + \frac{\partial q^*}{\partial \xi^*})\lambda}{D_{ref}} + \frac{\xi_{ref}^2 (-\triangle H_R) R}{D_{ref} T_{ref}} \tag{45}$$

The basic dimensionless continuity equation:

$$\frac{\partial c^*}{\partial t^*} + \frac{1}{\xi^{*2}} \frac{\partial}{\partial \xi^*}(\xi^{*2} c^* u_\xi^*) = (\frac{\xi_{ref}^2}{c_{ref} D_{ref}}) \sum_{i=1}^n R_i' \tag{46}$$

Wilke diffusion model:

$$J_i^* = -c^* \frac{D_{im}'}{D_{ref}} \frac{\partial x_i}{\partial \xi^*} \qquad D_{im}' = \frac{1 - x_i}{\sum_{\substack{j=1 \\ j \neq i}}^n \frac{x_j}{D_{ij}}} \tag{47}$$

Wilke–Bosanquet diffusion model:

$$J_i^* = -c^* \frac{D_{i,eff}'}{D_{ref}} \frac{\partial x_i}{\partial \xi^*} \qquad \frac{1}{D_{i,eff}'} = \frac{1}{D_{im}'} + \frac{1}{D_{iK}} \tag{48}$$

Maxwell-Stefan diffusion model:

$$J_i^* = \frac{-\frac{c^*}{D_{ref}} \frac{\partial x_i}{\partial \xi^*} + \sum_{\substack{j=1 \\ j \neq i}}^n \frac{J_j^* x_i}{D_{ij}}}{\sum_{\substack{j=1 \\ j \neq i}}^i \frac{x_j}{D_{ij}}} \tag{49}$$

Dusty gas diffusion model:

$$J_i^* = \frac{-\frac{c^*}{D_{ref}} \frac{\partial x_i}{\partial \xi^*} + \sum_{\substack{j=1 \\ j \neq i}}^n \frac{J_j^* x_i}{D_{ij}} - \frac{c^* x_i u^*}{D_{iK}}}{\sum_{\substack{j=1 \\ j \neq i}}^i \frac{x_j}{D_{ij}} + \frac{1}{D_{iK}}} \tag{50}$$

2.4 Numerical methods - Methods of weighted residuals[1]

In order to solve the system of equations a numerical solver has to be used. The basics of any numerical method is to transform the set of governing equations into a system of algebraic equations that can be solved using a computer. This can be achieved by multiple methods such as the finite difference method or the finite volume method. In this thesis a spectral method of weighted residuals is applied.

To solve the governing equations, two different subclasses in the methods of weighted residuals will be used: the orthogonal collocation method and the least squares method. The least squares method is expected to be the better method for the convective problems and the collocation method to perform best for the diffusive problems. Before the different subclasses are reviewed, the basics behind a spectral weighted residuals method is presented.

In the spectral weighted residuals method a numerical solution is obtained by finding an approximating function f belonging to a functional space X such that:

$$A(f, v) = F(v), \quad \forall v \in Z \tag{51}$$

where the space of functions Z may or may not be equivalent to X. The algebraic set of equations is then found when the search space is reduced from $X \subset X_N$ and considering trail function f_N that can be expanded as linear combinations of nodal-basis functions such that:

$$f \cong \overline{f_N} = \sum_j \alpha_j \psi_j \tag{52}$$

Then the equation 51 can be expanded to, when also reducing the test space Z to Z_N:

$$\sum_j A(\psi_j, \psi_k) = F(\psi_k) \quad , \quad \forall \psi_k \in Z_N \tag{53}$$

Rewriting the problem to matrix form:

$$A\overline{f} \cong F \tag{54}$$

where $[A]_{kj} = A(\psi_j, \psi_k)$, $[\overline{f}]_j = \alpha_j$ and $[F]_k = F(\psi_k)$.
However, this method will produce a residual unless $\overline{f} = f$, with the residual being:

$$A\overline{f} - F = R \tag{55}$$

A method of weighted residuals will then be applied in order to force the residuals to zero in some average sense over the domain:

$$\int_X R(X) W_i dx = 0 \qquad i = 1, 2, ..., n \tag{56}$$

Here the number of weight functions W_i is exactly the same as the number of unknown constants α_j in $\overline{f}$. This results in a set of n algebraic equations for the unknown constants α_i. The weight functions will then be specified either by the use of orthogonal collocation or least squares in this thesis.

2.4.1 Orthogonal collocation[3]

The orthogonal collocation method uses the weighting functions as the Dirac δ functions in the domain.

$$W_i(x) = \delta(x - x_i) \tag{57}$$

The Dirac δ function has the property that

$$\delta(x - x_i) = 1 \text{ if } x = x_i, = 0 \text{ otherwise} \tag{58}$$

Inserting and integrating up with the weighted residual statement 56, results in forcing the residual to zero at the specific points in the domain.

$$R(x_i) = 0 \tag{59}$$

2.4.2 Least squares method[3]

The least squares method minimizes the continuously summed up squared residuals.

$$S = \int_X R(x)R(x)dx = \int_X R^2(x)dx \tag{60}$$

The minimum of this scalar function implies that the derivatives of S with respect to all the unknown parameters also must be zero.

$$\frac{\partial S}{\partial \alpha_j} = 0 \tag{61}$$

$$2\int_X R(x)\frac{\partial R}{\partial \alpha_j}dx = 0 \tag{62}$$

Comparing the equation 62 to the method of weighted residuals statement 56, it can be seen that the weight functions for the least squares method are the derivatives of the residual with respect to the unknown constants.

$$W_i = 2\frac{\partial R}{\partial \alpha_j} \tag{63}$$

However the "2" can be dropped as it cancels out in the equation.

2.4.3   Under-relaxation and convergence criteria[1]

Since the numerical methods presented here are linear systems solvers we need to linearize the problem. In this thesis the method of Picard iteration is used. With the linearizion of the equations, some instability problems occur when considering the new solution that will used for the next iteration. To prevent this, some under-relaxation is needed in order to stabilize this process. The purpose of the under-relaxation is to only introduce a fraction of the new solution for each iteration to maintain a stable iterative process. The under-relaxation of the variables are defined as:

$$\overline{f} = \alpha \overline{f}^{it-1} + (1-\alpha)\overline{f}^{it} \tag{64}$$

Since the SMR pellet model is very diffusion limitied, steep gradients will occur in the pellet and a heavy under-relaxation is needed for a stable iterative process. However, with high under-relaxation more iterations are needed for a satisfying solution, resulting in computer costly models. An addition to the basic under-relaxation method was developed during the thesis, however the method is not fully investigated. The developed method and results are presented in appendix I.

Furthermore a convergence criteria for the iterative process has to be specified. In this thesis the residual is specified to be lower than 10^{-10} according to equation:

$$Residual = \sqrt{\int_{\Omega} R^2 d\Omega} = \sqrt{\int_{\Omega} (A\overline{f} - F)^2 d\Omega} \leq 10^{-10} \tag{65}$$

2.4.4 Spectral element methods[1]

To save computer cycles, the possibility of splitting up the domain in order to use more calculation points where there are steep gradients and fewer points where the profile is flat. The method for this is known as the spectral element methods. The method is fairly straight forward where the domain is separated and an individual amount of collocation points can be chosen for each element.

Looking at the problem matrix A for a one variable problem it can be seen how the method is implemented without elements:

$$
A = \begin{bmatrix}
A_{00} & A_{01} & \cdot & A_{0N} \\
A_{10} & A_{11} & \cdot & A_{0N} \\
\cdot & \cdot & \cdot & \cdot \\
A_{N0} & A_{N1} & \cdot & A_{NN}
\end{bmatrix}
\tag{66}
$$

Dividing this matrix into three elements will yield a matrix containing three sub matrices. The element matrices are joint together in such a way that the overlaps are only calculated once as seen in equation 68.

$$
A = \begin{bmatrix}
[A^{e1}] & 0 & 0 \\
0 & [A^{e2}] & 0 \\
0 & 0 & [A^{e3}]
\end{bmatrix}
\tag{67}
$$

By expanding the element matrices, it is apparent how the matrices are joint together. This is shown for whole system $Af = F$ using three elements with two points in each element.

$$
\begin{bmatrix}
A_{00}^1 & A_{01}^1 & 0 & 0 \\
A_{10}^1 & A_{11}^1 + A_{00}^2 & A_{10}^2 & 0 \\
0 & A_{10}^2 & A_{11}^2 + A_{00}^3 & A_{01}^3 \\
0 & 0 & A_{10}^3 & A_{11}^3
\end{bmatrix}
\begin{bmatrix}
x_1 \\
x_2 \\
x_3 \\
x_4
\end{bmatrix}
=
\begin{bmatrix}
F_1^1 \\
F_2^1 + F_1^2 \\
F_2^2 + F_1^3 \\
F_2^3
\end{bmatrix}
\tag{68}
$$

Using this method will give the opportunity to save computational power and increase the speed of the simulation. The possible speed increase will be looked into in the chapter where the numerical methods are compared in chapter 7.

2.5 Tetha method[1]

For the two dimensional problems where the transient terms are included, it is either needed to extend the already explained numerical methods to two dimensions or to discretise the transient terms using a finite difference method. In this thesis the latter method will be used as it is the simplest to implement and does not deviate much from the one-dimensional steady state implementation.

The finite difference θ method will be used to discretise the transient terms:

$$\frac{f^{t+1} - f^t}{\Delta t} + \theta[\mathcal{L}(f^{t+1}) - g^{t+1}] = -(1-\theta)[\mathcal{L}(f^t) - g^t] \tag{69}$$

here f represents the discretisized variable, $\mathcal{L}$ represents the term in the problem matrix(A) and g the term in source vector(F). the superscripts (t+1) and (t) represents the current and previous time-step respectively.

The value of θ indicates which method that is used.
1. Explicit forward Euler method $\theta = 0$
2. Implicit forward Euler method $\theta = 1$
3. Crank-Nicholson for $\theta = 0.5$

In the thesis only the second order Crank-Nicholson method will be considered as it gives the most accurate results. The equation is rearranged to show the implemented form:

$$f^{t+1} + \Delta t \theta \mathcal{L} f^{t+1} = \Delta t \theta g^{t+1} + \Delta t (1-\theta)(g^t - \mathcal{L} f^t) + f^t \tag{70}$$

3 Models on their simplest forms

Starting out with the most simplified model for simulating a pellet with the steam methane reforming reaction, gives the possibility to identify if the models on this level yield idientical results or deviates from each other.

With the models on their simplest form, steady state and no convective transport are assumed in the pellet. Basic boundary conditions are also used. The use of basic boundary conditions elimitates the effect of transfer resistances from the bulk to the pellet surface. A model on both mass and mole basis is to be derived. The method of implementation will also be shown in order to indicate how the problem is solved using orthogonal collocation.

3.1 Derivation of the model equations, mass and mole based

The temperature equation (A.56) for mass and (A.63) for the mole based model is solved in combination with Fouriers law. The temperature equation is only modified by introducing the assumptions for this case. Here, the heat flux is obtained from the temperature equation and the temperature is obtained from Fourier's law.

The species balance for respectively the mass and mole model (A.55) and (A.62), is used to calulate the fluxes. This is done by solving the species balance for N-1 components and the last component by the constitutive laws (A.39) and (A.41). In the species balance the continuity equation (A.57) and (A.64) is identified for the respective model and inserted giving the species balance used in the model.

The species fractions are solved by using one of the four different diffusion models in table B.2 for the mass based and B.6 for the mole based for N-1 components, the last component is solved by the appropriate constitutive law (A.40) and (A.42). These diffusion models are only reformulated from their general form presented in the theory to reflect their implemented form.

The equations used in these models are derived in detail in appendix B, with the mass based starting in chapter B.1 and the mole based in B.3. The solution strategy is shown in table B.1 and B.5 for the mass and the mole based model respectively. The visualization of the implementation is shown in figure B.1 and B.2.

A summary of the equations derived in detail in the appendix are shown in table 5 for the mass based and table 6 for the mole based model along with the boundary conditions and the constitutive laws used in the models. The reactor operating conditions are given in the theory, table 1.

Table 5: Mass based equations, constitutive laws and boundary conditions

Equations:	Constitutive Laws:
Temperature equation: $$\frac{2q^*}{\xi^*} + \frac{\partial q^*}{\partial \xi^*} = \frac{\xi^2_{ref}(-\triangle H_R)R}{T_{ref}\lambda} \qquad (71)$$	Fourier's law $$q^* + \frac{\partial T^*}{\partial \xi^*} = 0 \qquad (72)$$
Mass balance: $$\frac{2j_i^*}{\xi^*} + \frac{\partial j_i^*}{\partial \xi^*} = R_i \frac{\xi^2_{ref}}{D_{ref}\rho_{ref}} \qquad (73)$$	Definition: $$\sum_{i=1}^{n} j_i^* = 0 \qquad (74)$$
Diffusion model: One of the four diffusionmodels in table B.2 is used	Definition: $$\sum_{i=1}^{n} \omega_i = 1 \qquad (75)$$
Ideal gas law modified for density: $$\frac{p\overline{M}}{RT} = \rho \qquad (76)$$	
Boundary conditions in the symmetry point $\xi^* = 0$ $$j_i = 0 \qquad (77)$$ $$q = 0 \qquad (78)$$	Boundary conditions at the surface $\xi^* = \xi_p^*$ $$T = T^b \qquad (79)$$ $$\omega_i = \omega_i^b \qquad (80)$$

Table 6: Mole based equations, constitutive laws and boundary conditions

Equations:		Constitutive Laws:	
Temperature equation:		Fourier's law	
$$\frac{2q^*}{\xi^*} + \frac{\partial q^*}{\partial \xi^*} = \frac{\xi_{ref}^2(-\triangle H_R)R}{T_{ref}\lambda}$$	(81)	$$q^* + \frac{\partial T^*}{\partial \xi^*} = 0$$	(82)
Species mole balance:		Definition:	
$$\frac{2J_i^*}{\xi^{*2}} + \frac{\partial J_i^*}{\partial \xi^*} = (R_i' - x_i \sum_{i=1}^{n} R_i')\frac{\xi_{ref}^2}{D_{ref}c_{ref}}$$	(83)	$$\sum_{i=1}^{n} J_i^* = 0$$	(84)
Diffusion model:		Definition:	
One of the four diffusionmodels in table B.6 is used		$$\sum_{i=1}^{n} x_i = 1$$	(85)
Ideal gas law rearranged for concentration:			
$$\frac{p}{RT} = c$$	(86)		

Boundary conditions in the symmetry point $\xi^* = 0$		Boundary conditions at the surface $\xi^* = \xi_p^*$	
$J_i = 0$	(87)	$T = T^b$	(89)
$q = 0$	(88)	$x_i = x_i^b$	(90)

3.2 Results and discussion - The simple models

3.2.1 General for all simple models

As stated these are the models on their simplest forms with the assumption of steady state, no convective flow and simple boundary conditions. In the pellet the steam methane reforming reaction is simulated. The models are driven to a residual below 10^{-10} and are simulated using 60 collocation points.

The mole fractions of the reactants H_2O and CH_4 are expected to decrease from the surface to the center of the particle, and increase for the products CO_2, CO and H_2. The mole fraction of the inert gas N_2 is expected to increase slightly, on the contrary to what might be expected since the reaction generates mole. This happens because hydrogen easily diffusies out of the pellet, resulting in an effective mole consuming process for the heavier components in the pellet.

The simulation of the SMR reaction requires heavy under-relaxation of the diffusion model in order to converge. The Wilke-Bosanquet and the dusty gas diffusion model tend to be the most sensitive whereas the basic Wilke and Maxwell-Stefan models are the most robust. These simulations are underrelaxed by a factor of 1-2 in the order of 10^{-4} depending on the diffusion model.

3.2.2 Wilke and Wilke-Bosanquet models

Starting out with the Wilke and Wilke-bosanquet diffusion models on their simplest forms, one can immediately see from the result plots in figure 1 and 2 respectively, that the mole and mass based model does not yield the same results. The differences here are due to the inconsistensy in the Wilke model. Adding the effect of Knudsen diffusion in the Wilke-Bosanquet model does not have any effect on this problem.

The inconsistency can best be explained by looking at the mole fraction plot for nitrogen and comparing it with the Wilke equation on the different forms. The Wilke equation on mass basis is only dependent on the component which it is solving for. This means that nitrogen, since it does not react, will have a flat mass fraction profile. The increase seen in mole fraction is only due to the increase in molar weight. One would then expect a flat mole fraction profile for nitrogen when using the mole based Wilke model. However, in the mole based species balance it is accounted for mole generation by including the LHS of the continuity equation. This inclusion gives a rather significant change in the composition, however not in the expected direction.

The differences in the the temperature equations are due to the different reaction rates because of the inconsistent Wilke models. The same difference would also have been seen for the density or concentration and the average molecular weight since they are directly dependent on the primary variables, temperature and mole fractions. Result plots for these variables are by that reason not shown.

Additional result plots are given in appendix B, figure B.3 for Wilke and B.4 for Wilke-Bosanquet. Here the diffusive fluxes are compared since the convective

flow is not considered. The differences seen in the flux plots is the effect of not considering convective flow. Not considering convective flow is mainly causing the mole based model to deviate as the convective flow is negligible on mass basis. The effect of dis-considering convective flow on the mole based models will be further discussed in the more rigorous models.

3.2.3 Wilke
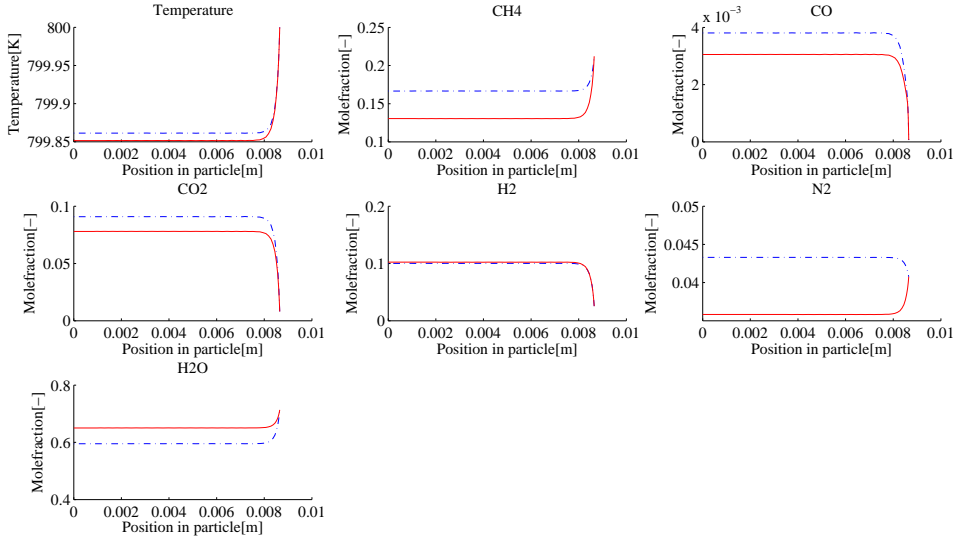
Figure 1: Mass(-.-.-) and mole(—) based simulations using the Wilke diffusion model. The mass based results are converted to mole fractions.

3.2.4 Wilke-Bosanquet
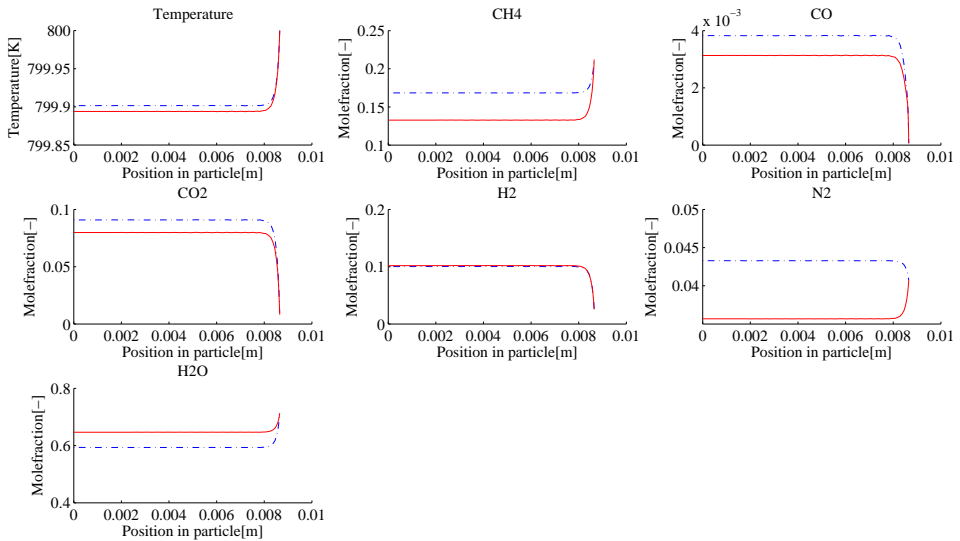
Figure 2: Mass(-.-.-) and mole(—) based simulations using the Wilke-Bosanquet diffusion model. The mass based results are converted to mole fractions.

3.2.5 Maxwell-Stefan and Dusty gas models

Looking at the results for the Maxwell-Stefan model in figure 3 and the dusty gas model in figure 4 one can immidately see that these models give much more comparable results between mass and mole based models compared to the Wilke diffusion models. One would also expect this since the Maxwell-Stefan and dusty gas models are more rigorous diffusion models which consider the other components as well. This is easily spotted comparing the diffusion equations in table B.2 for mass and table B.6 for the mole based models.

For the Maxwell-Stefan models only a small deviation between the mass and mole based models can be seen. The small deviation here is due to not considering convective flows. This will only affect the mole based model since the mass based model has negligible convective flow.

The results for the simplest form considering dusty gas diffusion is a bit different. The differences can be seen for the mole fractions in figure 4. This is a rigorous diffusion model along with the Maxwell-Stefan model, but with the addition of Knudsen diffusivites. The Knudsen diffusivities added in the dusty gas model introduces a convective term in the diffusion model, which is not considered in this simple case. This introduces a difference between the mass and the mole based models as the convective flows cannot be compared for the different models. When the models are compared in the chapter with convective flow one can see that the convective terms on mass basis are negligible but have a significant value on mole basis. This proves the differences seen on this level.

The temperature equation for both models are more similar than for the Wilke models due to the more similar reaction rates. The flux comparisons on mole and mass basis for all diffusion models in figure B.3,B.4,B.5 and B.6 all show great similarity between the diffusion models because of the very rapid reaction. The reaction is so rapid that the diffusion equations will yield almost no effect back to the species balances equations which is used to calculate the fluxes. Since the diffusion models have so small effect on the flux calculation, the difference here is mainly due to not considering convective flows.

3.2.6 Maxwell-Stefan
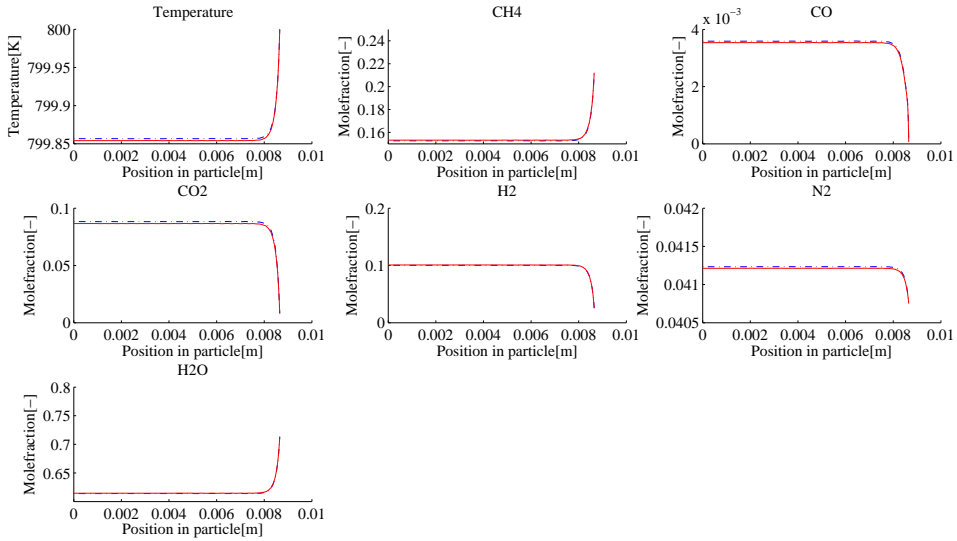
Figure 3: Mass(-.-.-) and mole(—) based simulations using the Maxwell-Stefan diffusion model. The mass based results are converted to mole fractions.

3.2.7 Dusty gas
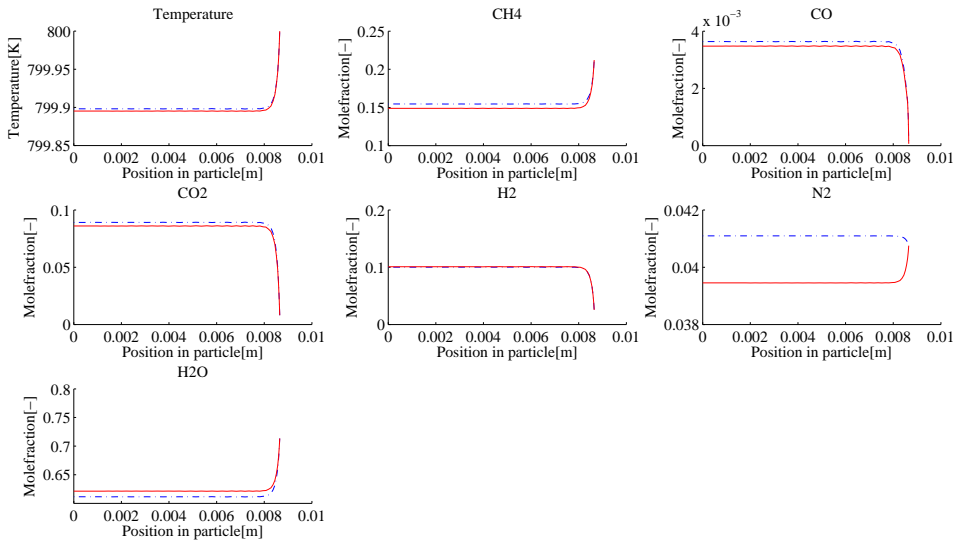
Figure 4: Mass(-.-.-) and mole(—) based simulations using the dusty gas diffusion model. The mass based results are converted to mole fractions.

4 Alternative methods for solving the simple models

In this chapter, it is looked into two alternative cases for solving the methods on their respective simplest forms. Firstly the effect of not assuming constant reference values when transforming the equations to a dimensionless form is investigated. This has been done for both the mole and the mass based model, but since they yielded the same conclusion only the mass based model will be presented.

Secondly, the use of the continuity equation(mass: eq. A.57 mole eq. A.64) in the species balance is investigated for the simplest models. For the simple models not considering convective flow the inclusion of the continuity equation in the species balance only has an effect on the mole based model. This is because the continuity equation on mass basis equals to zero and does not contribute with any new terms when dis-considering convective flow. However, the mole based continuity equation will have one remaining term which is not equal to zero. The effect of not including this term will be looked into.

For the more rigorous models on both mole and mass basis including convective flow, the use of the continuity equation to simplify the species balance is expected to not have any effect on the simulations.

4.1 Using non-constant values for making the fluxes dimensionless

It is speculated that some numerical errors may occur when using different methods of transforming the model equations to a dimensionless form. In order to investigate this, a new approach to how the diffusive fluxes are transformed to a dimensionless form will be trialled. The focus will be on the mass based model using the Maxwell-Stefan diffusion model, since this will yield the most differences compared to the method used previously in the thesis.

The derivation of the mass based model will only differ from the model presented in chapter 3.1 by not assuming constant reference values when making the fluxes dimensionless, i.e. variable density and diffusive term will now be used instead of the reference values. The model is solved in a completely similar manner and the walk-through of the equations can be found there. The model equations are derived in detail in appendix C with the addition of a solution strategy and a visualization of the collocation matrix. A summary of the derived equations is presented in table 7 along with the boundary conditions.

Table 7: Mass based equations, constitutive laws and boundary conditions

Equations:	Constitutive Laws:
Temperature equation:	Fourier's law
$$\frac{2q^*}{\xi^*} + \frac{\partial q^*}{\partial \xi^*} = \frac{\xi_{ref}^2(-\triangle H_R)R}{T_{ref}\lambda} \qquad (91)$$	$$q^* + \frac{\partial T^*}{\partial \xi^*} = 0 \qquad (92)$$
Mass balance:	Definition:
$$\frac{2j_i^*}{\xi^*} + \frac{\partial j_i^*}{\partial \xi^*} + \frac{j_i^*}{D_s}\frac{\partial D_s}{\partial \xi^*} + \frac{j_i^*}{c^*}\frac{\partial c^*}{\partial \xi^*} + \frac{j_i^*}{\overline{M}}\frac{\partial \overline{M}}{\partial \xi^*} = R_i\frac{\xi_{ref}^2}{\rho D_s}$$ $$(93)$$	$$\sum_{i=1}^{n} j_i^* D_s \rho = 0 \qquad (94)$$
Diffusion, Maxwell-Stefan:	Definition:
$$j_i^* = -\omega_i\frac{1}{\overline{M}}\frac{\partial \overline{M}}{\partial \xi^*} - \frac{\partial \omega_i}{\partial \xi^*} + \omega_i\sum_{\substack{j=1 \\ j\neq i}}^{n}\frac{j_j^* D_s \overline{M}}{M_j D_{ij}} \qquad (95)$$	$$\sum_{i=1}^{n} \omega_i = 1 \qquad (96)$$
Ideal gas law, concentration and density:	
$$\frac{p}{RT} = c \qquad \frac{p\overline{M}}{RT} = \rho \qquad (97)$$	

Boundary conditions in the symmetry point $\xi^* = 0$	Boundary conditions at the surface $\xi^* = \xi_p^*$
$$j_i = 0 \qquad (98)$$ $$q = 0 \qquad (99)$$	$$T = T^b \qquad (100)$$ $$\omega_i = \omega_i^b \qquad (101)$$

4.2   Results and discussion - Alternative dimensionless method

The effect of using constant vs variable density and diffusive term when making the diffusion fluxes dimensionless are compared for the mass based model in the figure 5. As expected, this yields no difference between the models. However, it is recommended to use constant reference values as this will yield a much simpler model. Using variable reference values will cause a more troublesome implementation, since the fluxes no longer will directly be in scale. The same results were seen for the mole based model, although this is not presented.

The simulations are run to a residual below 10^{-10} whilst using 60 collocation points.
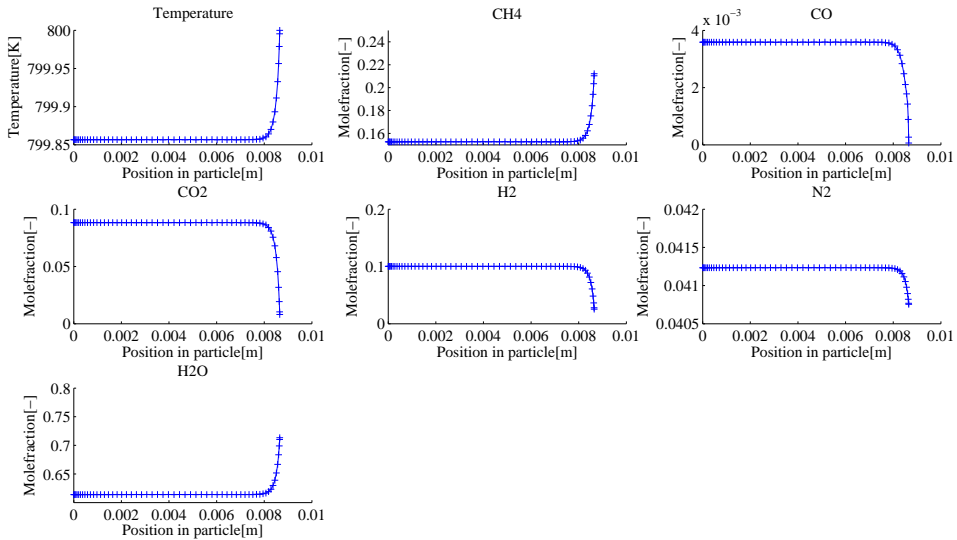
Figure 5: Mass based Maxwell-Stefan diffusion model comparing the use of constant(+++) vs variable(—) density and diffusive term for the species transport flux when transforming the equations to a dimensionless form.

4.3 Effect of continuity equation in the species balance

In this chapter the effect of including the continuity equation in the species balance will be investigated. This will as mentioned earlier in this chapter only have an effect for the mole based model for the cases not considering convective flow. The mass based model will not change in any manner for a non-conventive model since the mass based continuity equation does not contribute with any new terms. The mole based model will however change since the RHS of the continuity equation is a non-convective term which would not have been considered if it werent included in the species balance. The inclusion of the continuity equation in the species balance will be investigated both for a non-convective and a convective model.

A model for this particular case will be derived in detail in appendix C chapter C.3, with a solution strategy in table C.2 and a visualization of the implementation in figure C.2. A summary of the equations derived in the appendix along with the boundary conditions can be seen in table 8. The model is solved similarly to the simplest case in chapter 3 and the walkthroug of the equations can be found there.

For the rigorous models on both mole and mass basis alternative species balance equations not including the continuity equation are derived in short in appendix C chapter C.5. In the appendix, replacement equations for the rigorous models are suggested.

Table 8: Mole based equations, constitutive laws and boundary conditions

Equations:	Constitutive Laws:
Temperature equation: $$\frac{2q^*}{\xi^*} + \frac{\partial q^*}{\partial \xi^*} = \frac{\xi_{ref}^2(-\triangle H_R)R}{T_{ref}\lambda} \qquad (102)$$	Fourier's law $$q^* + \frac{\partial T^*}{\partial \xi^*} = 0 \qquad (103)$$
Species mole balance: $$\frac{2J_i^*}{\xi^{*2}} + \frac{\partial J_i^*}{\partial \xi^*} = R_i' \frac{\xi_{ref}^2}{D_{ref}c_{ref}} \qquad (104)$$	Definition: $$\sum_{i=1}^{n} J_i^* = 0 \qquad (105)$$
Diffusion, Maxwell-Stefan: $$\frac{j_i^* D_{ref}}{c^*} \sum_{\substack{j=1 \\ j \neq i}}^{i} \frac{x_j}{D_{ij}} + \frac{\partial x_i}{\partial \xi^*} = \frac{D_{ref}}{c^*} \sum_{\substack{j=1 \\ j \neq i}}^{n} \frac{j_j^* x_i}{D_{ij}} \qquad (106)$$	Definition: $$\sum_{i=1}^{n} x_i = 1 \qquad (107)$$
Ideal gas law rearranged for concentration: $$\frac{p}{RT} = c \qquad (108)$$	
Boundary conditions in the symmetry point $\xi^* = 0$ $$J_i = 0 \qquad (109)$$ $$q = 0 \qquad (110)$$	Boundary conditions at the surface $\xi^* = \xi_p^*$ $$T = T^b \qquad (111)$$ $$x_i = x_i^b \qquad (112)$$

4.4 Results and discussion - Effect of continuity equation

The big difference by not including the sum of reactions(RHS of the continuity equation) for the models dis-considering convective flow can be seen in figure 6. In the figure the results are compared to the model including the RHS of the continuity equation presented in the previous chapter. The inclusion of the RHS of the continuity equation in the models not considering convective flow will compensate for much of the loss where the convective terms have a significant value. The inclusion of the convective terms is especially important for the mole based SMR simulation as they have a significant value. This difference can easily be spotted in the figure 6 were a problem dis-considering convective flow is simulated with or without the continuity equation in the species balance.

However, if the convective terms were to be included it would not make any difference whether the convective terms are used or if they are replaced with the LHS of the continuity equation. This can be seen from the figures C.3 and C.4 in the additional results chapter presented in appendix C. No performance gain was seen for either of the models, meaning that the implementation method for models including convective flow will be optional.
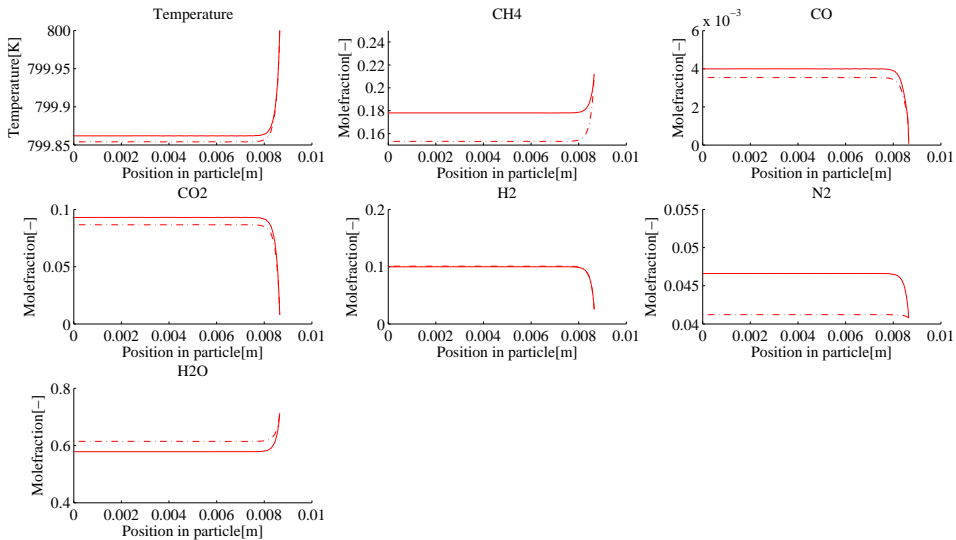
Figure 6: Comparing the inclusion of the LHS of the continuity equation for a mole based model assuming steady state, no convective transport and using basic boundary conditions. The model including the LHS of the continuity equation is seen as(-.-.-), while the model not considering the continuity equations is seen as(—).

5 Rigorous steady state models

Considering convective flow and transfer limitations in the boundary conditions will yield the fully rigorous steady state models of the SMR reaction in a catalyst particle. Firstly the convective terms will be added and later the transfer limitations, resulting in two different models for each case.

The addition of transfer limitations in the models will yield some inaccuracy since the mass transfer coefficients used in the boundary conditions are based on binary gas compositions [16]. However, the inaccuracy will be investigated by switching which component that is solved for by the sum of the rest(equation 14 and 16 for mass and mole respectively). Since the last component is solved without a boundary condition, there should not be any difference if consistent transfer limitations were used. However, by switching the order of the components a rough estimate of the yielded inaccuracy can be identified.

5.1 Derivation of the model equations

The basic model equations needed for the rigorous steady state models are equal to the simple models with the addition of the convective terms. In addition, equations for calculating the convective flow and the total pressure through the particle are needed. For the convective flow the continuity equation is used and pressure is calculated from Darcy's law.

The temperature equation (A.56) for mass and (A.63) for the mole based model is solved in combination with Fourier's law. The temperature equation is only modified by assuming steady state. The heat flux is obtained from the temperature equation and the temperature is obtained from Fourier's law. The temperature equation is dependent on mass averaged velocity, and for the mole based model the mass based velocity is obtained from the species transport fluxes according to equation A.35. For the mass based model the mass averaged velocity is obtained from the continuity equation.

The species balance for respectively the mass and mole model (A.55) and (A.62), is used to calculate the species transport fluxes. This is done by solving the species balance for N-1 components and the last component by the constitutive law's (A.39) and (A.41). In the species balance the continuity equation (A.57) and (A.64) is identified for the respective model and inserted giving the species balance used in the model.

The species fractions are solved by using one of the four different diffusion models in table 2. This is done for N-1 components, the last component is solved by the appropriate constitutive law (14) and (16). The diffusion models are only reformulated from their general form shown in the theory to reflect their implemented form.

The continuity equation A.57 and A.64 are used to obtain the mass and mole averaged velocity for the respective models. This equation is only modified by introducing the assumption of steady state. For comparison also the mole averaged velocity is calculated in the mass based model from the mass based fluxes using equation A.29, and vice versa for the mole based model with equation A.35.

The pressure is obtained from Darcy's law and the equation A.38 is used as it is given in the theory appendix A. This equation is also dependent on mass averaged velocity, so the mass averaged velocity obtained from the mole based fluxes are used for the mole based model.

The model derivation is presented in detail in appendix D. In the appendix all the needed model equations are derived and the mass based derivation is found in chapter D.1 whereas the mole based is found in chapter D.3. In the appendix the solution strategy is also presented in table D.1 and D.5 for the respective models and the visualization in figure D.1 and D.2. A summary of the derived equations along with the boundary conditions are presented in table 9 and 10 for convenience. The reactor operating conditions are given in the theory chapter table 1.

Table 9: Summary of the mass based model equations derived in chapter D.1 in Appendix D

Equations:	Constitutive Laws:
Temperature equation:	Fourier's law
$$\frac{D_{ref}}{\lambda}\rho^*\rho_{ref}v_r^*\sum_{i=1}^{n}\omega_i Cp_i\frac{\partial T^*}{\partial \xi^*} =$$ $$-(\frac{2q^*}{\xi^*}+\frac{\partial q^*}{\partial \xi^*})+\frac{\xi_{ref}^2(-\triangle H_R)R}{T_{ref}\lambda}$$ $\quad(113)$	$$q^*+\frac{\partial T^*}{\partial \xi^*}=0 \qquad (114)$$
Species mass balance, solved for N-1 equations:	Definition:
$$\frac{\partial \omega_i}{\partial \xi^*}(\rho^* v_\xi^*)+(\frac{2j_i^*}{\xi^*}+\frac{\partial j_i^*}{\partial \xi^*})=R_i\frac{\xi_{ref}^2}{D_{ref}\rho_{ref}} \qquad (115)$$	$$\sum_{i=1}^{n}j_i^*=0 \qquad (116)$$
Diffusion model, solved for N-1 equations:	Definition:
One of the four diffusionmodels in table D.2 is used	$$\sum_{i=1}^{n}\omega_i=1 \qquad (117)$$
Mass based continuity equation:	Mole averaged velocity
$$\frac{2}{\xi^*}v^*\rho^*+\frac{\partial \rho^*}{\partial \xi^*}v^*+\frac{\partial v^*}{\partial \xi^*}\rho^*=0 \qquad (118)$$	$$u=\sum_{i=1}^{N}\frac{j_i\overline{M}}{\rho M_i}+v \qquad (119)$$
Ideal gas law modified for density:	Darcy's law:
$$\frac{p\overline{M}}{RT}=\rho \qquad (120)$$	$$\frac{v^*\mu D_{ref}}{Bp_{ref}}+\frac{\partial p^*}{\partial \xi^*}=0 \;\;(121)$$

Boundary conditions in the symmetry point $\xi^*=0$	Boundary conditions at the surface $\xi^*=\xi_p^*$ with transfer limitations:
$$j_i=0 \qquad (122)$$ $$q=0 \qquad (123)$$ $$v=0 \qquad (124)$$	$$q_r+\rho Cp_g Tv=-h(T^b-T) \qquad (125)$$ $$-k_i(\rho_i^b-\omega_i\rho)=j_i+v\rho\omega_i \qquad (126)$$ $$p=p^b \qquad (127)$$ Boundary conditions at the surface $\xi^*=\xi_p^*$ without transfer limitations: $$T=T^b \qquad (128)$$ $$\omega_i=\omega_i^b \qquad (129)$$ $$p=p^b \qquad (130)$$

Table 10: Summary of the mole based model equations derived in chapter D.3 in Appendix D

Equations:	Constitutive Laws:
Temperature equation:	Fourier's law

$$\frac{D_{ref}}{\lambda} c^* c_{ref} v_r^* \sum_{i=1}^{n} x_i Cp_i' \frac{\partial T^*}{\partial \xi^*} + (\frac{2q^*}{\xi^*} + \frac{\partial q^*}{\partial \xi^*}) = \\ + \frac{\xi_{ref}^2(-\triangle H_R)R}{T_{ref}\lambda} \quad (131)$$

$$q^* + \frac{\partial T^*}{\partial \xi^*} = 0 \qquad (132)$$

Species mole balance, solved for N-1 equations: Definition:

$$\frac{\partial x_i}{\partial \xi^*}(c^* u_\xi^*) + (\frac{2J_i^*}{\xi^*} + \frac{\partial J_i^*}{\partial \xi^*}) = (R_i' - x_i \sum_{i=1}^{n} R_i')\frac{\xi_{ref}^2}{D_{ref}c_{ref}} \quad (133)$$

$$\sum_{i=1}^{n} J_i^* = 0 \qquad (134)$$

Diffusion model, solved for n-1 equations: Definition:

One of the four diffusionmodels in table D.6 is used

$$\sum_{i=1}^{n} x_i = 1 \qquad (135)$$

Continuity equation mole based: Mass averaged velocity:

$$\frac{2}{\xi^*}c^* u^* + \frac{\partial c^*}{\partial \xi^*}u^* + \frac{\partial u^*}{\partial \xi^*}c^* = (\frac{\xi_{ref}^2}{c_{ref}D_{ref}})\sum_{i=1}^{n} R_i' \quad (136)$$

$$v = \sum_{i=1}^{N} \frac{J_i M_i}{c\overline{M}} + u \quad (137)$$

Concentration: Darcy's law:

$$c = \frac{p}{RT} \qquad (138)$$

$$\frac{v^* \mu D_{ref}}{B p_{ref}} + \frac{\partial p^*}{\partial \xi^*} = 0 \quad (139)$$

Boundary conditions in the symmetry point $\xi^* = 0$	Boundary conditions at the surface $\xi^* = \xi_p^*$ with transfer limitations
$$J_i = 0 \qquad (140)$$ $$q = 0 \qquad (141)$$ $$u = 0 \qquad (142)$$	$$q_r + cCp_g'Tv = -h(T^b - T) \qquad (143)$$ $$-k_i(c_i^b - x_i c) = J_i + ucx_i \qquad (144)$$ $$p = p^b \qquad (145)$$ Boundary conditions at the surface $\xi^* = \xi_p^*$ without transfer limitations $$T = T^b \qquad (146)$$ $$x_i = x_i^b \qquad (147)$$ $$p = p^b \qquad (148)$$

5.2 Results and discussion - Rigorous models with simple boundary conditions

Moving on towards a fully rigorous steady state model gives the model where all terms are included except the transfer limitations in the boundary conditions. Without the transfer limitations the simple versions is used where $T = T^b$ and $\omega_i = \omega_i^b$ at the surface. The difference from the previous models is then the addition of the convective terms. This does have a positive effect for all the mole based models, but does not yield any change for the mass based models since the mass averaged velocity is supposed to be zero, i.e. negligible.

However since most of the convective terms in the mole based species balance are replaced by the LHS of the continuity equation, the change of adding the remaining convective terms is very small. The addition of these terms does not improve the differences from the mole and mass based models for the Wilke and Wilke-Bosanquet models figure 7 and 9 enough to make this change noticeable. The mole based Maxwell-Stefan and dusty gas models profits greatly by the addition of the convective terms and will now be identical as we can see from the figures 11 and 13. The inclusion of the mole based convective terms are especially important for the dusty gas model, since the diffusion model also relies on a convective term.

With the addition of the convective transport fluxes, it can now be seen that all the transport flux plots in figure(D.3,D.5,D.7 and D.9) are very similar. And due to the very slight back effect from the diffusion models, the differences that are seen for the mole fractions in the Wilke and Wilke-Bosanquet models, can only be spotted in the areas with steep gradients. There are however in general for all the mole based models, some problems with numerical errors when calculating the transport flux of nitrogen and some small oscillations are seen. Since the flux is supposed to be zero, small variations in the iteration easily leads to oscillatory behavior.

The oscillations seen in the convective flux of nitrogen transfers to the mass averaged velocity since the velocity is obtained from the fluxes in the mole based models. The numerical errors here are so small that it does not affect the other components. But, it gives an insignificant increase in pressure by approximately 0.04% for all the diffusion models on the mole based formulation, as we can see from the pressure plots in figure D.11. The mass based models do not show any increase in pressure as the numerical error does not appear here.

The secondary variables concentration, density and average molecular weight are calculated by algebraic equations outside of the solver system and will not be shown since they are directly dependent on the primary values. I.e the same differences that are seen for the primary variables will be seen for the secondary variables.

Looking at the effect of which component that is solved by the sum of other components with the constitutive law equation 14, it can be seen that this has no effect since the simple boundary conditions are used. This is as expected since the boundary conditions will be consistent, this is shown for three of the components in figure 15. However it is worth mentioning that it might be easier to get the model to converge using a component that has some presence, since the possibility of negative species fractions during iteration is reduced. But in this case there wasn't seen any major differences when simulating with the different components as the last in terms of convergence ability.

5.3   Results and discussion - Rigorous models with advanced boundary conditions

Adding the transfer limitations in the boundary conditions for the temperature and the diffusion models now gives a fully rigorous steady state model where all terms are considered. This addition does have an effect on the temperature and the mole fractions as we can see from the figures (8,10,12 and 14) for the different diffusion models, the changes are significant and can be easily spotted in the temperature plots. Also it is easy to see that the mole fractions at the surface are lower for the reactants because of the transfer limitations.

The transport fluxes behaves similarly to the models using basic boundary condition as we can see in the figures (D.4,D.6,D.8 and D.10), however the numerical error that occurs for calculating the transport flux of nitrogen is slightly lower, and the pressure increase seen in the pressure plots figure D.12 drops to 0.03%. However, this is considered insignificant for the simulation.

These models do not have any great differences from the models using the simple boundary conditions, and the same discussion applies here. The main difference can however be seen for the last component that is solved by the equation 16. Here the models will not give the same results changing the last component since the boundary conditions aren't consistent. They are however still identical on mass and mole basis, but this is not shown in a figure. The differences range from 0-3%, giving a noticeable difference. By the looks of the comparison for the methane figures it would be reasonable to assume that more comprehensive transfer limitations would range somewhere in between, meaning it's an acceptable error.

5.3.1 Wilke - Simple boundary conditions
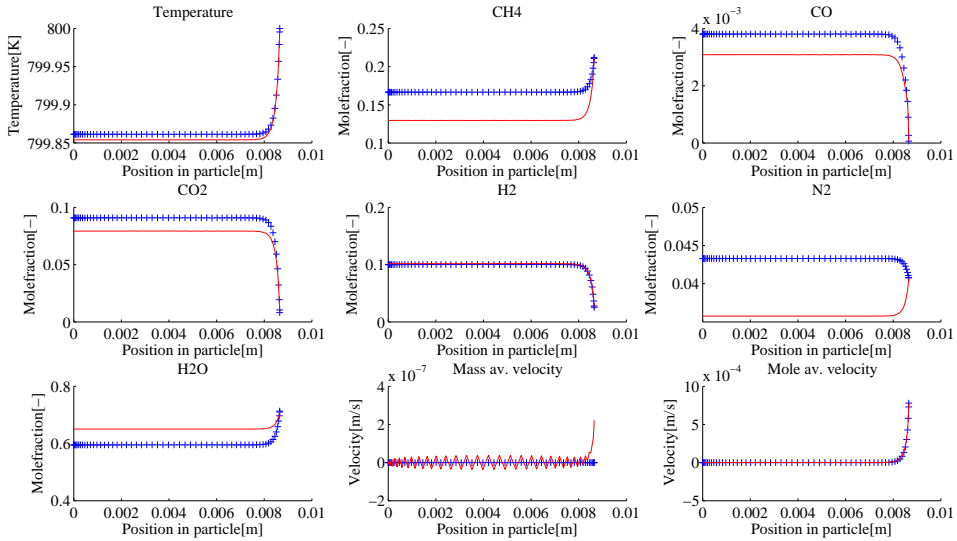
Figure 7: Comparison of the mole(—) and the mass (+++) based model, with the use of simple boundary conditions.

5.3.2 Wilke - Rigorous
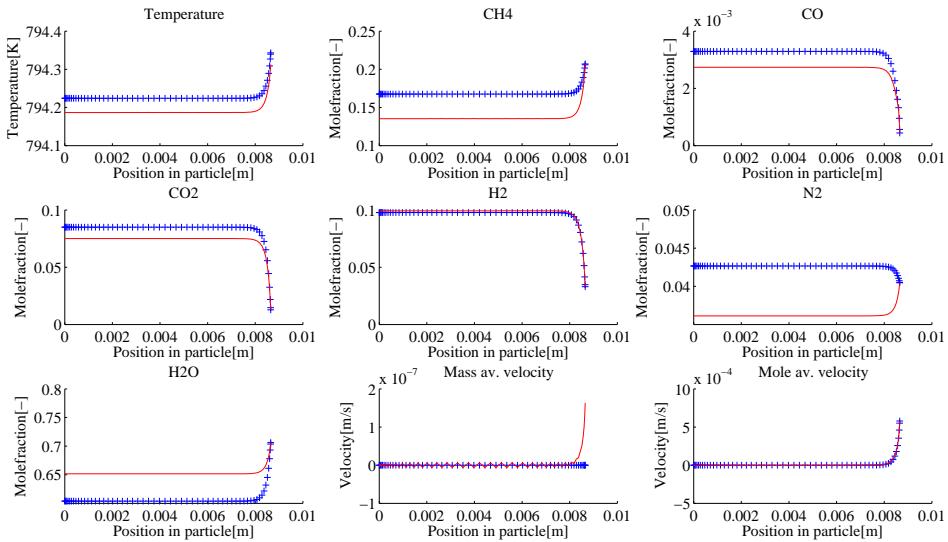
Figure 8: Comparison of the fully rigorous steady state mole(—) and the mass (+++) based model.

5.3.3 Wilke-Bosanquet - Simple boundary conditions
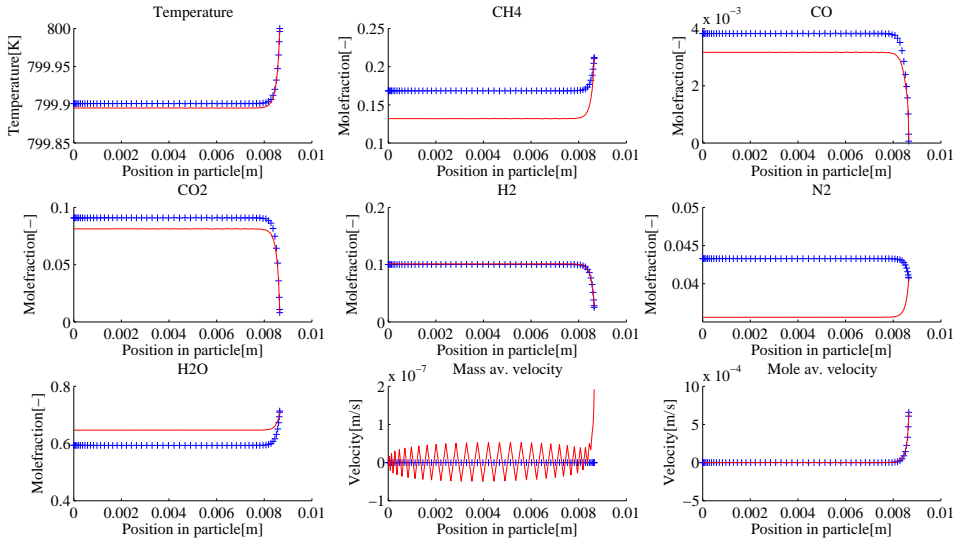
Figure 9: Comparison of the mole(—) and the mass $(+++)$ based model, with the use of simple boundary conditions.

5.3.4 Wilke-Bosanquet - Rigorous
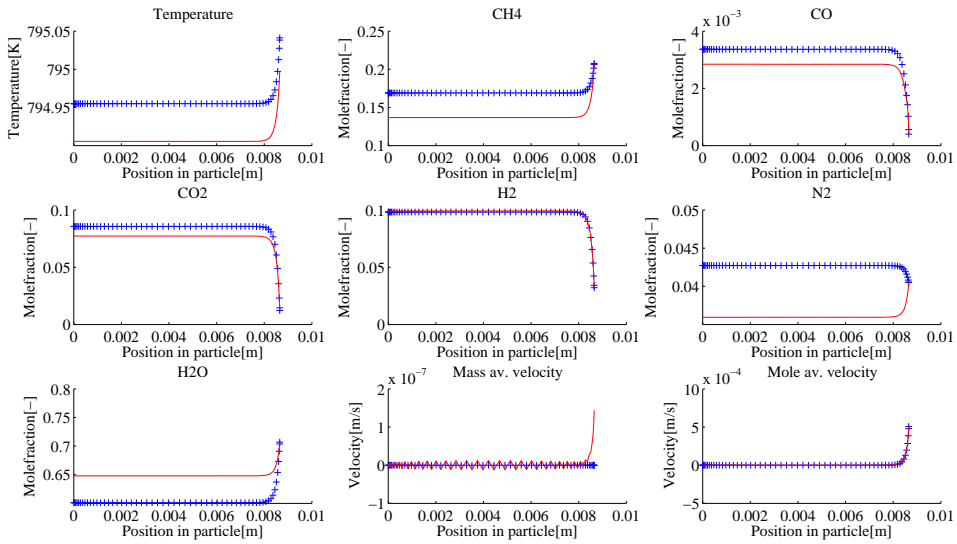
Figure 10: Comparison of the fully rigorous steady state mole(—) and the mass $(+++)$ based model.

5.3.5 Maxwell-Stefan - Simple boundary conditions
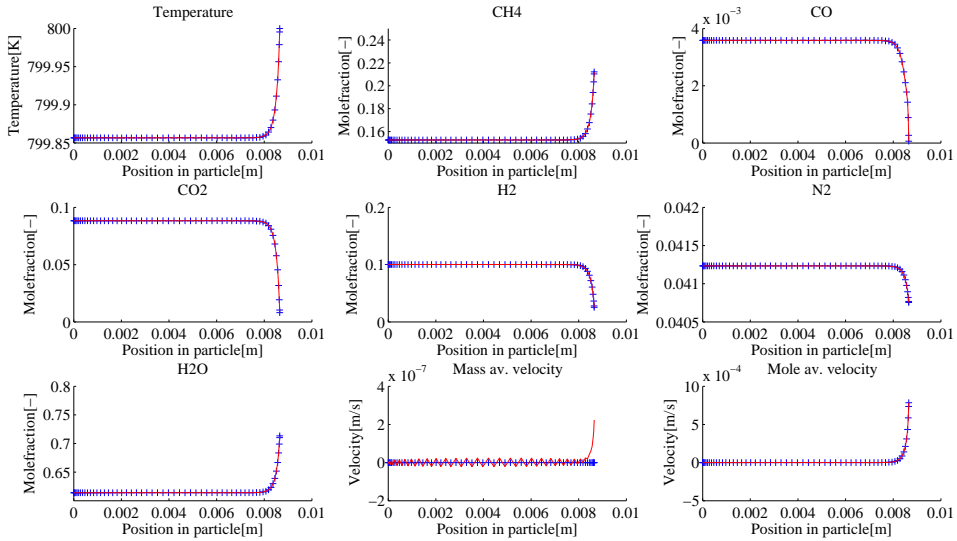
Figure 11: Comparison of the mole(—) and the mass (+++) based model, with the use of simple boundary conditions.

5.3.6 Maxwell-Stefan - Rigorous
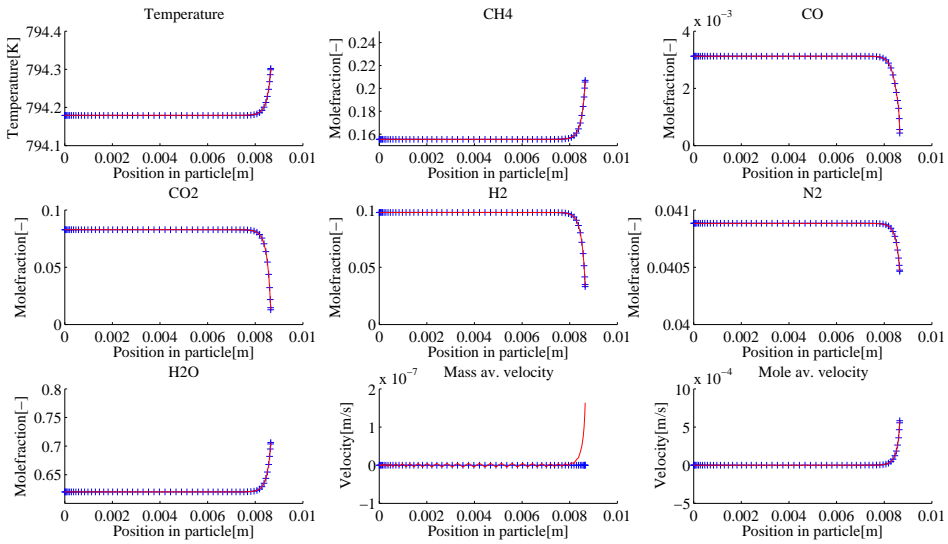
Figure 12: Comparison of the fully rigorous steady state mole(—) and the mass (+++) based model.

5.3.7 Dusty-gas - Simple boundary conditions
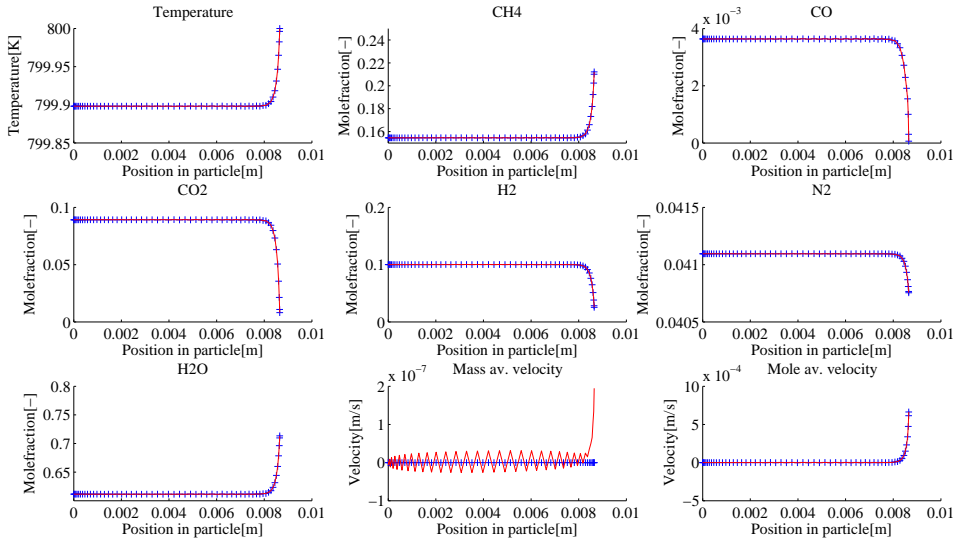
Figure 13: Comparison of the mole(—) and the mass (+++) based model, with the use of simple boundary conditions.

5.3.8 Dusty-gas - Rigorous
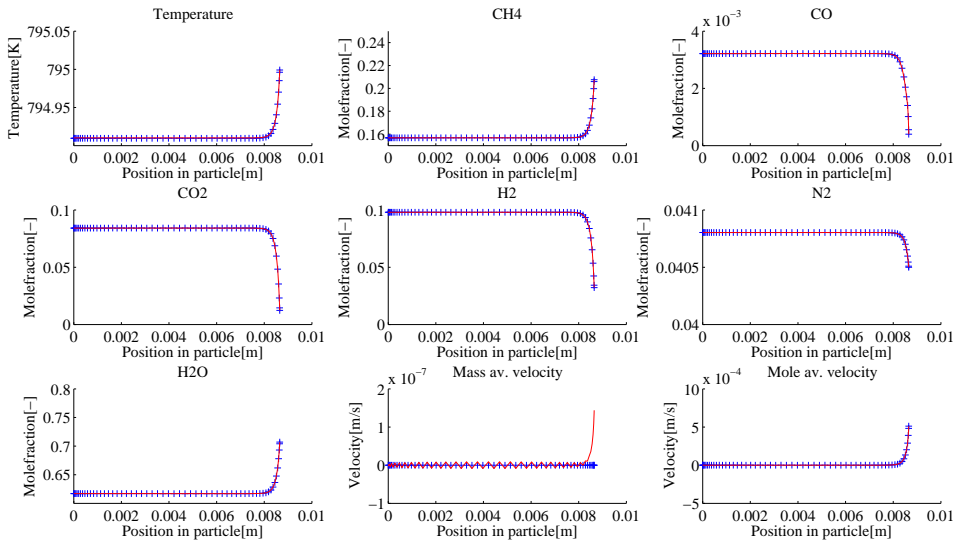
Figure 14: Comparison of the fully rigorous steady state mole(—) and the mass (+++) based model.

5.3.9 Effect of component solved with eqX
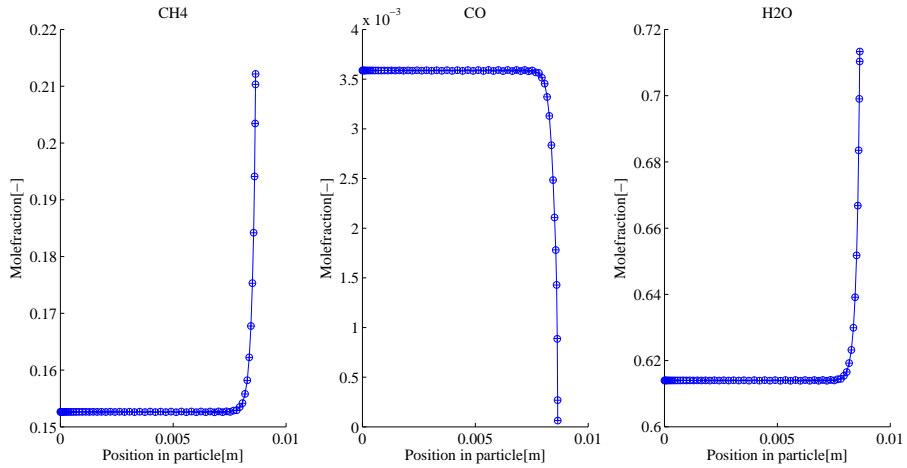
Figure 15: Comparing the effect of choosing a different component solved by the equation 14, using simple boundary conditions. $H_2O(—)$, $CH_4(+++)$,$CO(ooo)$.
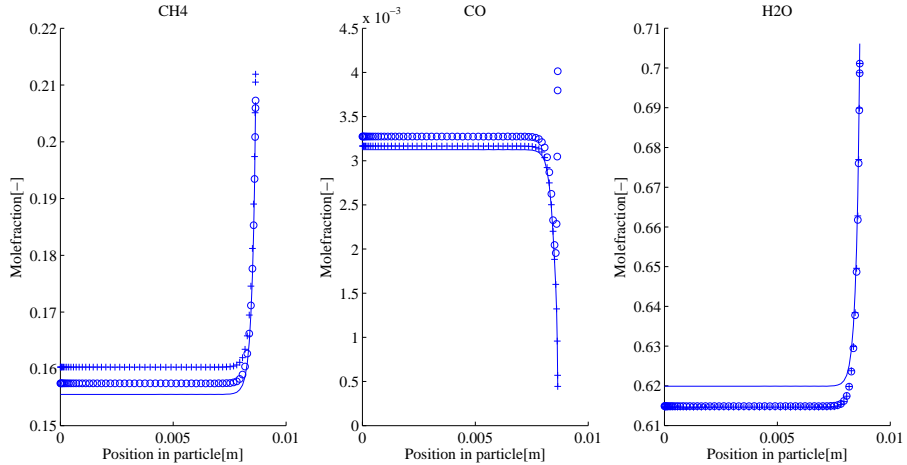
Figure 16: Comparing the effect of choosing a different component solved by the equation 14, including transfer limitations in the boundary conditions. $H_2O(—)$, $CH_4(+++)$,$CO(ooo)$.

6 Alternative rigorous steady state Wilke model

The Wilke and Wilke-Bosanquet diffusion models are both based on a simplified version of the Maxwell-Stefan diffusion model. The proposed method from Wilke is to reduce the Maxwell-Stefan equation to a multicomponent diffusion model based on the binary Fick's law form where the binary diffusivities are substituted by an effective multicomponent diffusivity[3]. The numerical errors introduced by the simplifications in the Wilke diffusion model will by solving the last component as a sum of the rest with the constitutive laws 14 and 16 only be included in this last component.

An alternative method was however presented, where it was suggested to solve both the fluxes and the diffusion models for N equations with the addition of a corrective diffusive velocity. This method will be investigated for the Wilke model and not for the Wilke-Bosanquet model since the addition of Knudsen diffusivities will not affect this alternative method.

$$\frac{\partial}{\partial t}(\rho \omega_i) + \nabla \cdot (\rho \omega_i v + v_c) = -\nabla \cdot (j_i) + R_i \qquad v_c = \sum_i D_{im} \nabla \cdot \omega_i \qquad (149)$$

$$\frac{\partial}{\partial t}(c x_i) + \nabla \cdot (c x_i u + u_c) = -\nabla \cdot (J_i) + R_i \qquad u_c = \sum_i D_{im} \nabla \cdot x_i \qquad (150)$$

Looking at the suggested modifications to the species mass balance it can be seen the addition to the equations is v_c/u_c when comparing to the general species balance equations (mass:8, mole:9) given in the theory. The corrective diffusive velocities are obtained from the effective diffusivities from the Wilke equation(mass:22, mole:26) and the gradient of the species fractions.

The introduction of the corrective velocity terms in the species balance equations will result in corrected continuity equations for both the mass and the mole based models. From the corrected continuity equations the new corrected velocity is obtained. However, since the method only seeks to correct the species mass balance, the original velocities are still needed for the temperature equation and Darcy's law. These velocities are easily obtained by subtracting the corrective term. A walk-through of the equations used in the alternative model will be given in appendix E.

6.1   Results and discussion - Alternative Wilke model

With the use of the modified Wilke model the mass fractions or mole fractions depending on the model basis will not sum to one, nor will the transport fluxes sum to zero. The results will by that reason be shown for the original results and scaled results. The results are easily scaled by dividing each component by the sum of the mass or mole fractions, in such a way that they sum to one.

In the figure 17 the original and the modified Wilke model is compared with the Maxwell-Stefan diffusion model using mass fractions. From the looks of the figure it can be seen that there are significant differences between the Wilke models, however they still deviate from the Maxwell-Stefan model. Though it is some times in opposite directions as seen for H_2O, the deviations are approximately in the same magnitude. The models are compared using mass fractions since the mass fractions do not sum to one and as we can see from the figure the mass fractions for the modified Wilke model increase approximately by 5%. Converting the mass fractions to mole fractions would have automatically scaled the mass fractions so that they sum to one, hence modifying the results.

Looking at the figure 18, the modified Wilke results have now been scaled so that the mass fraction sum to one. This has a very positive effect for the results, and the modified Wilke model is now approximately equal to the Maxwell-Stefan model. The model will however still have problems since the transport fluxes does not sum to zero and the use of the modified results are questionable.

The same can be seen for the mole based model, where no particular improvements can be seen for the unscaled results in figure 19. Scaling the results in such a what that the mole fractions sum to one, will have the same effect as for the mass based model and the mole based model will now be very comparable to the models using Maxwell-Stefan diffusion, this can be seen in figure 20. The modified Wilke mole based model deviates by approximately 11 percent in the sum of mole fractions for the non scaled results, which can be considered a significant loss i accuracy. Still, the modified Wilke model achieves reasonable results if scaling is used.

The modified Wilke models will also become more sensitive, resulting in longer simulation times than when using the Maxwell-Stefan model. This regards both the mole and the mass based models.

6.1.1 Mass based untouched results
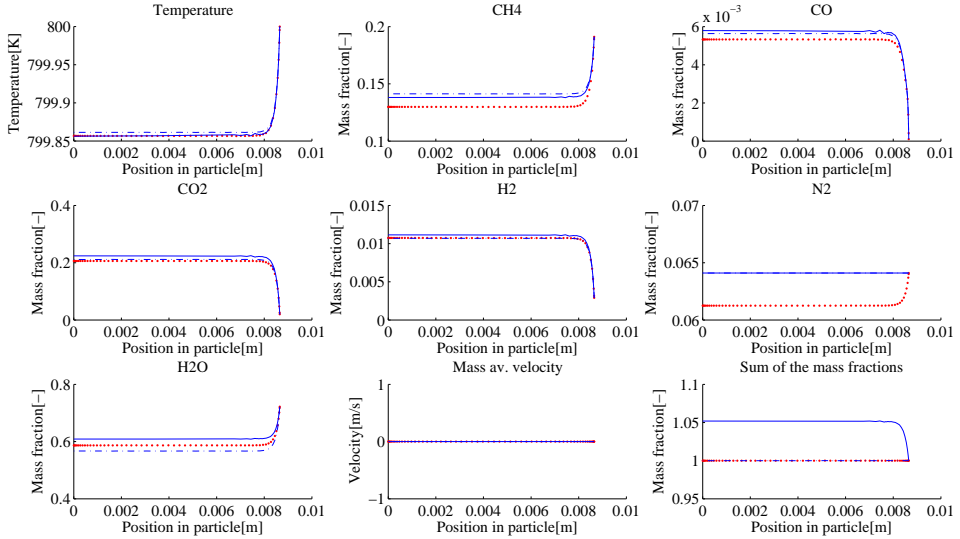
Figure 17: Comparison of the different mass based diffusion models using simple boundary conditions, original Wilke blue(-.-.-), modified Wilke blue(—), Maxwell-Stefan red($\cdots$)

6.1.2 Mass based scaled results
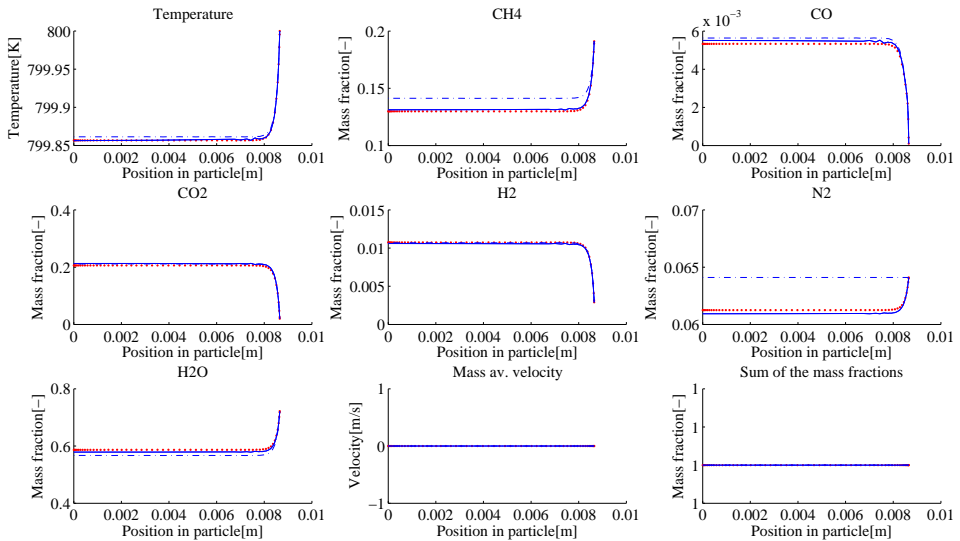
Figure 18: Comparison of the different mass based diffusion models using simple boundary conditions, original Wilke blue(-.-.-), modified scaled Wilke blue(—), Maxwell-Stefan red($\cdots$)

6.1.3 Mole based untouched results
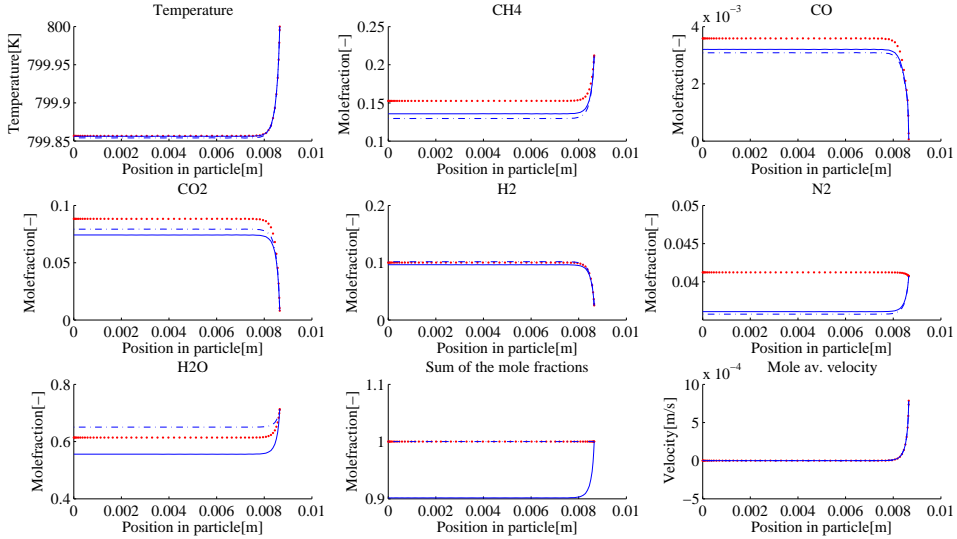
Figure 19: Comparison of the different mole based diffusion models using simple boundary conditions, original Wilke blue(-.-.-), modified Wilke blue(—), Maxwell-Stefan red($\cdots$)

6.1.4 Mole based scaled results
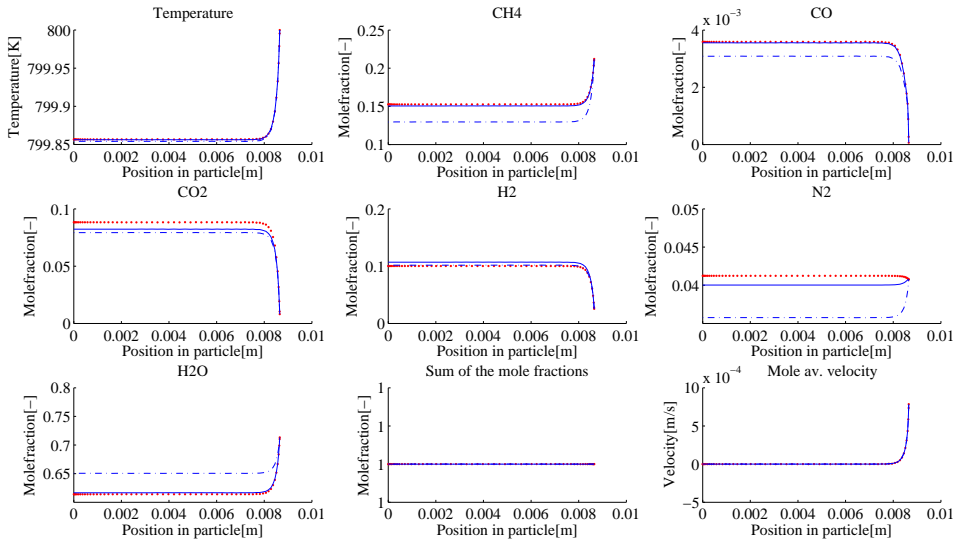
Figure 20: Comparison of the different mole based diffusion models using simple boundary conditions, original Wilke blue(-.-.-), modified scaled Wilke blue(—), Maxwell-Stefan red($\cdots$)

7 Alternative numerical methods for solving the rigorous steady state models

There are numerous different numerical methods. In this thesis only the numerical methods of weighted residuals are considered. So far the spectral method of orthogonal collocation has been used, which is the preferred method for pellet modeling[3]. The orthogonal collocation method will now be compared against the least squares method which is considered to be better for solving convective problems. These numerical methods will be compared for simulating the diffusion dominated pellet model in this chapter. The methods are also compared for convective dominated problems in chapter 9.

Both of these numerical methods will be solved as spectral elemental methods according to the theory chapter 2.4.4, in addition to the traditional spectral method. This is done in order to reduce the computational costs and reduce the simulation time whilst keeping the same level of accuracy. The spectral elemental methods are optimized to use the fewest amount of collocation points whilst maintaining an equal solution to the non element version. The numerical methods are are expected to behave differently with the least squares method to have less trouble with fewer collocation points. The orthogonal collocation method is however still expected to be the faster method as it requires much less computational effort for each iteration.

The methods are compared simulating a rigorous steady state pellet model on both mole and mass basis using the Maxwell-Stefan diffusion model. For the orthogonal collocation method the model equations are similar to the rigorous steady state models presented in chapter 5. For the least squares method the model derivation is the same, but the equations will have to be placed in a specific order in the problem matrix to obtain a stable system.

7.1 Derivation and visualization of the model equations

The models that are simulated using the orthogonal collocation method are solved as presented in the rigorous state state chapter 5 with the use of transfer limitations in the boundary conditions. This model is also used when the spectral element method is considered, however here the model is split into elements as shown in the theory chapter 2.4.4.

The model equations and the solution strategy used for the least squares method are identical to the orthogonal collocation models. However since the least squares method appears to be more sensitive to the variable sequence in the problem matrix, both matrices for the mass and mole based model will be showed to illustrate a working implementation strategy. This is presented in appendix F.

7.2 Results and discussion - Comparing the numerical methods

The numerical methods are compared as it can be seen from the figures (21-22) and (23-24) for mass and mole based models respectively. It is clear that both of the numerical methods yield identical results, with only some insignificant numerical differences for the mass averaged velocity and transport flux of nitrogen. Since the numerical methods yield identical results, the focus will be on the performance.

The methods will be compared by implementing the numerical methods both as spectral methods and as spectral element methods. For the spectral methods, both methods will be compared using a similar amount of collocation points. The spectral element methods will be optimized for each of the numerical methods to use the least amount of collocation points in such a way that the results still are identical to the non-element results. After obtaining the fastest possible run for each of the numerical methods, the novel pulse iteration method developed during this thesis will be applied to further reduce the simulation times.

Looking at the simulation results for the spectral methods in table 11, we can see that the orthogonal collocation method performs far better than the least squares method. Without the use of elements the least squares method seems to use approximately 200% additional time to reach the same residual as the orthogonal collocation method for the mass based formulation. The mole based formulation is in general a bit slower than its mass based counterpart since the mole based model needs additional under-relaxation of the convective term.

Moving on to the spectral element methods in table 12 it can seen that the differences between the mass and the mole based formulations increase. The mole based formulation tends to be more sensitive, and thus requiring additional collocation points in the steep gradients. The additional collocation points will result in a slower model. The same can also be seen for the least squares method and the orthogonal collocation method, where the least squares method tend to require less collocation points in the steep gradients. However, the least squares method is still approximately 150% slower since it requires more operations per iterations.

To further increase the performance of the numerical methods, the pulse iteration method presented in appendix I is applied to the models. The results are presented in table 13 and as it can be seen the novel under-relaxation method further reduces the simulation times by up to 76%. The weaker results from the least squares mole based model is because the model struggles to achieve a sufficient residual. For the more stable models the use of pulse iteration gives a very significant reduction in simulation times and in combination with a spectral element method this under-relaxation method can reduce the simulation times to only 8% of the simulation time used by a spectral method.

The lowest obtainable residual for the mass based formulations were 4×10^{-12} for the orthogonal collocation method and 5×10^{-11} for the least squares method. For the mole based formulation the residual obtained from the orthogonal collocation method remains unchanged while the acquired residual increases slightly to $4 \times$

10^{-10} for the least squares method. This is sufficiently low for all methods and the difference between them is insignificant.

Table 11: Mass based simulation results

Spectral models

Method	Simulation time	Increased simulation time	Collocation points
Mass OC*	97.6 Minutes	0%	60
Mole OC*	101 Minutes	3%	60
Mass LSM**	292 Minutes	199%	60
Mole LSM**	310 Minutes	217%	60

The mass based models are run to a residual of 10^{-10}, while the mole based are run to a residual of 10^{-9}. * Othogonal Collocation, ** least squares method.

Table 12: Mass based simulation results

Spectral element models

Method	Simulation time	Increased simulation time	Collocation points	Distribution of collocation points
Mass OC*	29 Minutes	0%	26	12%-6%-4%-78% 20-3-3-3
Mole OC*	49 Minutes	69%	31	12%-6%-4%-78% 24-4-3-3
Mass LSM**	72 Minutes	148%	21	12%-6%-4%-78% 15-3-3-3
Mole LSM**	87 Minutes	200%	24	12%-6%-4%-78% 18-3-3-3

The mass based models are run to a residual of 10^{-10}, while the mole based are run to a residual of 10^{-9}. * Othogonal Collocation, ** least squares method.

Table 13: Adding pulse iteration to the spectral element models to further improve speed

Spectral element models

Method	Simulation time	Simulation time with pulse iteration	Reduction in simulation time	Collocation points
Mass OC*	29 Minutes	8 Minutes	73%	26
Mole OC*	49 Minutes	14 Minutes	71%	31
Mass LSM**	72 Minutes	17 Minutes	76%	21
Mole LSM**	87 Minutes	50 Minutes	42%	24

The mass based models are run to a residual of 10^{-10}, while the mole based are run to a residual of 10^{-9}. * Othogonal Collocation, ** least squares method.

7.2.1 Maxwell-Stefan
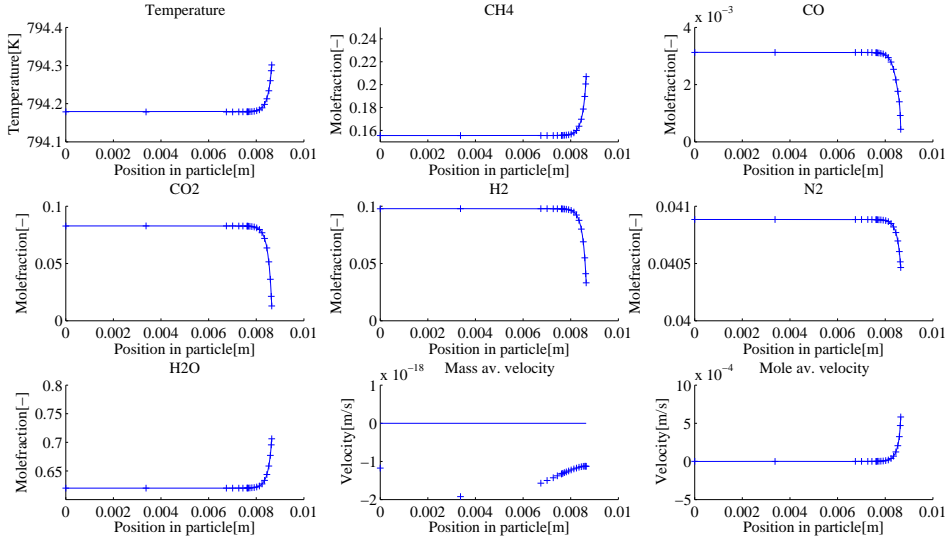
Figure 21: Comparison of the primary variables using the least squares(+++) and the orthogonal collocation(—) spectral element methods simulating a mass formulated Maxwell-Stefan model.
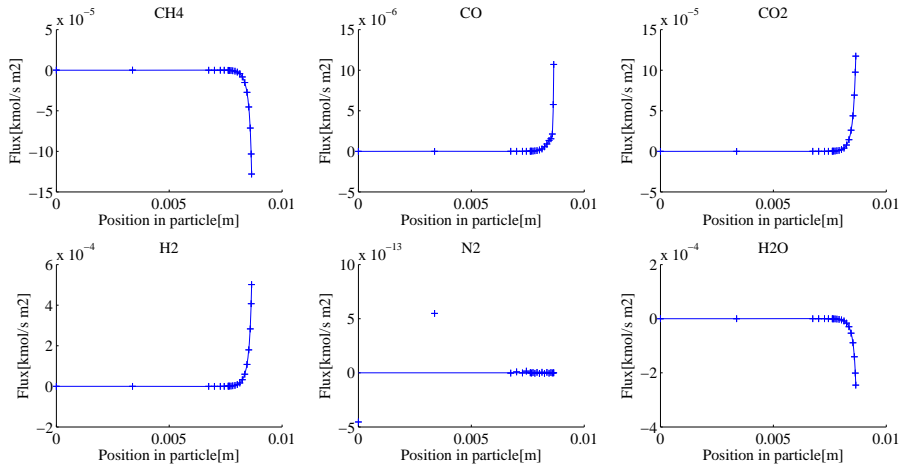
Figure 22: Comparison of the transport fluxes using the least squares(+++) and the orthogonal collocation(—) spectral element methods simulating a mass formulated Maxwell-Stefan model.

7.2.2 Maxwell-Stefan
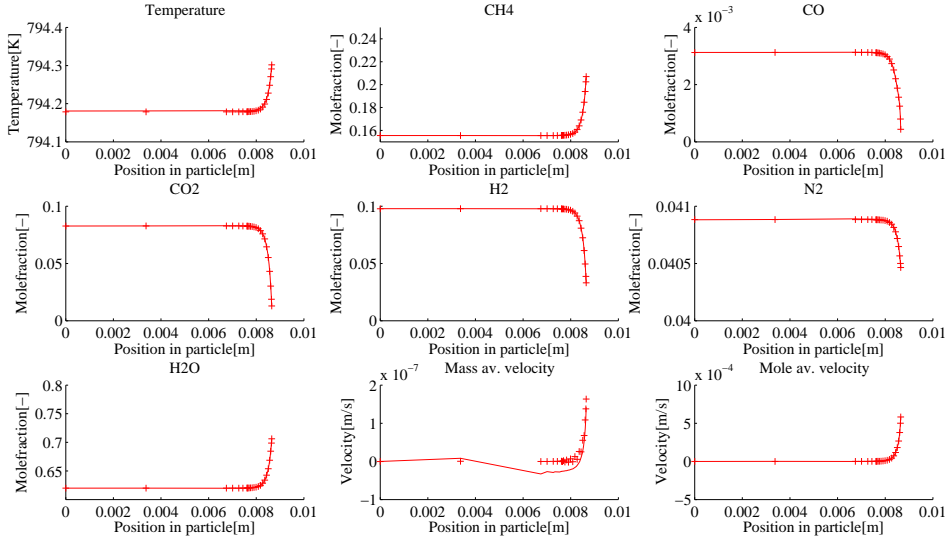
Figure 23: Comparison of the primary variables using the least squares(+++) and the orthogonal collocation(—) spectral element methods simulating a mole formulated Maxwell-Stefan model.
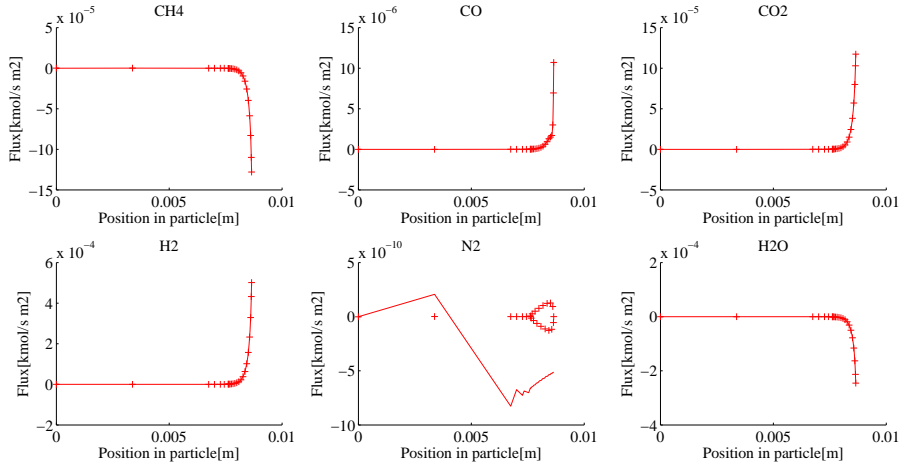
Figure 24: Comparison of the transport fluxes using the least squares(+++) and the orthogonal collocation(—) spectral element methods simulating a mole formulated Maxwell-Stefan model.

8 Rigorous transient models

Thus far the steady state models have been examined and it has been seen that the mole and mass based models yield identical results when the models include the convective terms and a consistent diffusion model are used. The transient term will now be implemented to see if the models still yield identical results. The focus will be on the consistent diffusion models Maxwell-Stefan and dusty gas. The inconsistent diffusion models Wilke and Wilke-Bosanquet will not be considered in this part since they did not yield identical results for the steady state models.

For the rigorous transient models, both of the numerical methods used in the previous chapter will be used. This is done to see if a difference between the numerical methods appear in the obtained steady state solutions.

8.1 Derivation of the model equations

The transient models are comparable to the rigorous models with the addition of the transient terms. The transient terms are discretized using the theta method as described in the theory chapter 2.5. Here a theta value of 0.5 is used meaning that the second order Crank-Nicholson method is applied.

The temperature equation (A.56) for mass and (A.63) for the mole based model is solved in combination with Fourier's law. The transient term is discretized using the theta method and the equation is rearranged for implementation. The heat flux and the time dependent temperature change are obtained from the temperature equation and the temperature is obtained from Fourier's law. The temperature equation is dependent on mass averaged velocity. The mass based velocity is calculated from the mole based fluxes according to equation A.35 for the mole based model. For the mass based model the mass averaged velocity is obtained from the continuity equation.

The species balance for the mass(A.55) and mole(A.62) formulation, is used to calulate the fluxes and the time dependent change of the species fractions. This is done by solving the species balance for N-1 components and the last component by the constitutive laws (A.39) and (A.41). In the species balance the continuity equation (A.57) and (A.64) is identified for the respective model and inserted giving the species balance used in the model. Swapping the terms in the species balance with the RHS of the continuity equation will in the transient models also replace one of the transient terms, yielding a simpler yet fully rigorous equation. The remaining transient term is discretisized using the aforementioned method.

The species fractions are solved by using the Maxwell-Stefan or dusty gas diffusion model given in the rigorous steady state chapter, table D.2 for the mass based and D.6 for the mole based. The diffusion model is solved for N-1 components, and the last component is solved by the appropriate constitutive law (A.40) and (A.42). The diffusion models are only reformulated from their general form shown in the theory to reflect their implemented form.

The continuity equation A.57 and A.64 are for the previous models used to obtain the mass and mole averaged velocity for the respective models. Adding the transient term to the equation will now also include the density or concentration change with time for the mass or mole based model respectively. The mass averaged velocity is obtained from the equation A.35 in the mole based model.

The pressure is obtained from Darcy's law equation A.38, no modifications are needed. This equation is also dependent on mass averaged velocity, so the mass averaged velocity obtained from the mole based fluxes are used for the mole based model.

When introducing the transient term it is also convenient for a more stable system to include the ideal gas law eq. A.36 for the mole based model and the density equation A.37 for the mass based model in the problem matrix.

The equations are derived in detail in appendix G, chapter G.1 for the mass based model and chapter G.3 for the mole based. The solution strategy for the respective models are given in table G.1 and G.4, while the visualization of the implemented equations are given in figure G.1 and G.2 respectively. The equations derived in detail in the appendix are presented in table 14 and 15 respectively with the used initial and boundary conditions for convenience.

Table 14: Mass based equations, constitutive laws and boundary conditions

Equations:	Constitutive Laws:
Temperature equation: Equation G.4 is used	Fourier's law $$q^* + \frac{\partial T^*}{\partial \xi^*} = 0 \qquad (151)$$
Species mass balance for N-1 components: Equation G.12 is used	Definition: $$\sum_{i=1}^{n} j_i^* = 0 \qquad (152)$$
Diffusion model for N-1 components: Maxwell-Stefan or dusty gas diffusion model are used from table D.2	Definition: $$\sum_{i=1}^{n} \omega_i = 1 \qquad (153)$$
Mass based continuity equation: Equation G.7 is used	Mole averaged velocity, eq. A.29 $$u = \sum_{i=1}^{N} \frac{j_i \overline{M}}{\rho M_i} + v \qquad (154)$$
Density, dimensionless: $$\frac{p p_{ref} \overline{M}}{R T \rho_{ref}} = \rho^* \qquad (155)$$	Darcy's law: $$\frac{v^* \mu D_{ref}}{B p_{ref}} + \frac{\partial p^*}{\partial \xi^*} = 0 \quad (156)$$

Boundary conditions in the symmetry point $\xi^* = 0$	Boundary conditions at the surface $\xi^* = \xi_p^*$ with transfer limitations:
$$j_i = 0 \qquad (157)$$ $$q = 0 \qquad (158)$$ $$v = 0 \qquad (159)$$	$$q_r + \rho C p_g T v = -h(T^b - T) \qquad (160)$$ $$-k_i(\rho_i^b - \omega_i \rho) = j_i + v \rho \omega_i \qquad (161)$$ $$p = p^b \qquad (162)$$

Initial conditions at t=0, $\forall \xi$:
$q = 0 \qquad T = T^b \qquad j_i = 0 \qquad \omega_i = \omega_i^b \qquad v_\xi = 0 \qquad p = p^b \qquad \rho = \rho^b$ (163)

Table 15: Mole based equations, constitutive laws and boundary conditions

Equations:	Constitutive Laws:
Temperature equation: Equation G.27 is used	Fourier's law $$q^* + \frac{\partial T^*}{\partial \xi^*} = 0 \qquad (164)$$
Species mole balance for N-1 components: Equation G.35 is used	Definition: $$\sum_{i=1}^{n} J_i^* = 0 \qquad (165)$$
Diffusion model for N-1 components: Maxwell-Stefan or dusty gas diffusion model are used from table D.6	Definition: $$\sum_{i=1}^{n} x_i = 1 \qquad (166)$$
Continuity equation mole based: Equation G.30 is used	Mass averaged velocity(A.35): $$v^* = \sum_{i=1}^{N} \frac{J_i^* M_i}{c_i^* \overline{M}} + u^* \qquad (167)$$
Concentration, dimensionless: $$c^* = \frac{p p_{ref}}{RT c_{ref}} \qquad (168)$$	Darcy's law: $$\frac{v^* \mu D_{ref}}{B p_{ref}} + \frac{\partial p^*}{\partial \xi^*} = 0 \qquad (169)$$

Boundary conditions in the symmetry point $\xi^* = 0$	Boundary conditions at the surface $\xi^* = \xi_p^*$ with transfer limitations
$$J_i = 0 \qquad (170)$$ $$q = 0 \qquad (171)$$ $$u = 0 \qquad (172)$$	$$q_r + cCp'_g Tv = -h(T^b - T) \qquad (173)$$ $$-k_i(c_i^b - x_i c) = J_i + ucx_i \qquad (174)$$ $$p = p^b \qquad (175)$$

Initial conditions at t=0, $\forall \xi$:

$$q = 0 \qquad T = T^b \qquad J_i = 0 \qquad x_i = x_i^b \qquad u_\xi = 0 \qquad p = p^b \qquad c = c^b \tag{176}$$

8.2   Results and discussion - The transient models

Investigating the Maxwell-Stefan diffusion model, it can be seen in the figures (25, 26, 27 and 28) that the models are identical for the numerical methods and on the different formulations. Some insignificant differences can be seen for the numerical methods in the peaks, but this occurs due to the different amount of collocation points in each element for each method.

Examining the results further shows that the models reach steady state. This is shown for the mass based models for both numerical methods in appendix G, figure G.7 and G.8 for the Maxwell-Stefan and dusty gas diffusion model respectively. The exact same behavior is seen for the mole based formulations, allthough this is not shown. Also the development of the components all seem reasonable, except for the spikes seen for the hydrogen and nitrogen mole fractions. However the spikes seen appear because of diffusion limitations in the pellet. As the reaction starts a dramatic production of hydrogen will occur, resulting in a massive mole production in the pellet causing the nitrogen concentration to plummet. During this initial phase a pressure increase is also seen due to the sudden increase in moles. When the reaction progresses the produced hydrogen can easily diffuse out of the pellet preventing pressure increase and cause the total reaction to appear mole consuming. The bigger nitrogen molecule is unable to diffuse out of the pellet at a comparable rate and experiences a slight increase in mole fraction. This is easy to see from the steady state figures.

The same can be said for the dusty gas diffusion model. The model behaves similarly and the only difference is the addition of Knudsen diffusion, this can be seen from the figures (G.3, G.4, G.5 and G.6). The steady state data obtained from the transient models are as for the Maxwell-Stefan diffusion model identical to the data obtained from the steady state models.

The results are obtained using spectral element methods using a time step varying between 5×10^{-3} and 0.1 seconds. The under-relaxation value has to be adjusted accordincly since a higher timestep will require a lower under-relaxation value.
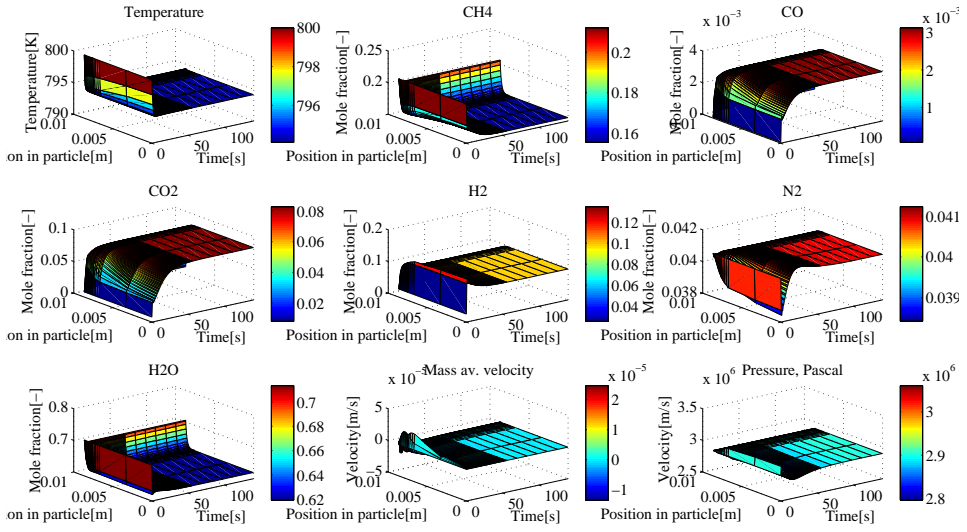
Figure 25: Rigorous Transient mass based model using the Maxwell-Stefan diffusion model simulated with the orhogonal collocation method.
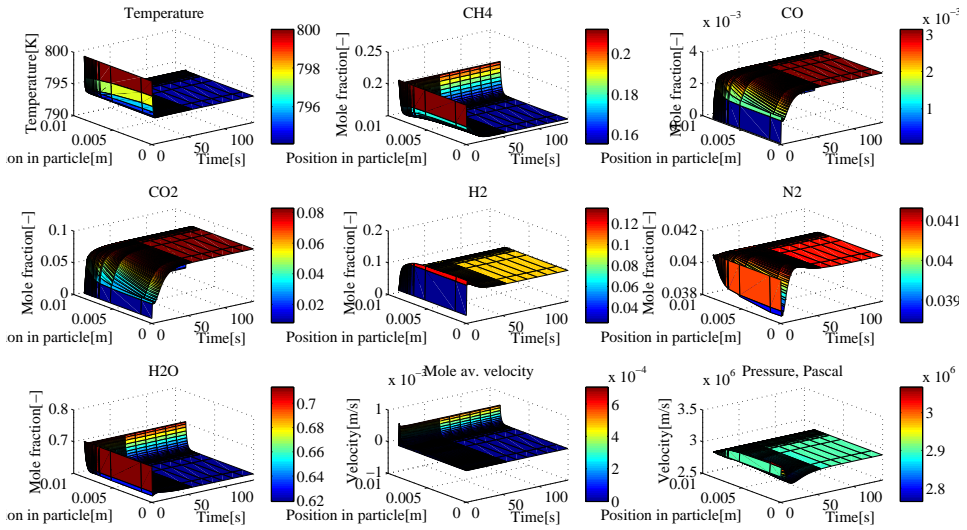
Figure 26: Rigorous Transient mole based model using the Maxwell-Stefan diffusion model simulated with the orhogonal collocation method.
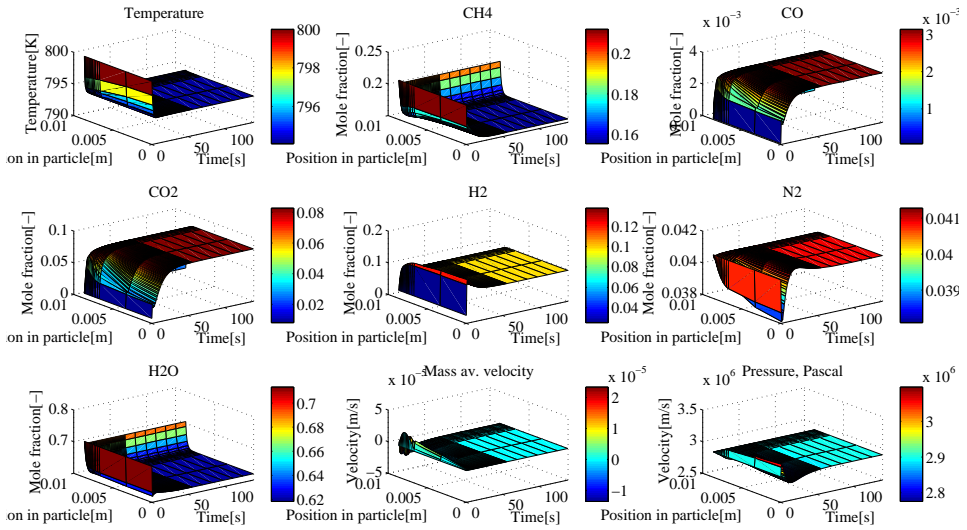
Figure 27: Rigorous Transient mass based model using the Maxwell-Stefan diffusion model simulated with the least squares method.
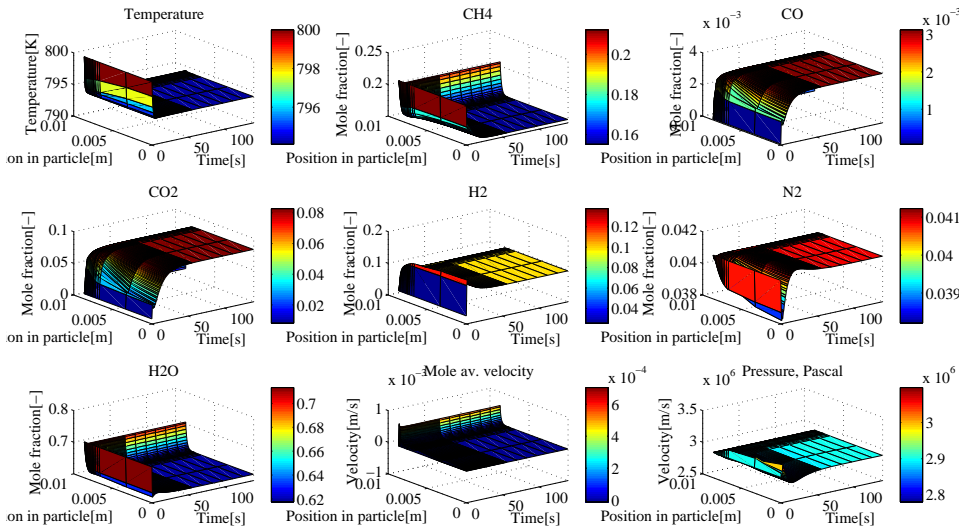
Figure 28: Rigorous Transient mole based model using the Maxwell-Stefan diffusion model simulated with the least squares method.

9 Comparing the numerical methods

So far the focus has been on the diffusion dominated pellet equations for both of the numerical methods presented in this thesis and both methods have produced satisfactory results. We will now look into convection-dominated problems to see if any weaknesses in the numerical methods can be found. It is known that the method of orthogonal collocation should have greater difficulty solving convection dominated problems than the least squares methods[3]. This claim will be tested by solving the equations for a pseudo-homogeneous reactor and the advection equation.

Solving the advection equation will serve the purpose as an extreme test, where only convection is present. This is meant to give good insight in how the methods behave in convective dominated problems. Here a discontinuity will be introduced in the model to see how the different numerical methods behaves during the transport throughout the reactor.

By looking into the more practical application of a pseudo-homogeneous reactor model using the steam methane reforming reaction, a good comparison for both numerical methods will be achieved when a very fast reaction is used in order to create a steep gradient in a reactor dominated by convective flow. The already existing diffusion in the problem will also be reduced by a factor in order to provoke the differences in the numerical methods. Also a discontinuity will be introduced in the simulation to see how the methods cope during a sudden change in the reactor feed.

9.1 Simulation of the advection equation

9.1.1 Derivation of the model equation

Starting out from the advection equation:

$$\frac{\partial \rho}{\partial t} + v \frac{\partial \rho}{\partial z} = 0 \tag{177}$$

The equation is made dimensionless according to correlations given in A.9:

$$\frac{\partial \rho^*}{\partial t^*} + v^* \frac{\partial \rho^*}{\partial z^*} = 0 \tag{178}$$

The transient term is discretisized using the theta model presented in chapter 2.5.

$$\rho^{*(t+1)} + \Delta t \theta v^* \frac{\partial \rho^{*(t+1)}}{\partial z^*} = \Delta t (1-\theta)(-v^* \frac{\partial \rho^{*(t)}}{\partial z^*}) + \rho^{*(t)} \tag{179}$$

9.1.2 Solution strategy of the advection equation

The equation is solved in the traditional matrix setup as shown for the pellet equations:

$$\left[1 \bullet + \Delta t \theta v^* \frac{\partial}{\partial z^*} \right] \left[\rho^{*(t+1)} \right] = \left[\Delta t (1-\theta)(-v^* \frac{\partial \rho^{*(t)}}{\partial z^*}) + \rho^{*(t)} \right] \tag{180}$$

With the boundary condition $\rho^*_{z=0} = 0.1$ and the initial condition $\rho^*_{\forall z} = 1$. The dimensionless constant velocity is set to 1.

9.2   Results and discussion - Advection equation

When simulating a front moving through the reactor with the advective equation it can be seen that both methods struggles with high oscillations. This is however an extreme test as there are no diffusive forces in the equation and the discontinuity introduced will not smoothen out over time. The time dependent variables are discretized using the method of Crank-Nicholson which is a second order method giving a high accuracy.

The least squares and the orthogonal collocation methods are compared using both high order polynomials and low order polynomials. A high order polynomial is obtained when using a high amount of collocation points, whereas a low order polynomials are obtained using a few collocation points in each element. As it can be seen from figure 29, when low order polynomials are introduced the small oscillations far from the discontinuity are removed and a better solution is achieved. However the oscillations near the discontinuity are still to high to prove acceptable. The opposite can be seen for the orthogonal collocation method where the solution suffers when low order polynomials are introduced to the solving method. In all cases the error near the discontinuity will be in the order of 20%.

Both methods yield unacceptable results and in order to remove the oscillations numerical diffusion has to be introduced. This would defeat the purpose of comparing the methods for simulation of a purely convective problem.
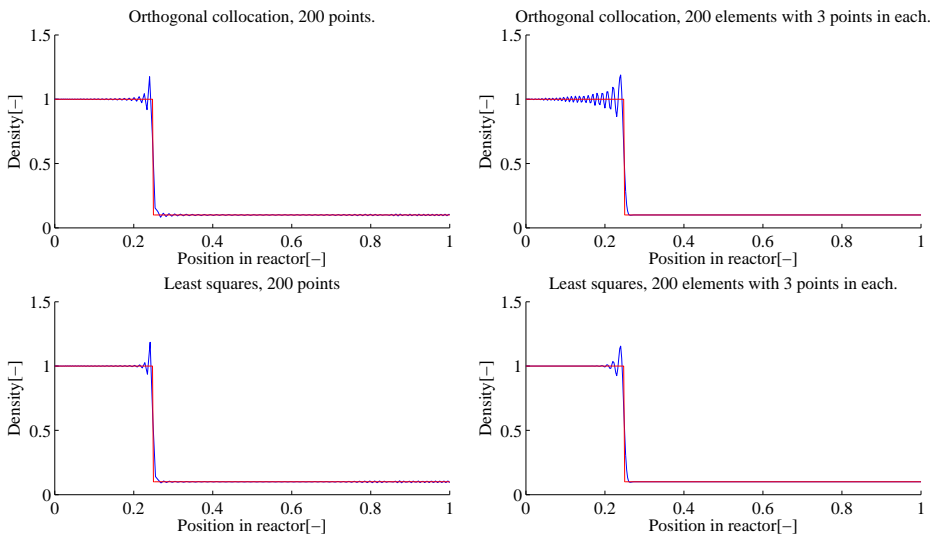
Figure 29: Comparing the different numerical methods(blue (—)) for solving the advection equation using both a non-element and an element method against the analytical solution(red (—)).

9.3   Simulation of a SMR reactor

The model for a SMR reactor is somewhat similar to the fully rigorous pellet equations, however here we will take basis in a cylindrical reactor rather than a sphere. This model will aslo be reduced to a one dimensional problem where symmetry is assumed around the axial direction, giving that there are no changes in the radial direction or with the azimuth angle.

The reactor is assumed to be pseudo homogeneous and will thereby not account for any limitations introduced by the catalyst particle. To include this effect some efficiency factors will need to be introduced to compensate for the diffusion resistances within the catalyst particle. These factors will effectively reduce the reaction rate to simulate the catalyst behavior. The efficiency factors presented by Solsvik et al.[2] are used in this thesis.

The initial conditions in the reactor will mainly be the boundary conditions in the whole system except for the mass fractions. For the mass fractions the initial conditions will mainly contain steam with some methane present, this is done to see how the numerical methods cope with a discontinuity traveling through the reactor system.

9.3.1   Model derivation

As for the other models the derivation of the model equations for the pseudo homogeneous SMR reactor will be derived in detail in appendix H along with a solution strategy and a visualization of the implementation. The focus in this chapter will be on a short explanatory approach with a summary of the equations derived in the appendix presented in table 16 along with the boundary and initial conditions.

The temperature equation 4 will as for the pellet models be solved in combination with Fourier's law to acquire a set of first order partial differential equations. The temperature is obtained from Fourier's law while the heat flux and the temperature change with time are obtained from the temperature equation. In the reactor model, heat transfer from the walls will also be included.

The species balance 8 is now used to calculate the dispersion fluxes and the change in mass fractions with time in the reactor for N-1 components. The last component is solved using the constitutive law 13. The mass fractions are obtained from the dispersion equation H.14 again for N-1 components with the last being solved from the constitutive law 14.

The continuity equation 30 is used to obtain the mass averaged velocity, which then can be used to solve the pressure with Ergun's equation H.15. The density is obtained from the modified ideal gas law equation A.37.

Both models are solved completely similar for both the orthogonal collocation and the least squares method.

Table 16: Mass based equations, constitutive laws and boundary conditions

Equations:	Constitutive Laws:
Temperature equation: Equation H.4 is used	Fourier's law $$q^* + \frac{\partial T^*}{\partial \xi^*} = 0 \qquad (181)$$
Species mass balance for N-1 components: Equation H.13 is used	Definition: $$\sum_{i=1}^{n} j_i^* = 0 \qquad (182)$$
Dispersion equation for N-1 components: $$j^* = -\frac{D_{disp}}{v_{ref} z_{ref}} \rho^* \frac{\partial \omega_i}{\partial z^*} \qquad (183)$$	Definition: $$\sum_{i=1}^{n} \omega_i = 1 \qquad (184)$$
Mass based continuity equation: Equation H.8 is used	Ergun's equation $$\frac{\partial p^*}{\partial z^*} = -\frac{f \rho^* v_z^{*2}}{d_p} \frac{\rho_{ref} v_{ref}^{*2} z_{ref}}{p_{ref}}$$ $$(185)$$
Ideal gas law modified for density: $$\frac{p\overline{M}}{RT} = \rho \qquad (186)$$	

Boundary conditions at the inlet $z = 0$	Boundary conditions at the outlet $z = z_{out}$ with transfer limitations:
$$T = T^b \qquad (187)$$ $$\omega_i = \omega_i^b \qquad (188)$$ $$v_z = v_z^b \qquad (189)$$	$$q = 0 \qquad (190)$$ $$j_i = 0 \qquad (191)$$ $$p = p^b \qquad (192)$$

Initial conditions at t=0, $\forall \xi$:
$q = 0 \qquad T = T^b \qquad j_i = 0 \qquad \omega_i = \omega_i^{\neq b} \qquad v_\xi = 0 \qquad p = p^b \qquad \rho = \rho^b$ $$(193)$$

9.4   Results and discussion - Simulation of a SMR reactor

The focus of the comparison will be on the development of steady state in the model, rather than just comparing the steady state results. To examine how the methods tackle steep gradients in the progress to steady state a plug will travel through the system in the initiating phase. Looking at the initial and boundary condition plot in figure 30, it can be seen how much the initial conditions differ from the boundary conditions. The boundary conditions are here stipulated over the whole of the reactor to make it more easy to compare it to the initial conditions. As the simulation starts the initial conditions will travel out of the reactor as a plug.

Looking at the system in figure 31 when two seconds have passed, it can be seen that both methods behaves similarly with some oscillations near the discontinuity introduced as initial conditions. The methods are simulated using 60 collocation points with a time-step of 0.1 seconds. The least squares method behaves more stable and can run with a relative high under-relaxation value compared to the orthogonal collocation method. This makes the least squares method the fastest and uses only 25% of the simulation time the orthogonal collocation method uses. Although the orthogonal method requires a much lower under-relaxation parameter to obtain results, it is much more versatile when it comes to the time step size. It will have no problem with any time step size, whereas the least squares method will have trouble if the time-step is reduced further.

Since the methods are supposed to behave different for a convective dominated problem, the dispersion rate is artificially reduced by a factor of 100. As it can be seen from the results in figure 32, these methods are still identical. But, this is also as expected since they behaved similar for the advection equation. However, the time spent on simulating is further increased for the orthogonal collocation method, since a lower under-relaxation value are required to obtain the solution. The least squares method does not need this and use the same amount of time, resulting in that it only needs 15% of the time to obtain the same results.

Introducing elements to the problem is expected to cause the orthogonal collocation method to oscillate, while the least squares method remains more or less the same as it has been seen for the advection equation. For the next simulation there will be used 30 elements, evenly distributed with 3 collocation points in each. As expected this doesn't significantly affect the least squares method, however the orthogonal collocation method is now unable to produce the results due to oscillations. The results for this is not shown since a comparison cant be made, but the least squares method is compared against the method using 60 collocation points in figure 33. From the figure it is easy to see that the effect of introducing elements reduces the amount of oscillations near the discontinuity. However new oscillations will occur at the entry of the reactor.
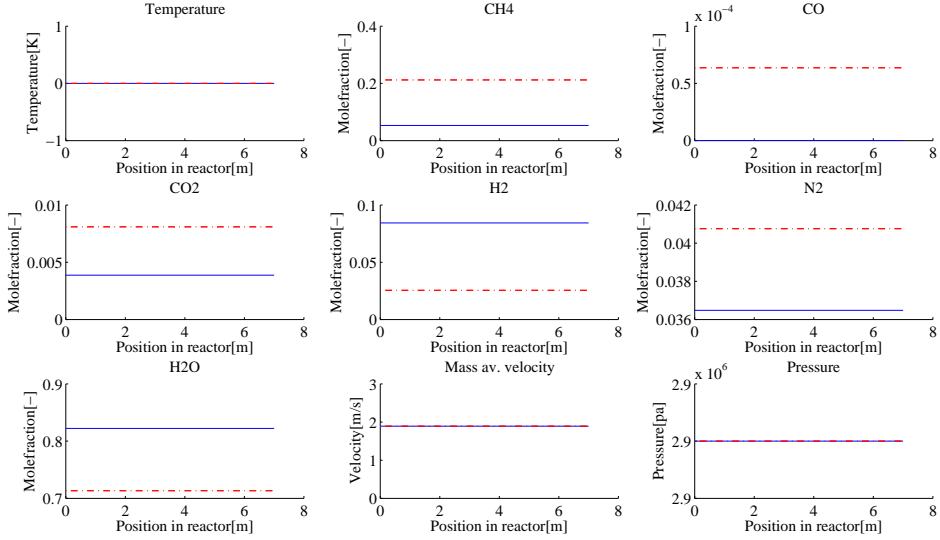
Figure 30: Visualization of the initial(blue (—)) and boundary(red (-.-.-)) conditions used in the simulation, the boundary conditions are stipulated through the reactor for convenience.
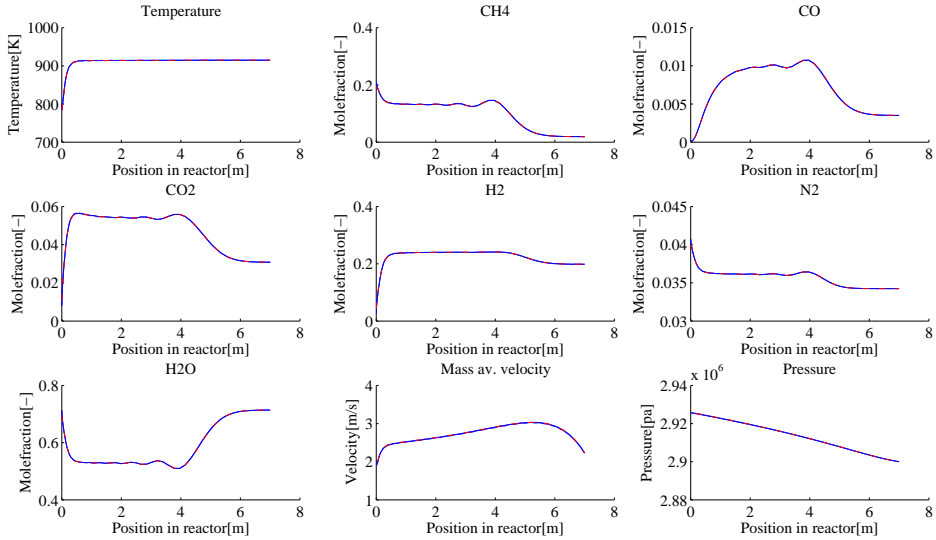
Figure 31: Comparison of the least squares method(red (- - -)) and the orthogonal collocation method(blue (—)) using 60 collocation points and a time step of 0.1 seconds. This is the simulated behavior two seconds after reaction initialization.
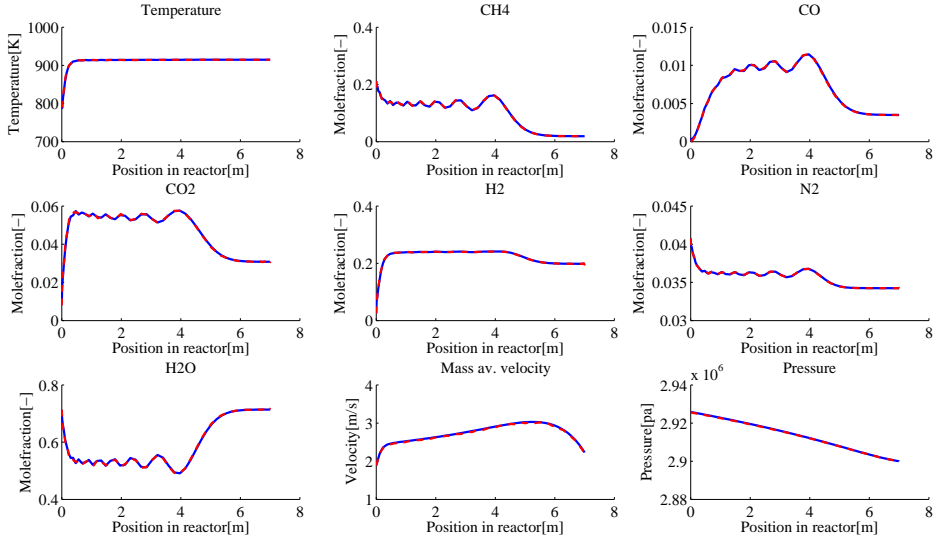
Figure 32: Comparison of the least squares method(red (- - -)) and the orthogonal collocation method(blue (—)) using 60 collocation points and a time step of 0.1 seconds. The dispersion rate are artificially reduced by a factor of 100. This is the simulated behavior two seconds after reaction initialization.
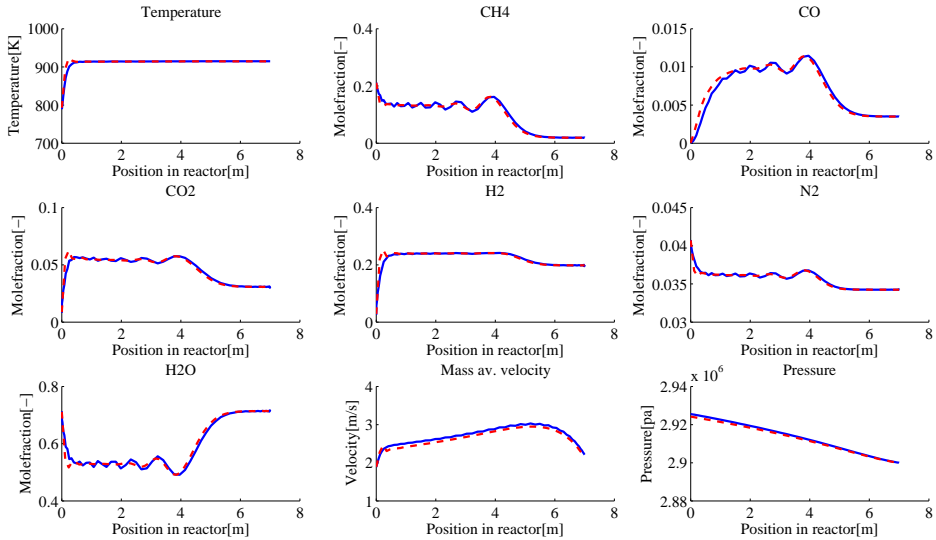
Figure 33: Comparison of the least squares method using 60 collocation points(blue (—)) vs 30 elements and 3 points(red (- - -)) in each with a time-step of 0.1 seconds. The dispersion rate are artificially reduced by a factor of 100. This is the simulated behavior two seconds after reaction initialization.

10 Conclusions and closing remarks

10.1 Steam methane reforming - pellet models

10.1.1 Wilke and Wilke-Bosanquet models

The Wilke and Wilke-Bosanquet diffusion models are simplified versions of the Maxwell-Stefan and dusty gas diffusion models, respectively. Based on the obtained results they are unable to yield identical results even when the models are fully comprehensive.

The Wilke diffusion model on both formulations, were however able to obtain comparable results to the Maxwell-Stefan diffusion model if the scaled results from the alternative Wilke method was used. The reliability and use of these scaled results are however questionable and is not recommended. The Wilke-Bosanquet model were not compared to the dusty gas model in the same manner.

Furthermore the Wilke diffusion model was only seen to be 5% faster than the Maxwell-Stefan diffusion model, meaning that the speed difference between these models are insignificant.

10.1.2 Maxwell-Stefan and dusty gas models

When using the more rigorous Maxwell-Stefan and dusty gas diffusion models identical results were obtained. However, this was only possible if the convective terms were included for the mole based formulation. Based on the results in the thesis it is important to differentiate between the convective terms on the different formulations, since they are proven not to be comparable. The mass based convective terms are negligible, but the mole based convective terms are not.

If convective flow was to be assumed negligible on both formulations, it would be possible to counteract most of the accuracy loss by replacing most of the convective terms in the species mole balance with the LHS of the mole based continuity equation. The last neglected convective term in the species mole balance would still yield some accuracy loss. The use of the continuity equation in the species balance are however optional if the convective terms are included and no performance gain nor accuracy loss was seen for either of the implementation methods.

The same problem arises for the dusty gas diffusion model since a convective term is included in the diffusion model. As for the species balance this term will be negligible on mass basis but not on mole basis.

For the Maxwell-Stefan model the method of transforming the model equations to a dimensionless form was also investigated. The chosen method was proven to be optional, but the traditional method using constant reference values is recommended, since it yields less troublesome implementations of the equations.

10.2   Numerical methods and performance

10.2.1   Diffusion dominated problems - Pellet model

The orthogonal collocation method is superior to the least squares method when considering a diffusion dominated problem. Both methods yields accurate and identical results apart from some insignificant numerical differences. However, the orthogonal collocation method uses only 33% of the simulation time compared to the least squares method under optimized circumstances for both methods. The orthogonal collocation method is also more robust since it is unaffected by the variable sequence in the problem matrix.

The diffusion dominated problems were also further improved performance-wise by the use of pulse iteration, and a decrease in simulation time by up to 76% was obtained.

10.2.2   Convective dominated problems

For the convective dominated problems the methods continue to yield accurate and identical results as proven in the reactor model. However here the least squares method will prove to be superior in the terms of performance as it only uses 25% of the simulation time to obtain the same results. By artificial reduction of the diffusion these performance differences continue to grow.

Identical results are also seen for the advection equation when the numerical methods are implemented as spectral methods. However, if the methods where to be optimized by the use of elements, it would become a requirement to use the least squares method, as the orthogonal collocation method would oscillate and under some circumstances be unable to converge properly.

10.3   General recommendations for building a pellet model

When building a steam methane reforming pellet model it is recommended to use a rigorous diffusion model, i.e. Maxwell-Stefan or the dusty gas diffusion model. Also the mass based formulation is recommended since the model is easier to implement and overall faster than the mole based formulation. Based on the results obtained in the thesis it is safe to assume no mass averaged velocity and pressure changes.

To solve the problem the numerical method of orthogonal collocation is recommended since it is the fastest method for diffusion dominated problems.

Bibliography

[1] Hugo A. Jakobsen. Solution of simple model problems to illustrate the least squares method of implementation. *NTNU*, 2011.

[2] Jannike Solsvik and Hugo A. Jakobsen. Modeling of multicomponent mass diffusion in porous spherical pellets: Application to steam methane reforming and methanol synthesis. *Chemical Engineering Science*, 66:1986–2000, 2011.

[3] Hugo A. Jakobsen. *Chemical Reactor Modeling: Multiphase Reactive Flows.* Springer, 2008.

[4] Gilbert F. Froment Jianguo Xu. Methane steam reforming, methanation and water-gas shift: I. intrinsic kinetics. *AIChE Journal*, 35:88–96, 1989.

[5] C.R. Wilke. Modeling of multicomponent mass diffusion in porous spherical pellets: Application to steam methane reforming and methanol synthesis. *Chem. Eng. Prog.*, 46:95–104, 1950.

[6] J.C. Maxwell. On the dynamical theory of gases. *Philos. Trans R. Soc*, 157:49–88, 1866.

[7] J. Stefan. Über das gleichgewicht und die bewegung insbesondere die diffusion von gasgemengden. *Sitszber, Akad. Wiss. Wien 63*, pages 63–124, 1871.

[8] C.H. Bosanquet. British ta report br-507. 1944.

[9] R. Jackson. Transport in porous catalysts. *Elsevier*, 1977.

[10] E.A. Mason and A.P Malinauskas. Gas transport in porous media: The dusty gas model. *Elsevier*, 1983.

[11] Bruce E. Poling, John M. Prausnitz, and John P. O'Connell. *The properties of gases and liquids.* McGraw-Hill, New York, USA, 2001.

[12] Cheng Huang Deqiang Mu, Zhong-Sheng Liu and Ned Djilali. Determination of the effective diffusion coefficient in porous media including knudsen effects. *Microfluidics and Nanofluidics*, 4:257–260, 2008.

[13] J. M. Smith. *Chemical Engineering Kintetics.* McGraw-Hill, 1981.

[14] R. Byron Bird, Warrend E. Steward, and Edwin N.Lightfoot. *Transport Phenomena.* John Wiley and Sons, 2007.

[15] R. Krishna. Problems and pitfalls in the use of the fick formulation for intraparticle diffusion. *Chem. Eng. Sci.*, 48:845–961, 1993.

[16] Ross Taylor and R. Krishna. *Multicomponent mass transfer.* Wiley, New York, USA, 1993.

A 2 Theory - Derivation of governing equations

The basic governing equations used in this thesis are to be derived from general governing equations. This is done to make the derivation for each case shorter and more specific. During the deduction of these basic equations the different terms are also explained. For all equations the divergence needs to be specified in spherical coordinates for both a vector and a scalar. These equations can be defined respectively as:

$$\nabla \cdot \vec{v} = \frac{1}{\xi^2} \frac{\partial}{\partial \xi}(\xi^2 v_\xi) + \frac{1}{\xi^2 \sin\theta} \frac{\partial}{\partial \theta}(v_\theta \sin\theta) + \frac{1}{\xi^2 \sin\theta} \frac{\partial v_\phi}{\partial \phi} \tag{A.1}$$

$$\nabla \cdot s = \frac{\partial s}{\partial \xi}\hat{e}_i + \frac{1}{\xi}\frac{\partial s}{\partial \theta}\hat{e}_j + \frac{1}{\xi \sin\theta}\frac{\partial s}{\partial \phi}\hat{e}_k \tag{A.2}$$

These equations can be further simplified for this thesis. The catalyst particle is assumed to be spherical, so it is reasonable to assume symmetry around the center of the particle - i.e., no change when changing the inclination angle θ or the azimuth angle ϕ. Hence the derivatives in θ and ϕ may be dis-considered. As a result the divergence of a vector and scalar in this thesis will be given respectively as:

$$\nabla \cdot \vec{v} = \frac{1}{\xi^2} \frac{\partial}{\partial \xi}(\xi^2 v_\xi) \tag{A.3}$$

$$\nabla \cdot s = \frac{\partial s}{\partial \xi}\hat{e}_i \tag{A.4}$$

A.1 Mass based basic governing equations

A.1.1 Species mass balance

Differential equations describing the change in mass fractions for the different components in radial direction within the catalyst pellets are to be derived. The different terms are explained in table A.1, and general species mass balance for a component i is given as:

$$\frac{\partial}{\partial t}(\rho\omega_i) + \nabla \cdot (\rho\omega_i v) = -\nabla \cdot (j_i) + R_i \qquad (A.5)$$

Table A.1: Explanation of the different terms in the species mass balance

$\frac{\partial}{\partial t}(\rho\omega_i)$	Represents the change in density for each species i with time
$\nabla \cdot (\rho\omega_i v)$	Represents the convective transport
$\nabla \cdot (j_i)$	Represents the diffusional transport
R_i	Represents the reaction rate

Introducing the divergence of a vector (A.3) for both the diffusional and convective term gives the simplified species mass balance:

$$\frac{\partial}{\partial t}(\rho\omega_i) + \frac{1}{\xi^2}\frac{\partial}{\partial \xi}(\xi^2 \rho\omega_i v_\xi) = -\frac{1}{\xi^2}\frac{\partial}{\partial \xi}(\xi^2 j_i) + R_i \qquad (A.6)$$

A.1.2 The continuity equation

A simplified equation for the continuity equation is to be derived. The terms are explained in table A.2. The governing continuity equation on mass basis can be defined as:

$$\frac{\partial \rho}{\partial t} + \nabla \cdot (\rho v) = 0 \tag{A.7}$$

Table A.2: Explanation of the terms in the general continutity equation

$\dfrac{\partial \rho}{\partial t}$	Represents the change of density with time
$\nabla \cdot (\rho v)$	Represents the change of mass or moles in the control volume

Introducing the divergence of a vector (A.3) for the second term gives the simplified mass based continuity equation:

$$\frac{\partial \rho}{\partial t} + \frac{1}{\xi^2}\frac{\partial}{\partial \xi}(\xi^2 \rho v_\xi) = 0 \tag{A.8}$$

A.1.3   Temperature equation

A differential equation describing the radial temperature profile within the catalyst particles is to be derived. The contributions from the different terms in the general energy equation are explained in table A.3. The general governing energy equation can be given as:

$$\left((1-\epsilon)\rho_p Cp_p + \epsilon\rho \sum_{i=1}^{n} \omega_i Cp_i\right)\frac{\partial T}{\partial t} + \rho \sum_{i=1}^{n} \omega_i Cp_i v \, \nabla \cdot T = -\nabla \cdot q + (-\triangle H_R)R + Q$$

(A.9)

Table A.3: Explanation of the terms in the general energy equation

$\left((1-\epsilon)\rho_p Cp_p + \epsilon\rho \sum_{i=1}^{n} \omega_i Cp_i\right)\frac{\partial T}{\partial t}$	Represents the change of heat content with time
$\rho \sum_{i=1}^{n} \omega_i Cp_i v \, \nabla \cdot T$	Represents the advective transport
$\nabla \cdot q$	Represents the heat transport by conduction
$(-\triangle H_R)R$	Represents the heat from chemical reactions
Q	Represents the radiation heat flux

The radiation heat flux is not considered in the next parts of deriving a simplified energy equation. Introducing the divergence of a scalar (A.4) for the advective term and the divergence of a vector (A.3) for the conduction term gives the simplified energy equation on mass form:

$$\left((1-\epsilon)\rho_p Cp_p + \epsilon\rho \sum_{i=1}^{n} \omega_i Cp_i\right)\frac{\partial T}{\partial t} + \rho \sum_{i=1}^{n} \omega_i Cp_i v \frac{\partial T}{\partial \xi} = -\frac{1}{\xi^2}\frac{\partial}{\partial \xi}(\xi^2 q) + (-\triangle H_R)R$$

(A.10)

A.2 Mass based diffusion models

The general diffusion models are only modified from their original state given in table A.4 by introducing the simplified divergence for the pellet and introducing the effective binary and Knudsen diffusitivies as shown in the theory chapter 2.2.2. This is however not shown, but the diffusion models are represented with the simplified divergences and effective diffusivities included on a dimensionless form in table A.10.

Table A.4: Mass based diffusion models, standard form

Wilke

$$j_i = -\rho D_{im} \nabla \omega_i \qquad D_{im} = \frac{1 - \omega_i}{\overline{M} \sum_{\substack{j=1 \\ j \neq i}}^{n} \frac{\omega_j}{M_j D_{ij}}} \qquad (A.11)$$

Wilke–Bosanquet

$$j_i = -\rho D_{i,eff} \nabla \omega_i \qquad \frac{1}{D_{i,eff}} = \frac{1}{D_{im}} + \frac{1}{D_{iK}} \qquad (A.12)$$

Maxwell-Stefan

$$j_i = \frac{-\rho \omega_i \nabla ln(\overline{M}) - \rho \nabla \omega_i + \overline{M} \omega_i \sum_{\substack{j=1 \\ j \neq i}}^{n} \frac{j_j}{M_j D_{ij}}}{\overline{M} \sum_{\substack{j=1 \\ j \neq i}}^{i} \frac{\omega_j}{M_j D_{ij}}} \qquad (A.13)$$

Dusty gas

$$j_i = \frac{M^2 \sum_{\substack{j=1 \\ j \neq i}}^{n} \frac{\omega_i j_j}{M_j D_{ij}} - \frac{v \rho_i M}{D_{iK}} - \rho(\omega_i \nabla M + M \nabla \omega_i)}{M^2 \sum_{\substack{j=1 \\ j \neq i}}^{n} \frac{\omega_j}{M_j D_{ij}} + \frac{M}{D_{iK}}} \qquad (A.14)$$

A.3   Mole based basic governing equations

A.3.1   Species mole balance

Differential equations describing the change in mole fractions for the different components in radial direction within the catalyst pellets are to be derived. The different terms are explained in table A.5, and general species mole balance for a component i is given as:

$$\frac{\partial}{\partial t}(cx_i) + \nabla \cdot (cx_i u) = -\nabla \cdot (J_i) + R'_i \tag{A.15}$$

Table A.5: Explanation of the different terms in the species mass balance

$\frac{\partial}{\partial t}(cx_i)$	Represents the change in concentration for the different species i with time
$\nabla \cdot (cx_i u)$	Represents the convective transport
$\nabla \cdot (J_i)$	Represents the diffusional transport
R'_i	Represents the reaction rate

Introducing the divergence of a vector (A.3) for both the diffusional and convective term gives the simplified species mole balance:

$$\frac{\partial}{\partial t}(cx_i) + \frac{1}{\xi^2}\frac{\partial}{\partial \xi}(\xi^2 cx_i u_\xi) = -\frac{1}{\xi^2}\frac{\partial}{\partial \xi}(\xi^2 J_i) + R'_i \tag{A.16}$$

A.3.2 The continuity equation

A simplified equation for the continuity equation is to be derived. The terms are explained in table A.6. The governing continuity equation on mole basis can be defined as:

$$\frac{\partial c}{\partial t} + \nabla \cdot (cu) = \sum_{i=1}^{n} R_i' \tag{A.17}$$

Table A.6: Explanation of the terms in the general continutity equation

$\dfrac{\partial c}{\partial t}$	Represents the change of concentration with time
$\nabla \cdot (cu)$	Represents the change of moles in the control volume
$\displaystyle\sum_{i=1}^{n} R_i'$	Represents the sum of the reactions(mole generation rate)

Introducing the divergence of a vector (A.3) for the second term gives the simplified mole based continuity equation:

$$\frac{\partial c}{\partial t} + \frac{1}{\xi^2} \frac{\partial}{\partial \xi} (\xi^2 c u_\xi) = \sum_{i=1}^{n} R_i' \tag{A.18}$$

A.3.3 Temperature equation

A differential equation describing the radial temperature profile within the catalyst particles is to be derived. The contributions from the different terms in the general energy equation are explained in table A.7. The general governing energy equation can be given as:

$$((1-\epsilon)\rho_p Cp_p + \epsilon\rho\sum_{i=1}^{n}x_i Cp_i')\frac{\partial T}{\partial t} + c\sum_{i=1}^{n}x_i Cp_i' v\nabla T = -\nabla\cdot q + (-\triangle H_R)R + Q$$

$$(A.19)$$

Table A.7: Explanation of the terms in the general energy equation

$((1-\epsilon)\rho_p Cp_p + \epsilon\rho\sum_{i=1}^{n}x_i Cp_i')\frac{\partial T}{\partial t}$	Represents the change of heat content with time
$c\sum_{i=1}^{n}x_i Cp_i' v\nabla T$	Represents the advective transport
∇q	Represents the heat transport by conduction
$(-\triangle H_R)R$	Represents the heat from chemical reactions
Q	Represents the radiation heat flux

The radiation heat flux is not considered further as it is not needed. Introducing the divergence of a scalar (A.4) for the advective term and the divergence of a vector (A.3) for the conduction term gives the simplified energy equation on mole basis:

$$((1-\epsilon)\rho_p Cp_p + \epsilon c\sum_{i=1}^{n}x_i Cp_i')\frac{\partial T}{\partial t} + c\sum_{i=1}^{n}x_i Cp_i' v\frac{\partial T}{\partial \xi} = -\frac{1}{\xi^2}\frac{\partial}{\partial \xi}(\xi^2 q) + (-\triangle H_R)R$$

$$(A.20)$$

A.4   Mole based diffusion models

The general diffusion models are only modified from their original state given in table A.8 by introducing the simplified divergence for the pellet and introducing the effective binary and Knudsen diffusitivies as shown in the theory chapter 2.2.2. This is however not shown, but the diffusion models are represented with the simplified divergences and effective diffusivities included on a dimensionless form in table A.11.

Table A.8: Mole based diffusion models, standard form

Wilke

$$j_i = -cD'_{im} \nabla \cdot x_i \qquad D'_{im} = \frac{1 - x_i}{\sum_{\substack{j=1 \\ j \neq i}}^{n} \frac{x_j}{D_{ij}}} \tag{A.21}$$

Wilke–Bosanquet

$$j_i = -cD'_{i,eff} \nabla \cdot x_i i \qquad \frac{1}{D'_{i,eff}} = \frac{1}{D'_{im}} + \frac{1}{D_{iK}} \tag{A.22}$$

Maxwell-Stefan

$$j_i = \frac{-cx_i + \sum_{\substack{j=1 \\ j \neq i}}^{n} \frac{j_j x_i}{D_{ij}}}{\sum_{\substack{j=1 \\ j \neq i}}^{i} \frac{x_j}{D_{ij}}} \tag{A.23}$$

Dusty gas

$$j_i = \frac{\sum_{\substack{j=1 \\ j \neq i}}^{n} \frac{j_j x_i}{D_{ij}} - \frac{c_i u}{D_{iK}} - c\nabla x_i}{\sum_{\substack{j=1 \\ j \neq i}}^{i} \frac{x_j}{D_{ij}} + \frac{1}{D_{iK}}} \tag{A.24}$$

A.5   Supportive equations

The equations needed to complete the model equations are presented here.

A.5.1   Mass based flux-velocity conversion[14]

Optional equation, only included for comparing the obtained velocities from the continuity equations.

$$j_i = \rho_i(u_i - v) \tag{A.25}$$

$$u - v = \sum_{i=1}^{N} x_i(u_i - v) \tag{A.26}$$

$$\omega_i = \frac{x_i M_i}{\overline{M}} \tag{A.27}$$

Inserting the first into the second:

$$u - v = \sum_{i=1}^{N} \frac{x_i j_i}{\rho_i} \tag{A.28}$$

writing out ρ_i as $\omega_i \rho$ and using equation A.27, gives the conversion equation:

$$u - v = \sum_{i=1}^{N} \frac{j_i \overline{M}}{\rho M_i} \tag{A.29}$$

A.5.2   Mole based flux-velocity conversion[14]

This is an important equation for the mole based models as the mass averaged velocity is needed for the temperature equation and Darcy's Law.

$$J_i = c_i(u_i - u) \tag{A.30}$$

$$v - u = \sum_{i=1}^{N} \omega_i(u_i - u) \tag{A.31}$$

$$x_i = \frac{\omega_i \overline{M}}{M_i} \tag{A.32}$$

Inserting the first into the second:

$$v - u = \sum_{i=1}^{N} \omega_i \frac{J_i}{c_i} \tag{A.33}$$

$$\tag{A.34}$$

writing out c_i as $x_i c$ and using equation A.32 gives the conversion equation:

$$v - u = \sum_{i=1}^{N} \frac{J_i M_i}{c_i \overline{M}} \tag{A.35}$$

A.5.3   Ideal gas law

Different versions of the ideal gas law is used for the different cases. The standard is used for concentration:

$$pV = nRT$$
$$\frac{p}{RT} = c \tag{A.36}$$

multiplied with moleweight gives the density equation used:

$$\frac{p\overline{M}}{RT} = \rho \tag{A.37}$$

A.5.4   Darcy's law[15]

$$v = -\frac{B}{\mu}\frac{\partial p}{\partial \xi} \qquad B = \frac{\epsilon}{\tau}\frac{d_0^2}{32} \tag{A.38}$$

A.5.5   Constitutive laws[14]

for mass based models:

$$\sum_{i=1}^{n} j_i = 0 \tag{A.39}$$

$$\sum_{i=1}^{n} \omega_i = 1 \tag{A.40}$$

for mole based models:

$$\sum_{i=1}^{n} J_i = 0 \tag{A.41}$$

$$\sum_{i=1}^{n} x_i = 1 \tag{A.42}$$

A.5.6   Viscosity and heat capacities

These variables are obtained from the equations given in the properties of liquids and gases[11]. However these equations are considered less important in the thesis as the same equations are used for both the mass and mole based models, and will not yield any difference for the models.

A.6 Transforming the simplified equations to the dimensionless form

The simplified general equations are made dimensionless using the correlations in table A.9. By using these correlations in the simplified equations we will acquire the basic dimensionless equations used in this thesis.

Table A.9: Correlations used to make the equations dimensionless

$$\xi^* = \frac{\xi}{\xi_{ref}} \quad \text{(A.43)} \qquad u^* = \frac{u}{u_{ref}} \quad \text{(A.44)} \qquad q^* = \frac{q_\xi \xi_{ref}}{\lambda T_{ref}} \quad \text{(A.45)}$$

$$u_{ref} = \frac{Dref}{\xi_{ref}} \quad \text{(A.46)} \qquad p^* = \frac{p}{p_{ref}} \quad \text{(A.47)} \qquad \rho^* = \frac{\rho}{\rho_{ref}} \quad \text{(A.48)}$$

$$c^* = \frac{c}{c_{ref}} \quad \text{(A.49)} \qquad j^* = \frac{j}{\frac{D_{ref}\rho_{ref}}{\xi_{ref}}} \quad \text{(A.50)} \qquad J^* = \frac{J}{\frac{D_{ref}c_{ref}}{\xi_{ref}}} \quad \text{(A.51)}$$

$$t^* = \frac{t}{\frac{\xi_{ref}^2}{Dref}} \quad \text{(A.52)} \qquad M_w^* = \frac{M_w}{M_{ref}} \quad \text{(A.53)} \qquad T^* = \frac{T}{T_{ref}} \quad \text{(A.54)}$$

A.7 Summary of the dimensionless equations on mole and mass basis

The general dimensionless basis equations used for all the pellet models are given in table A.10 for the mass based models and table A.11 for the mole based models.

Table A.10: Mass based model equations on dimensionless form

Species mass balance:

$$\frac{\partial}{\partial t^*}(\rho^*\omega_i) + \frac{1}{\xi^{*2}}\frac{\partial}{\partial \xi^*}(\xi^{*2}\rho^*\omega_i v_\xi^*) = -\frac{1}{\xi^{*2}}\frac{\partial}{\partial \xi^*}(\xi^{*2}j_i^*) + R_i\frac{\xi_{ref}^2}{D_{ref}\rho_{ref}} \qquad (A.55)$$

The basic dimensionless temperature equation:

$$((1-\epsilon)\rho_p Cp_p + \epsilon\rho^*\rho_{ref}\sum_{i=1}^{n}\omega_i Cp_i)\frac{\partial T^*}{\partial t^*} =$$

$$-\rho^*\rho_{ref}v_r^*\sum_{i=1}^{n}\omega_i Cp_i\frac{\partial T^*}{\partial \xi^*} - \frac{(\frac{2q^*}{\xi^*} + \frac{\partial q^*}{\partial \xi^*})\lambda}{D_{ref}} + \frac{\xi_{ref}^2(-\triangle H_R)R}{D_{ref}T_{ref}} \qquad (A.56)$$

The basic dimensionless continuity equation:

$$\frac{\partial \rho^*}{\partial t^*} + \frac{1}{\xi^{*2}}\frac{\partial}{\partial \xi^*}(\xi^{*2}\rho^* v^*) = 0 \qquad (A.57)$$

Wilke diffusion model:

$$j_i^* = -\rho^*\frac{D_{im}}{D_{ref}}\frac{\partial \omega_i}{\partial \xi^*} \qquad D_{im} = \frac{1-\omega_i}{\overline{M}\sum_{\substack{j=1\\j\neq i}}^{n}\frac{\omega_j}{M_j D_{ij}^e}} \qquad (A.58)$$

Wilke–Bosanquet diffusion model:

$$j_i^* = -\rho^*\frac{D_{i,eff}}{D_{ref}}\frac{\partial \omega_i}{\partial \xi^*} \qquad \frac{1}{D_{i,eff}} = \frac{1}{D_{im}} + \frac{1}{D_{iK}} \qquad (A.59)$$

Maxwell-Stefan diffusion model:

$$j_i^* = \frac{\frac{-\rho^*\omega_i}{D_{ref}}\frac{1}{\overline{M}}\frac{\partial \overline{M}}{\partial \xi^*} - \frac{\rho^*}{D_{ref}}\frac{\partial \omega_i}{\partial \xi^*} + \overline{M}\omega_i\sum_{\substack{j=1\\j\neq i}}^{n}\frac{j_j^*}{M_j D_{ij}^e}}{\overline{M}\sum_{\substack{j=1\\j\neq i}}^{i}\frac{\omega_j}{M_j D_{ij}^e}} \qquad (A.60)$$

Dusty gas diffusion model:

$$j_i^* = \frac{\overline{M}^2\sum_{\substack{j=1\\j\neq i}}^{n}\frac{\omega_i j_j^*}{M_j D_{ij}^e} - \frac{v^*\omega_i\overline{M}}{D_{iK}^e} - \frac{\omega_i\rho^*}{D_{ref}}\frac{\partial \overline{M}}{\partial \xi^*} - \frac{\rho^*\overline{M}}{D_{ref}}\frac{\partial \omega_i}{\partial \xi^*}}{\overline{M}^2\sum_{\substack{j=1\\j\neq i}}^{n}\frac{\omega_j}{M_j D_{ij}^e} + \frac{\overline{M}}{D_{iK}^e}} \qquad (A.61)$$

Table A.11: Mole based model equations on dimensionless form

Species mole balance:

$$\frac{\partial}{\partial t^*}(c^* x_i) + \frac{1}{\xi^{*2}} \frac{\partial}{\partial \xi^*}(\xi^{*2} c^* x_i u_\xi^*) = -\frac{1}{\xi^{*2}} \frac{\partial}{\partial \xi^*}(\xi^{*2} J_i^*) + R_i' \frac{\xi_{ref}^2}{D_{ref} c_{ref}} \qquad (A.62)$$

The basic dimensionless temperature equation:

$$((1-\epsilon)\rho_p Cp_p + \epsilon c^* c_{ref} \sum_{i=1}^{n} x_i Cp_i') \frac{\partial T^*}{\partial t^*} =$$

$$-c^* c_{ref} v_r^* \sum_{i=1}^{n} x_i Cp_i' \frac{\partial T^*}{\partial \xi^*} - \frac{(\frac{2q^*}{\xi^*} + \frac{\partial q^*}{\partial \xi^*})\lambda}{D_{ref}} + \frac{\xi_{ref}^2 (-\triangle H_R) R}{D_{ref} T_{ref}} \qquad (A.63)$$

The basic dimensionless continuity equation:

$$\frac{\partial c^*}{\partial t^*} + \frac{1}{\xi^{*2}} \frac{\partial}{\partial \xi^*}(\xi^{*2} c^* u_\xi^*) = (\frac{\xi_{ref}^2}{c_{ref} D_{ref}}) \sum_{i=1}^{n} R_i' \qquad (A.64)$$

Wilke diffusion model:

$$J_i^* = -c^* \frac{D_{im}'}{D_{ref}} \frac{\partial x_i}{\partial \xi^*} \qquad D_{im}' = \frac{1-x_i}{\sum_{\substack{j=1 \\ j \neq i}}^{n} \frac{x_j}{D_{ij}^e}} \qquad (A.65)$$

Wilke–Bosanquet diffusion model:

$$J_i^* = -c^* \frac{D_{i,eff}'}{D_{ref}} \frac{\partial x_i}{\partial \xi^*} \qquad \frac{1}{D_{i,eff}'} = \frac{1}{D_{im}'} + \frac{1}{D_{iK}^e} \qquad (A.66)$$

Maxwell-Stefan diffusion model:

$$J_i^* = \frac{-\frac{c^*}{D_{ref}} \frac{\partial x_i}{\partial \xi^*} + \sum_{\substack{j=1 \\ j \neq i}}^{n} \frac{J_j^* x_i}{D_{ij}^e}}{\sum_{\substack{j=1 \\ j \neq i}}^{i} \frac{x_j}{D_{ij}^e}} \qquad (A.67)$$

Dusty gas diffusion model:

$$J_i^* = \frac{-\frac{c^*}{D_{ref}} \frac{\partial x_i}{\partial \xi^*} + \sum_{\substack{j=1 \\ j \neq i}}^{n} \frac{J_j^* x_i}{D_{ij}^e} - \frac{c^* x_i u^*}{D_{iK}^e}}{\sum_{\substack{j=1 \\ j \neq i}}^{i} \frac{x_j}{D_{ij}^e} + \frac{1}{D_{iK}^e}} \qquad (A.68)$$

B 3 Models on their simplest forms

In this appendix the equations needed for the pellet model on its simplest form will be derived on both mass and mole basis. Also some additional results are presented here to give a complete overview of the simulation.

B.1 Mass based model derivation

As this is the simplest model, it will only be necessary to derive an equation for the temperature balance and the species mass balance. The respective fluxes will be calculated with the Fourier's law and the diffusion models.

B.1.1 The temperature balance

The general temperature balance derived earlier (A.56):

$$
((1-\epsilon)\rho_p Cp_p + \epsilon\rho^*\rho_{ref}\sum_{i=1}^{n}\omega_i Cp_i)\frac{\partial T^*}{\partial t^*} =
$$
$$
-\rho^*\rho_{ref}v_r^*\sum_{i=1}^{n}\omega_i Cp_i\frac{\partial T^*}{\partial\xi^*} - \frac{(\frac{2q^*}{\xi^*}+\frac{\partial q^*}{\partial\xi^*})\lambda}{D_{ref}} + \frac{\xi_{ref}^2(-\triangle H_R)R}{D_{ref}T_{ref}}
$$
(B.1)

Steady state is assumed:

$$
0 = -\rho^*\rho_{ref}v_r^*\sum_{i=1}^{n}\omega_i Cp_i\frac{\partial T^*}{\partial\xi^*} - \frac{(\frac{2q^*}{\xi^*}+\frac{\partial q^*}{\partial\xi^*})\lambda}{D_{ref}} + \frac{\xi_{ref}^2(-\triangle H_R)R}{D_{ref}T_{ref}}
$$
(B.2)

no convective transport is assumed:

$$
0 = -\frac{(\frac{2q^*}{\xi^*}+\frac{\partial q^*}{\partial\xi^*})\lambda}{D_{ref}} + \frac{\xi_{ref}^2(-\triangle H_R)R}{D_{ref}T_{ref}}
$$
(B.3)

The equation is rearranged and the used equation is given as:

$$
\frac{2q^*}{\xi^*} + \frac{\partial q^*}{\partial\xi^*} = \frac{\xi_{ref}^2(-\triangle H_R)R}{T_{ref}\lambda}
$$
(B.4)

B.1.2 Species mass balance

The mass based fluxes are obtained from the species mass balance. The general dimensionless equation is given as derived earlier (A.55):

$$
\frac{\partial}{\partial t^*}(\rho^*\omega_i) + \frac{1}{\xi^{*2}}\frac{\partial}{\partial\xi^*}(\xi^{*2}\rho^*\omega_i v_\xi^*) = -\frac{1}{\xi^{*2}}\frac{\partial}{\partial\xi^*}(\xi^{*2}j_i^*) + R_i\frac{\xi_{ref}^2}{D_{ref}\rho_{ref}}
$$
(B.5)

Steady state is assumed.

$$
\frac{1}{\xi^{*2}}\frac{\partial}{\partial\xi^*}(\xi^{*2}\rho^*\omega_i v_\xi^*) = -\frac{1}{\xi^{*2}}\frac{\partial}{\partial\xi^*}(\xi^{*2}j_i^*) + R_i\frac{\xi_{ref}^2}{D_{ref}\rho_{ref}}
$$
(B.6)

The first term is written out to identify the continuity equation.

$$\frac{1}{\xi^{*2}}\frac{\partial \omega_i}{\partial \xi^*}(\xi^{*2}\rho^* v_\xi^*) + \omega_i \frac{1}{\xi^{*2}}\frac{\partial}{\partial \xi^*}(\xi^{*2}\rho^* v_\xi^*) = -\frac{1}{\xi^{*2}}\frac{\partial}{\partial \xi^*}(\xi^{*2}j_i^*) + R_i \frac{\xi_{ref}^2}{D_{ref}\rho_{ref}} \quad (B.7)$$

The second term is identified as the LHS of the mass based continuity equation (A.57) when steady state is assumed, swapped for the RHS of the mass based continuity equation gives:

$$\frac{1}{\xi^{*2}}\frac{\partial \omega_i}{\partial \xi^*}(\xi^{*2}\rho^* v_\xi^*) = -\frac{1}{\xi^{*2}}\frac{\partial}{\partial \xi^*}(\xi^{*2}j_i^*) + R_i \frac{\xi_{ref}^2}{D_{ref}\rho_{ref}} \quad (B.8)$$

No convective transport is assumed, and the equation is rearranged:

$$\frac{1}{\xi^{*2}}\frac{\partial}{\partial \xi^*}(\xi^{*2}j_i^*) = R_i \frac{\xi_{ref}^2}{D_{ref}\rho_{ref}} \quad (B.9)$$

The first term is expanded to reflect the implemented equation:

$$\frac{2j_i^*}{\xi^*} + \frac{\partial j_i^*}{\partial \xi^*} = R_i \frac{\xi_{ref}^2}{D_{ref}\rho_{ref}} \quad (B.10)$$

B.1.3 Wilke diffusion model

The general Wilke diffusion model as given in (A.58):

$$j_i^* = -\rho^* \frac{D_{im}}{D_{ref}}\frac{\partial \omega_i}{\partial \xi^*} \qquad D_{im} = \frac{1-\omega_i}{\overline{M}\sum_{\substack{j=1 \\ j\neq i}}^{n}\frac{\omega_j}{M_j D_{ij}^e}} \quad (B.11)$$

Rearranged to the implemented form:

$$j_i^* \frac{D_{ref}}{D_{im}\rho^*} + \frac{\partial \omega_i}{\partial \xi^*} = 0 \qquad D_{im} = \frac{1-\omega_i}{\overline{M}\sum_{\substack{j=1 \\ j\neq i}}^{n}\frac{\omega_j}{M_j D_{ij}^e}} \quad (B.12)$$

B.1.4 Wilke-Bosanquet diffusion model

$$j_i^* = -\rho^* \frac{D_{i,eff}}{D_{ref}}\frac{\partial \omega_i}{\partial \xi^*} \qquad \frac{1}{D_{i,eff}} = \frac{1}{D_{im}} + \frac{1}{D_{iK}^e} \quad (B.13)$$

Rearranged to the implemented form:

$$j_i^* \frac{D_{ref}}{D_{i,eff}'\rho^*} + \frac{\partial \omega_i}{\partial \xi^*} = 0 \qquad \frac{1}{D_{i,eff}'} = \frac{1}{\frac{1-\omega_i}{\overline{M}\sum_{\substack{j=1 \\ j\neq i}}^{n}\frac{\omega_j}{M_j D_{ij}^e}}} + \frac{1}{D_{iK}^e} \quad (B.14)$$

B.1.5 Maxwell-Stefan diffusion model

The general Maxwell-Stefan model as given in (A.60):

$$j_i^* = \frac{\frac{-\rho^* \omega_i}{D_{ref}} \frac{1}{\overline{M}} \frac{\partial}{\partial \xi^*}(\overline{M}) - \frac{\rho^*}{D_{ref}} \frac{\partial \omega_i}{\partial \xi^*} + \overline{M} \omega_i \sum_{\substack{j=1 \\ j \neq i}}^{n} \frac{j_j^*}{M_j D_{ij}^e}}{\overline{M} \sum_{\substack{j=1 \\ j \neq i}}^{i} \frac{\omega_j}{M_j D_{ij}^e}} \tag{B.15}$$

Rearranged to the implemented form:

$$j_i^* \frac{\overline{M} D_{ref}}{\rho^*} \sum_{\substack{j=1 \\ j \neq i}}^{i} \frac{\omega_j}{M_j D_{ij}^e} + \frac{\partial \omega_i}{\partial \xi^*} = \frac{-\omega_i}{\overline{M}} \frac{\partial \overline{M}}{\partial \xi^*} + \frac{\overline{M} D_{ref}}{\rho^*} \omega_i \sum_{\substack{j=1 \\ j \neq i}}^{n} \frac{j_j^*}{M_j D_{ij}^e} \tag{B.16}$$

B.1.6 Dusty gas diffusion model

The general Maxwell-Stefan model as given in (A.61):

$$j_i^* = \frac{\overline{M}^2 \sum_{\substack{j=1 \\ j \neq i}}^{n} \frac{\omega_i j_j^*}{M_j D_{ij}^e} - \frac{v^* \omega_i \overline{M}}{D_{iK}^e} - \frac{\omega_i \rho^*}{D_{ref}} \frac{\partial \overline{M}}{\partial \xi^*} - \frac{\rho^* \overline{M}}{D_{ref}} \frac{\partial \omega_i}{\partial \xi^*}}{\overline{M}^2 \sum_{\substack{j=1 \\ j \neq i}}^{n} \frac{\omega_j}{M_j D_{ij}^e} + \frac{\overline{M}}{D_{iK}^e}} \tag{B.17}$$

Rearranged to the implemented form:

$$j_i^* \frac{D_{ref}}{\rho^*} \left(\overline{M} \sum_{\substack{j=1 \\ j \neq i}}^{n} \frac{\omega_j}{M_j D_{ij}^e} + \frac{1}{D_{iK}^e} \right) + \frac{\partial \omega_i}{\partial \xi^*} = \frac{\overline{M} D_{ref}}{\rho^*} \sum_{\substack{j=1 \\ j \neq i}}^{n} \frac{\omega_i j_j^*}{M_j D_{ij}^e} - \frac{v^* \omega_i D_{ref}}{D_{iK}^e \rho^*} - \frac{\omega_i}{\overline{M}} \frac{\partial \overline{M}}{\partial \xi^*} \tag{B.18}$$

Assuming no convective transport:

$$j_i^* \frac{D_{ref}}{\rho^*} \left(\overline{M} \sum_{\substack{j=1 \\ j \neq i}}^{n} \frac{\omega_j}{M_j D_{ij}^e} + \frac{1}{D_{iK}^e} \right) + \frac{\partial \omega_i}{\partial \xi^*} = \frac{\overline{M} D_{ref}}{\rho^*} \sum_{\substack{j=1 \\ j \neq i}}^{n} \frac{\omega_i j_j^*}{M_j D_{ij}^e} - \frac{\omega_i}{\overline{M}} \frac{\partial \overline{M}}{\partial \xi^*} \tag{B.19}$$

B.1.7 Density equation

The density is obtained from modified ideal gas law given earlier A.37

$$\frac{p \overline{M}}{RT} = \rho \tag{B.20}$$

B.2 Mass based solution strategy

The different equations are discussed in short and the main summary of the solution strategy is given in table B.1. In the table the used equations combined with boundary conditions are shown. The solution strategy is also visualized in the form on how it would be implemented by the use of orthogonal collocation, shown in figure B.1.

B.2.1 Temperature equation

The temperature equation is solved in combination with Fourier's law in order to obtain two first order partial differential equations. Here the heat flux is obtained from the temperature equation and the temperature is obtained from Fourier's law. The temperature is specified at the surface for the Fourier's law, while the flux is specified at the center of the particle for the temperature equation.

B.2.2 Species mass balance and diffusion models

The species mass balance is solved to obtain the mass based fluxes. The mass based fluxes are then used to obtain the mass fractions throughout the catalyst particle using the different diffusion models. This is done for N-1 components for both the transport fluxes and the mass fractions, the last component is solved with a fitting constitutive law as seen in the solution strategy table. As boundary conditions the mass fractions are specified at the surface for the diffusion model, while the fluxes are specified at the center for the species mass balence.

B.2.3 Density

The density is obtained by the ideal gas law multiplied with averaged molecular weight. These values are obtained using previous iterative values and is solved outside of the matrix system.

Table B.1: Summary of the solution strategy

Equations, LHS represents terms in the problem matrix and the RHS represents the terms in the source vector:	Boundary conditions:
Fourier's law $$q^* + \frac{\partial T^*}{\partial \xi^*} = 0 \qquad (B.21)$$	Boundary condition at $\xi = \xi^p$ $$T = T^b \qquad (B.22)$$
Temperature equation: $$\frac{2q^*}{\xi^*} + \frac{\partial q^*}{\partial \xi^*} = \frac{\xi_{ref}^2 (-\triangle H_R) R}{T_{ref} \lambda} \qquad (B.23)$$	Boundary condition at $\xi = 0$ $$q = 0 \qquad (B.24)$$
Species mass balance, used for N-1 components: $$\frac{2j_i^*}{\xi^*} + \frac{\partial j_i^*}{\partial \xi^*} = R_i \frac{\xi_{ref}^2}{D_{ref} \rho_{ref}} \qquad (B.25)$$	Boundary condition at $\xi = 0$ $$j_i = 0 \qquad (B.26)$$
Last flux(H2O) in the species balance is solved by: $$\sum_{i=1}^{n} j_i^* = 0 \qquad (B.27)$$	No boundary condition $$-$$
A diffusion model is used for N-1 components: One of the four diffusion models in table B.2 is used	Boundary condition at $\xi = \xi^p$: $$\omega_i = \omega_i^b \qquad (B.28)$$
Last massfraction(H2O) in the species balance is solved by: $$\sum_{i=1}^{n} \omega_i = 1 \qquad (B.29)$$	No boundary condition $$-$$
Ideal gas law modified for density*: $$\frac{p\overline{M}}{RT} = \rho \qquad (B.30)$$	No boundary condition $$-$$

*Solved outside of the numerical collocation system and calculated from previous iteration values

Table B.2: Diffusion models on their implemented form

LHS is implemented in the collocation matrix, and the RHS is implemented in the source vector

Wilke:

$$j_i^* \frac{D_{ref}}{D_{im}\rho^*} + \frac{\partial \omega_i}{\partial \xi^*} = 0 \qquad D_{im} = \frac{1 - \omega_i}{\overline{M} \sum_{\substack{j=1 \\ j \neq i}}^{n} \frac{\omega_j}{M_j D_{ij}^e}} \tag{B.31}$$

Wilke-Bosanquet:

$$j_i^* \frac{D_{ref}}{D_{i,eff}\rho^*} + \frac{\partial \omega_i}{\partial \xi^*} = 0 \qquad \frac{1}{D_{i,eff}} = \frac{1}{\frac{1 - \omega_i}{\overline{M} \sum_{\substack{j=1 \\ j \neq i}}^{n} \frac{\omega_j}{M_j D_{ij}^e}}} + \frac{1}{D_{i,K}^e} \tag{B.32}$$

Maxwell-Stefan:

$$j_i^* \frac{\overline{M} D_{ref}}{\rho^*} \sum_{\substack{j=1 \\ j \neq i}}^{i} \frac{\omega_j}{M_j D_{ij}^e} + \frac{\partial \omega_i}{\partial \xi^*} = \frac{-\omega_i}{\overline{M}} \frac{\partial \overline{M}}{\partial \xi^*} + \frac{\overline{M} D_{ref}}{\rho^*} \omega_i \sum_{\substack{j=1 \\ j \neq i}}^{n} \frac{j_j^*}{M_j D_{ij}^e} \tag{B.33}$$

Dusty gas:

$$j_i^* \frac{D_{ref}}{\rho^*} \left(\overline{M} \sum_{\substack{j=1 \\ j \neq i}}^{n} \frac{\omega_j}{M_j D_{ij}^e} + \frac{1}{D_{iK}^e} \right) + \frac{\partial \omega_i}{\partial \xi^*} = \frac{\overline{M} D_{ref}}{\rho^*} \sum_{\substack{j=1 \\ j \neq i}}^{n} \frac{\omega_i j_j^*}{M_j D_{ij}^e} - \frac{\omega_i}{\overline{M}} \frac{\partial \overline{M}}{\partial \xi^*}$$

$$\tag{B.34}$$

$$
\begin{bmatrix}
1\bullet & 0 & & & & & & & & & & & \\
\frac{2}{\xi^*}\bullet+\frac{\partial}{\partial\xi^*} & \frac{\partial}{\partial\xi^*} & & & & & & & & & & & \\
0 & 0 & DM_1\bullet & & & & & & & & & & \\
0 & 0 & 0 & DM_1\bullet & & & & & & & & & \\
0 & 0 & 0 & 0 & DM_1\bullet & & & & & & & & \\
0 & 0 & 0 & 0 & 0 & DM_1\bullet & & & & & & & \\
0 & 0 & 1\bullet & 1\bullet & 1\bullet & 1\bullet & 0 & 0 & & & & & \\
0 & 0 & \frac{2}{\xi^*}\bullet+\frac{\partial}{\partial\xi^*} & \frac{2}{\xi^*}\bullet+\frac{\partial}{\partial\xi^*} & \frac{2}{\xi^*}\bullet+\frac{\partial}{\partial\xi^*} & \frac{2}{\xi^*}\bullet+\frac{\partial}{\partial\xi^*} & 0 & 0 & & & & & \\
\end{bmatrix}
\begin{bmatrix}
q \\ T \\ j_{CH_4} \\ j_{CO} \\ j_{CO_2} \\ j_{H_2} \\ j_{N_2} \\ j_{H_2O} \\ \omega_{CH_4} \\ \omega_{CO} \\ \omega_{CO_2} \\ \omega_{H_2} \\ \omega_{N_2} \\ \omega_{H_2O}
\end{bmatrix}
=
\begin{bmatrix}
0 \\ \frac{-\Delta H_r\,\xi^{*2}}{T_{ref}\,\lambda}\,DM_2 \\ DM_2 \\ DM_2 \\ DM_2 \\ DM_2 \\ 0 \\ SB_1 \\ SB_1 \\ SB_1 \\ SB_1 \\ SB_1 \\ 1
\end{bmatrix}
$$

Figure B.1: Collocation matrix, mass based. Explanation on the labeled terms can be seen in table B.3 and B.4

Table B.3: Terms in the collocation matrix

Label in matrix	Collocation matrix terms:	multiplied with:
DM_1	Wilke: $$\frac{D_{ref}}{D_{im}\rho^*}$$	j_i^*
DM_1	Wilke-Bosanquet: $$\frac{D_{ref}}{D_{i,eff}\rho^*}$$	j_i^*
DM_1	Maxwell-Stefan: $$\frac{\overline{M}D_{ref}}{\rho^*}\sum_{\substack{j=1 \\ j\neq i}}^{i}\frac{\omega_j}{M_j D_{ij}^e}$$	j_i^*
DM_1	Dusty gas: $$\frac{D_{ref}}{\rho^*}(\overline{M}\sum_{\substack{j=1 \\ j\neq i}}^{n}\frac{\omega_j}{M_j D_{ij}^e}+\frac{1}{D_{iK}^e})$$	j_i^*

Table B.4: Terms in the source vector

Label in source vector	Source vector
DM_2	Wilke: $$0$$
DM_2	Wilke-Bosanquet: $$0$$
DM_2	Maxwell-Stefan: $$\frac{-\omega_i}{\overline{M}}\frac{\partial \overline{M}}{\partial \xi^*} + \frac{\overline{M}D_{ref}}{\rho^*}\omega_i \sum_{\substack{j=1 \\ j\neq i}}^{n} \frac{j_j^*}{M_j D_{ij}^e}$$
DM_2	Dusty gas: $$\frac{\overline{M}D_{ref}}{\rho^*}\sum_{\substack{j=1 \\ j\neq i}}^{n} \frac{\omega_i j_j^*}{M_j D_{ij}^e} - \frac{\omega_i}{\overline{M}}\frac{\partial \overline{M}}{\partial \xi^*}$$
SB_1	Source term species balance: $$R_i \frac{\xi_{ref}^2}{D_{ref}\rho_{ref}}$$

B.3 Mole based model derivation

The mole based model will be derived similar to the mass based model.

B.3.1 The temperature balance

The general temperature balance derived earlier (A.63):

$$
((1-\epsilon)\rho_p Cp_p + \epsilon c^* c_{ref} \sum_{i=1}^{n} x_i Cp_i') \frac{\partial T^*}{\partial t^*} =
$$
$$
-c^* c_{ref} v_r^* \sum_{i=1}^{n} x_i Cp_i' \frac{\partial T^*}{\partial \xi^*} - \frac{(\frac{2q^*}{\xi^*} + \frac{\partial q^*}{\partial \xi^*})\lambda}{D_{ref}} + \frac{\xi_{ref}^2 (-\triangle H_R)R}{D_{ref} T_{ref}}
$$
(B.35)

Steady state is assumed:

$$
0 = -c^* c_{ref} v_r^* \sum_{i=1}^{n} x_i Cp_i' \frac{\partial T^*}{\partial \xi^*} - \frac{(\frac{2q^*}{\xi^*} + \frac{\partial q^*}{\partial \xi^*})\lambda}{D_{ref}} + \frac{\xi_{ref}^2 (-\triangle H_R)R}{D_{ref} T_{ref}}
$$
(B.36)

no convective transport is assumed:

$$
0 = -\frac{(\frac{2q^*}{\xi^*} + \frac{\partial q^*}{\partial \xi^*})\lambda}{D_{ref}} + \frac{\xi_{ref}^2 (-\triangle H_R)R}{D_{ref} T_{ref}}
$$
(B.37)

The equation is rearranged and the used equation is given as:

$$
\frac{2q^*}{\xi^*} + \frac{\partial q^*}{\partial \xi^*} = \frac{\xi_{ref}^2 (-\triangle H_r)R}{T_{ref} \lambda}
$$
(B.38)

B.3.2 Species mole balance

The mole based fluxes are obtained from the species mole balance. The general dimensionless equation is given as derived earlier (A.62):

$$
\frac{\partial}{\partial t^*}(c^* x_i) + \frac{1}{\xi^{*2}} \frac{\partial}{\partial \xi^*}(\xi^{*2} c^* x_i u_\xi^*) = -\frac{1}{\xi^{*2}} \frac{\partial}{\partial \xi^*}(\xi^{*2} J_i^*) + R_i' \frac{\xi_{ref}^2}{D_{ref} c_{ref}}
$$
(B.39)

Steady state is assumed.

$$
\frac{1}{\xi^{*2}} \frac{\partial}{\partial \xi^*}(\xi^{*2} c^* x_i u_\xi^*) = -\frac{1}{\xi^{*2}} \frac{\partial}{\partial \xi^*}(\xi^{*2} J_i^*) + R_i' \frac{\xi_{ref}^2}{D_{ref} c_{ref}}
$$
(B.40)

The first term is written out to identify the continuity equation.

$$
\frac{1}{\xi^{*2}} \frac{\partial x_i}{\partial \xi^*}(\xi^{*2} c^* u_\xi^*) + x_i \frac{1}{\xi^{*2}} \frac{\partial}{\partial \xi^*}(\xi^{*2} c^* u_\xi^*) = -\frac{1}{\xi^{*2}} \frac{\partial}{\partial \xi^*}(\xi^{*2} J_i^*) + R_i' \frac{\xi_{ref}^2}{D_{ref} c_{ref}}
$$
(B.41)

The second term is identified as the LHS of the mole based continuity equation (A.64) when steady state is assumed, swapped for the RHS of the mole based continuity equation gives:

$$
\frac{1}{\xi^{*2}} \frac{\partial x_i}{\partial \xi^*}(\xi^{*2} c^* u_\xi^*) + x_i (\frac{\xi_{ref}^2}{c_{ref} D_{ref}}) \sum_{i=1}^{n} R_i' = -\frac{1}{\xi^{*2}} \frac{\partial}{\partial \xi^*}(\xi^{*2} J_i^*) + R_i' \frac{\xi_{ref}^2}{D_{ref} c_{ref}}
$$
(B.42)

No convective transport is assumed and the equation is rearranged:

$$\frac{1}{\xi^{*2}}\frac{\partial}{\partial \xi^*}(\xi^{*2}J_i^*) = (R_i' - x_i \sum_{i=1}^{n} R_i')\frac{\xi_{ref}^2}{D_{ref}c_{ref}} \tag{B.43}$$

Expanding the first terms to reflect the equation used in the model:

$$\frac{2J_i^*}{\xi^{*2}} + \frac{\partial J_i^*}{\partial \xi^*} = (R_i' - x_i \sum_{i=1}^{n} R_i')\frac{\xi_{ref}^2}{D_{ref}c_{ref}} \tag{B.44}$$

B.3.3 Wilke diffusion model

The general Wilke diffusion model on mole basis as given in A.65:

$$J_i^* = -c^* D_{im}' \frac{\partial x_i}{\partial \xi^*} \qquad D_{im}' = \frac{1 - x_i}{\sum_{\substack{j=1 \\ j \neq i}}^{n} \frac{x_j}{D_{ij}^e}} \tag{B.45}$$

Rearranged to the implemented form:

$$J_i^* \frac{D_{ref}}{c^* D_{im}'} + \frac{\partial x_i}{\partial \xi^*} = 0 \qquad D_{im}' = \frac{1 - x_i}{\sum_{\substack{j=1 \\ j \neq i}}^{n} \frac{x_j}{D_{ij}^e}} \tag{B.46}$$

B.3.4 Wilke-Bosanquet diffusion model

$$j_i^* = -c^* \frac{D_{i,eff}'}{D_{ref}} \frac{\partial x_i}{\partial \xi^*} \qquad \frac{1}{D_{i,eff}'} = \frac{1}{D_{im}'} + \frac{1}{D_{i,K}^e} \tag{B.47}$$

Rearranged to the implemented form:

$$j_i^* \frac{D_{ref}}{D_{i,eff}' c^*} + \frac{\partial x_i}{\partial \xi^*} = 0 \qquad \frac{1}{D_{i,eff}'} = \frac{1}{\frac{1-x_i}{\sum_{\substack{j=1 \\ j \neq i}}^{n} \frac{x_j}{D_{ij}^e}}} + \frac{1}{D_{i,K}^e} \tag{B.48}$$

B.3.5 Maxwell-Stefan diffusion model

The general Maxwell-Stefan model on mole basis as given in A.67:

$$j_i^* = \frac{-c^* \frac{\partial x_i}{\partial \xi^*} + \sum_{\substack{j=1 \\ j \neq i}}^{n} \frac{j_j^* x_i}{D_{ij}^e}}{\sum_{\substack{j=1 \\ j \neq i}}^{i} \frac{x_j}{D_{ij}^e}} \tag{B.49}$$

Rearranged to the implemented form:

$$\frac{j_i^* D_{ref}}{c^*} \sum_{\substack{j=1 \\ j \neq i}}^{i} \frac{x_j}{D_{ij}^e} + \frac{\partial x_i}{\partial \xi^*} = \frac{D_{ref}}{c^*} \sum_{\substack{j=1 \\ j \neq i}}^{n} \frac{j_j^* x_i}{D_{ij}^e} \tag{B.50}$$

B.3.6 Dusty gas diffusion model

The general Maxwell-Stefan model on mole basis as given in A.68:

$$J_i^* = \frac{-\frac{c^*}{D_{ref}}\frac{\partial x_i}{\partial \xi^*} + \sum_{\substack{j=1\\j\neq i}}^{n} \frac{J_j^* x_i}{D_{ij}^e} - \frac{c^* x_i u^*}{D_{iK}^e}}{\sum_{\substack{j=1\\j\neq i}}^{i} \frac{x_j}{D_{ij}^e} + \frac{1}{D_{iK}^e}} \tag{B.51}$$

Rearranged to the implemented form:

$$J_i^* \frac{D_{ref}}{c^*}\left(\sum_{\substack{j=1\\j\neq i}}^{i} \frac{x_j}{D_{ij}^e} + \frac{1}{D_{iK}^e}\right) = -\frac{\partial x_i}{\partial \xi^*} + \frac{D_{ref}}{c^*}\sum_{\substack{j=1\\j\neq i}}^{n} \frac{J_j^* x_i}{D_{ij}^e} - \frac{D_{ref} x_i u^*}{D_{iK}^e} \tag{B.52}$$

B.3.7 Concentration equation

The concentration is obtained from the ideal gas law.

$$\frac{p}{RT} = c \tag{B.53}$$

B.4   Mole based solution strategy

The different equations are first discussed in short and the main summary of the solution strategy is given in table B.5. In the table the used equations combined with boundary conditions are shown. The solution strategy is also visualized in the form on how it would be implemented by the use of orthogonal collocation, shown in figure B.2.

B.4.1   Temperature equation

The temperature equation combined with the Fourier's law is solved separately to obtain the temperature. Similar to the mass based model the temperature is obtained from Fourier's law while the heat flux is obtained from the temperature equation. The same boundary conditions are also used where the temperature is specified at the surface for the Fourier's law, while the flux is specified at the center for the species mass balance.

B.4.2   Species Mole balance and Maxwell-Stefan diffusion

The species mole balance is solved to obtain the mole based fluxes. The mole based fluxes are then used to obtain the mole fractions throughout the catalyst particle using the different diffusion models given in table B.6. As for the mass based model this is also done for N-1 components for both the fluxes and the mole fractions, the last component is solved with a fitting constitutive law. The mole fractions are specified at the surface for the diffusion models, while the transport flux is specified at the center for the species mole balance.

B.4.3   Concentration

The concentration is solved outside the matrix system and is solved using the previous iterative values.

Table B.5: Summary of the solution strategy

Equations, LHS represents terms in the problem matrix and the RHS represents the terms in the source vector:	Boundary conditions:
Fourier's law $$q^* + \frac{\partial T^*}{\partial \xi^*} = 0 \qquad (B.54)$$	Boundary condition at $\xi = \xi^p$ $$T = T^b \qquad (B.55)$$
Temperature equation: $$\frac{2q^*}{\xi^*} + \frac{\partial q^*}{\partial \xi^*} = \frac{\xi_{ref}^2(-\triangle H_R)R}{T_{ref}\lambda} \qquad (B.56)$$	Boundary condition at $\xi = 0$ $$q = 0 \qquad (B.57)$$
Species mole balance, used for N-1 components: $$\frac{2J_i^*}{\xi^{*2}} + \frac{\partial J_i^*}{\partial \xi^*} = (R_i' - x_i \sum_{i=1}^{n} R_i')\frac{\xi_{ref}^2}{D_{ref}c_{ref}} \quad (B.58)$$	Boundary condition at $\xi = 0$ $$J_i = 0 \qquad (B.59)$$
Last flux(H2O) in the species balance is solved by: $$\sum_{i=1}^{n} J_i^* = 0 \qquad (B.60)$$	No boundary condition $-$
A diffusion model is used for N-1 components: One of the four diffusion models in table B.6 is used	Boundary condition at $\xi = \xi^p$: $$x_i = x_i^b \qquad (B.61)$$
Last mass fraction(H2O) in the species balance is solved by: $$\sum_{i=1}^{n} x_i = 1 \qquad (B.62)$$	No boundary condition $-$
Ideal gas law modified for concentration*: $$\frac{p}{RT} = c \qquad (B.63)$$	No boundary condition $-$

*Solved outside of the numerical collocation system and calculated from previous iteration values

Table B.6: Diffusion models on their implemented form

LHS is implemented in the collocation matrix, and the RHS is implemented in the source vector

Wilke:

$$J_i^* \frac{D_{ref}}{c^* D_{im}'} + \frac{\partial x_i}{\partial \xi^*} = 0 \qquad D_{im}' = \frac{1 - x_i}{\sum_{\substack{j=1 \\ j \neq i}}^{n} \frac{x_j}{D_{ij}^e}} \tag{B.64}$$

Wilke-Bosanquet:

$$j_i^* \frac{D_{ref}}{D_{i,eff}' c^*} + \frac{\partial x_i}{\partial \xi^*} = 0 \qquad \frac{1}{D_{i,eff}'} = \frac{1}{\frac{1 - x_i}{\sum_{\substack{j=1 \\ j \neq i}}^{n} \frac{x_j}{D_{ij}^e}}} + \frac{1}{D_{i,K}^e} \tag{B.65}$$

Maxwell-Stefan:

$$\frac{j_i^* D_{ref}}{c^*} \sum_{\substack{j=1 \\ j \neq i}}^{i} \frac{x_j}{D_{ij}^e} + \frac{\partial x_i}{\partial \xi^*} = \frac{D_{ref}}{c^*} \sum_{\substack{j=1 \\ j \neq i}}^{n} \frac{j_j^* x_i}{D_{ij}^e} \tag{B.66}$$

Dusty gas:

$$J_i^* \frac{D_{ref}}{c^*} \left(\sum_{\substack{j=1 \\ j \neq i}}^{i} \frac{x_j}{D_{ij}^e} + \frac{1}{D_{iK}^e} \right) + \frac{\partial x_i}{\partial \xi^*} = \frac{D_{ref}}{c^*} \sum_{\substack{j=1 \\ j \neq i}}^{n} \frac{J_j^* x_i}{D_{ij}^e} - \frac{D_{ref} x_i u^*}{D_{iK}^e} \tag{B.67}$$

$$
\begin{bmatrix}
\end{bmatrix}
\begin{bmatrix}
q \\
T \\
J_{CH_4} \\
J_{CO} \\
J_{CO_2} \\
J_{H_2} \\
J_{N_2} \\
J_{H_2O} \\
x_{CH_4} \\
x_{CO} \\
x_{CO_2} \\
x_{H_2} \\
x_{N_2} \\
x_{H_2O}
\end{bmatrix}
=
\begin{bmatrix}
0 \\
\frac{-\triangle H_r \, \xi^{*2}}{T_{ref} \, \lambda} \\
DM_2 \\
DM_2 \\
DM_2 \\
DM_2 \\
DM_2 \\
0 \\
SB_1 \\
SB_1 \\
SB_1 \\
SB_1 \\
SB_1 \\
1
\end{bmatrix}
$$

Figure B.2: Collocation matrix, mole based. Explanation on the labeled terms can be seen in table B.7 and B.8

Table B.7: Terms in the collocation matrix

Label in matrix	Collocation matrix terms:	multiplied with:
DM_1	Wilke: $$\frac{D_{ref}}{D'_{im}c^*}, \qquad D'_{im} = \frac{1-x_i}{\sum_{\substack{j=1\\j\neq i}}^{n}\frac{x_j}{D^e_{ij}}}$$	J_i^*
DM_1	Wilke-Bosanquet: $$\frac{D_{ref}}{D'_{i,eff}c^*}, \qquad \frac{1}{D'_{i,eff}} = \frac{1}{\frac{1-x_i}{\sum_{\substack{j=1\\j\neq i}}^{n}\frac{x_j}{D^e_{ij}}}} + \frac{1}{D^e_{iK}}$$	J_i^*
DM_1	Maxwell-Stefan: $$\frac{D_{ref}}{c^*}\sum_{\substack{j=1\\j\neq i}}^{i}\frac{x_j}{D^e_{ij}}$$	J_i^*
DM_1	Dusty gas: $$\frac{D_{ref}}{c^*}(\sum_{\substack{j=1\\j\neq i}}^{i}\frac{x_j}{D^e_{ij}} + \frac{1}{D^e_{iK}})$$	J_i^*

Table B.8: Terms in the source vector

Label in source vector	Source vector
DM_2	Wilke: $$0$$
DM_2	Wilke-Bosanquet: $$0$$
DM_2	Maxwell-Stefan: $$\frac{D_{ref}}{c^*} \sum_{\substack{j=1 \\ j \neq i}}^{n} \frac{J_j^* x_i}{D_{ij}^e}$$
DM_2	Dusty gas: $$\frac{D_{ref}}{c^*} \sum_{\substack{j=1 \\ j \neq i}}^{n} \frac{J_j^* x_i}{D_{ij}^e} - \frac{D_{ref} x_i u^*}{D_{iK}^e}$$
SB_1	Source term species balance: $$\left(R_i' - x_i \sum_{i=1}^{n} R_i'\right) \frac{\xi_{ref}^2}{D_{ref} c_{ref}}$$

B.5 Additional result plots

Wilke
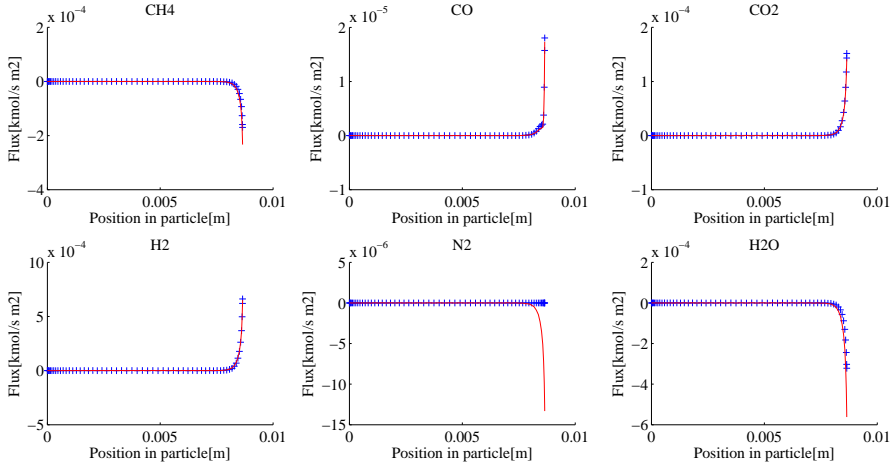
Figure B.3: Mole(—) and mass(+++) based diffusive transport fluxes using the Wilke diffusion model.

Wilke-Bosanquet
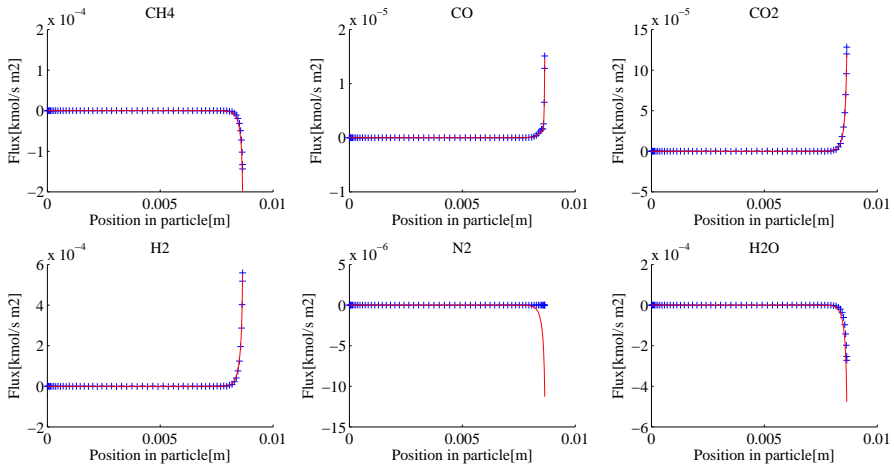
Figure B.4: Mole(—) and mass(+++) based diffusive transport fluxes using the Wilke-Bosanquet diffusion model.

Maxwell-Stefan
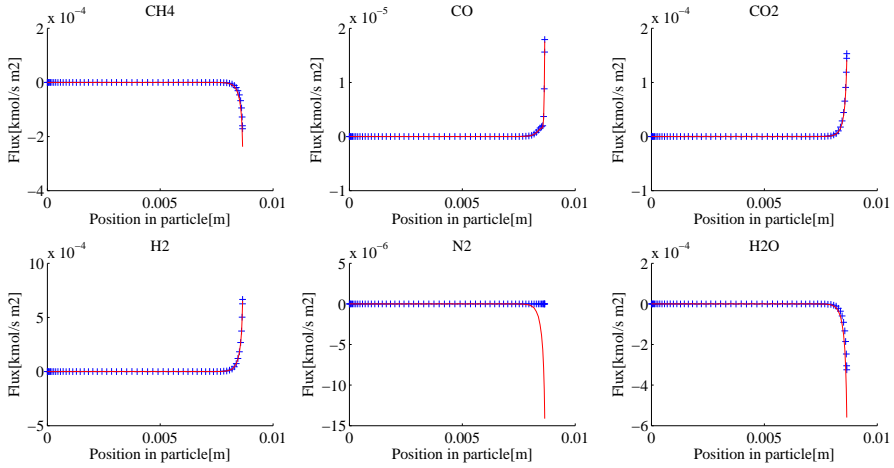
Figure B.5: Mole(—) and mass(+++) based diffusive transport fluxes using the Maxwell-Stefan diffusion model.

Dusty gas
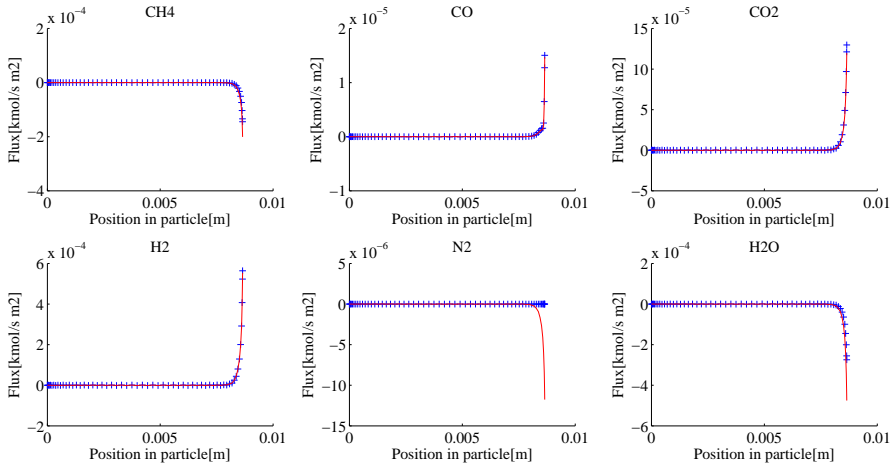
Figure B.6: Mole(—) and mass(+++) based diffusive transport fluxes using the dusty gas diffusion model.

C 4 Alternative methods for solving the simple models

In this appendix the equations needed for the alternative pellet model formulations will be derived.

C.1 Mass based model - Alternative dimensionless method

The model equations will be derived for the mass based formulation using Maxwell-Stefan diffusion.

C.1.1 The temperature balance

The general temperature balance derived earlier (A.56):

$$((1-\epsilon)\rho_p Cp_p + \epsilon\rho^*\rho_{ref}\sum_{i=1}^{n}\omega_i Cp_i)\frac{\partial T^*}{\partial t^*} =$$
$$-\rho^*\rho_{ref}v_r^*\sum_{i=1}^{n}\omega_i Cp_i\frac{\partial T^*}{\partial \xi^*} - \frac{(\frac{2q^*}{\xi^*} + \frac{\partial q^*}{\partial \xi^*})\lambda}{D_{ref}} + \frac{\xi_{ref}^2(-\triangle H_R)R}{D_{ref}T_{ref}} \tag{C.1}$$

Steady state is assumed:

$$0 = -\rho^*\rho_{ref}v_r^*\sum_{i=1}^{n}\omega_i Cp_i\frac{\partial T^*}{\partial \xi^*} - \frac{(\frac{2q^*}{\xi^*} + \frac{\partial q^*}{\partial \xi^*})\lambda}{D_{ref}} + \frac{\xi_{ref}^2(-\triangle H_R)R}{D_{ref}T_{ref}} \tag{C.2}$$

No convective transport is assumed:

$$0 = -\frac{(\frac{2q^*}{\xi^*} + \frac{\partial q^*}{\partial \xi^*})\lambda}{D_{ref}} + \frac{\xi_{ref}^2(-\triangle H_R)R}{D_{ref}T_{ref}} \tag{C.3}$$

The equation is rearranged and the used equation is given as:

$$\frac{2q^*}{\xi^*} + \frac{\partial q^*}{\partial \xi^*} = \frac{\xi_{ref}^2(-\triangle H_R)R}{T_{ref}\lambda} \tag{C.4}$$

C.1.2 Species mass balance

The mass based fluxes are obtained from the species mass balance. To account for the alternative method of making the flux dimensionless, we will start out from the general species mass balance with dimensions. The general equation is given as noted earlier (A.6):

$$\frac{\partial}{\partial t}(\rho\omega_i) + \frac{1}{\xi^2}\frac{\partial}{\partial \xi}(\xi^2\rho\omega_i v_\xi) = -\frac{1}{\xi^2}\frac{\partial}{\partial \xi}(\xi^2 j_i) + R_i \tag{C.5}$$

Steady state is assumed.

$$\frac{1}{\xi^2}\frac{\partial}{\partial \xi}(\xi^2\rho\omega_i v_\xi) = -\frac{1}{\xi^2}\frac{\partial}{\partial \xi}(\xi^2 j_i) + R_i \tag{C.6}$$

The first term is written out to identify the continuity equation.

$$\frac{\partial \omega_i}{\partial \xi}(\rho v_\xi) + \omega_i \frac{1}{\xi^2}\frac{\partial}{\partial \xi}(\xi^2 \rho v_\xi) = -\frac{1}{\xi^2}\frac{\partial}{\partial \xi}(\xi^2 j_i) + R_i \tag{C.7}$$

The second term is identified as the LHS of the mass based continuity equation (A.8) when steady state is assumed, swapped for the RHS of the mass based continuity equation gives:

$$\frac{\partial \omega_i}{\partial \xi}(\rho v_\xi) = -\frac{1}{\xi^2}\frac{\partial}{\partial \xi}(\xi^2 j_i) + R_i \tag{C.8}$$

No convective transport is assumed, and the equation is rearranged:

$$\frac{1}{\xi^2}\frac{\partial}{\partial \xi}(\xi^2 j_i) = R_i \tag{C.9}$$

The first term is expanded to reflect the implemented equation:

$$\frac{2j_i}{\xi} + \frac{\partial j_i}{\partial \xi} = R_i \tag{C.10}$$

Alternative method for making the fluxes dimensionless:

$$j_i^* = \frac{j\xi_{ref}}{D_s\rho} \tag{C.11}$$

where ρ can be written out to:

$$j_i^* = \frac{j\xi_{ref}}{D_s c^* c_{ref}\overline{M}} \tag{C.12}$$

Introducing the last equation into the species mass balance to transform it to a dimensionless form:

$$\frac{2j_i^* D_s c^* c_{ref}\overline{M}}{\xi^* \xi_{ref}^2} + \frac{c_{ref}}{\xi ref^2}\frac{\partial}{\partial \xi^*}(j_i^* D_s c^*\overline{M}) = R_i \tag{C.13}$$

Rearranging and writing out the differential:

$$\frac{2j_i^* D_s c^*\overline{M}}{\xi^*} + D_s c^*\overline{M}\frac{\partial j_i^*}{\partial \xi^*} + j_i^* c^*\overline{M}\frac{\partial D_s}{\partial \xi^*} +$$
$$j_i^* D_s\overline{M}\frac{\partial c^*}{\partial \xi^*} + j_i^* D_s c^*\frac{\partial \overline{M}}{\partial \xi^*} = R_i\frac{\xi_{ref}^2}{c_{ref}} \tag{C.14}$$

Cleaning up the equation:

$$\frac{2j_i^*}{\xi^*} + \frac{\partial j_i^*}{\partial \xi^*} + \frac{j_i^*}{D_s}\frac{\partial D_s}{\partial \xi^*} + \frac{j_i^*}{c^*}\frac{\partial c^*}{\partial \xi^*} + \frac{j_i^*}{\overline{M}}\frac{\partial \overline{M}}{\partial \xi^*} = R_i\frac{\xi_{ref}^2}{\rho D_s} \tag{C.15}$$

C.1.3 Constitutive law for the species balance

a modified constitutive law is needed as now the dimensionless fluxes will not sum to 0.

$$\sum_{i=1}^{n} j_i^* D_s c^*\overline{M} = 0 \tag{C.16}$$

C.1.4 Maxwell-Stefan diffusion model

The general Maxwell-Stefan model with dimension as given in (A.13):

$$j_i = \frac{-\rho \omega_i \nabla ln(\overline{M}) - \rho \nabla \omega_i + \overline{M}\omega_i \sum_{\substack{j=1 \\ j \neq i}}^{n} \frac{j_j}{M_j D_{ij}^e}}{\overline{M} \sum_{\substack{j=1 \\ j \neq i}}^{i} \frac{\omega_j}{M_j D_{ij}^e}} \tag{C.17}$$

Specifies that:

$$D_s^{-1} = \overline{M} \sum_{\substack{j=1 \\ j \neq i}}^{i} \frac{\omega_j}{M_j D_{ij}^e} \tag{C.18}$$

Transforming to dimensionless form:

$$j_i^* = \xi_{ref} \frac{-\rho \omega_i \frac{1}{\overline{M}} \frac{\partial \overline{M}}{\partial \xi^* \xi_{ref}} - \rho \frac{\partial \omega_i}{\partial \xi^* \xi_{ref}} + \overline{M}\omega_i \sum_{\substack{j=1 \\ j \neq i}}^{n} \frac{j_j^* D_s c^* c_{ref} \overline{M}}{M_j D_{ij}^e \xi_{ref}}}{c^* c_{ref} \overline{M}} \tag{C.19}$$

Cleaning the equation:

$$j_i^* = -\omega_i \frac{1}{\overline{M}} \frac{\partial \overline{M}}{\partial \xi^*} - \frac{\partial \omega_i}{\partial \xi^*} + \omega_i \sum_{\substack{j=1 \\ j \neq i}}^{n} \frac{j_j^* D_s \overline{M}}{M_j D_{ij}^e} \tag{C.20}$$

C.1.5 Concentration equation

The concentration is obtained from the ideal gas law:

$$\frac{p}{RT} = c \tag{C.21}$$

C.2 Solution strategy

The different equations are first discussed in short and the main summary of the solution strategy is given in table C.1. In the table the used equations combined with boundary conditions are shown. The solution strategy is also visualized in the form on how it would be implemented by the use of orthogonal collocation, shown in figure C.1.

C.2.1 Temperature equation

The temperature equation combined with the Fourier's law are solved separately to obtain the temperature. Here the temperature is obtained from Fourier's law and the heat flux is obtained from the temperature equation. The temperature is specified at the surface for the Fourier's law and the flux is specified at the center for the temperature equations.

C.2.2 Species Mass balance and Maxwell-Stefan diffusion

The species mass balance is solved for N-1 components to obtain the mass based fluxes. The mass based fluxes are then used to obtain the mass fractions throughout the catalyst particle using the Maxwell-Stefan diffusion model also here for N-1 components. The last flux and mass fractions are solved using their respective constitutive law given in the solution strategy. The mass fraction is specified at the surface for the diffusion model, while the flux is specified at the center for the species mass balance.

C.2.3 Concentration

The ideal gas law is solved outside the numerical problem and is solved using the previous iterative values.

Table C.1: Summary of the solution strategy

Equations, LHS represents terms in the problem matrix and the RHS represents the terms in the source vector:	Boundary conditions:
Fourier's law $$q^* + \frac{\partial T^*}{\partial \xi^*} = 0 \qquad (C.22)$$	Boundary condtion at $\xi = \xi^p$ $$T = T^b \qquad (C.23)$$
Temperature equation: $$\frac{2q^*}{\xi^*} + \frac{\partial q^*}{\partial \xi^*} = \frac{\xi_{ref}^2(-\triangle H_R)R}{T_{ref}\lambda} \qquad (C.24)$$	Boundary condition at $\xi = 0$ $$q = 0 \qquad (C.25)$$
Species mass balance, used for N-1 components: $$\frac{2j_i^*}{\xi^*} + \frac{\partial j_i^*}{\partial \xi^*} = R_i \frac{\xi_{ref}^2}{\rho D_s} - \frac{j_i^*}{D_s}\frac{\partial D_s}{\partial \xi^*} - \frac{j_i^*}{c^*}\frac{\partial c^*}{\partial \xi^*} - \frac{j_i^*}{\overline{M}}\frac{\partial \overline{M}}{\partial \xi^*}$$ (C.26)	Boundary condition at $\xi = 0$ $$j_i = 0 \qquad (C.27)$$
Last flux(H2O) in the species balance is solved by: $$\sum_{i=1}^{n} j_i^* D_s \rho = 0 \qquad (C.28)$$	No boundary condition $-$
Maxwell-Stefan diffusion model for N-1 components: $$j_i^* + \frac{\partial \omega_i}{\partial \xi^*} = -\omega_i \frac{1}{\overline{M}}\frac{\partial \overline{M}}{\partial \xi^*} + \omega_i \sum_{\substack{j=1 \\ j\neq i}}^{n} \frac{j_j^* D_s \overline{M}}{M_j D_{ij}^e} \quad (C.29)$$	Boundary condition at $\xi = \xi^p$: $$\omega_i = \omega_i^b \qquad (C.30)$$
Last mass fraction(H2O) in the species balance is solved by: $$\sum_{i=1}^{n} \omega_i = 1 \qquad (C.31)$$	No boundary condition $-$
Ideal gas law, concentration and density*: $$\frac{p}{RT} = c \qquad \frac{p\overline{M}}{RT} = \rho \qquad (C.32)$$	No boundary condition $-$

*Solved outside of the numerical collocation system and calculated from previous iteration values

$$
[\cdots] \begin{bmatrix} q \\ T \\ j_{CH_4} \\ j_{CO} \\ j_{CO_2} \\ j_{H_2} \\ j_{N_2} \\ j_{H_2O} \\ \omega_{CH_4} \\ \omega_{CO} \\ \omega_{CO_2} \\ \omega_{H_2} \\ \omega_{N_2} \\ \omega_{H_2O} \end{bmatrix} = \begin{bmatrix} 0 \\ \dfrac{-\Delta H_r \xi^{*2} \lambda}{T_{ref}} \\ MS_1 \\ MS_1 \\ MS_1 \\ MS_1 \\ MS_1 \\ 0 \\ SB_1 \\ SB_1 \\ SB_1 \\ SB_1 \\ SB_1 \\ 1 \end{bmatrix}
$$

Figure C.1: Mass based collocation matrix using the Maxwell-Stefan diffusion model.

$$
MS_1 = -\omega_i \frac{1}{\overline{M}} \frac{\partial \overline{M}}{\partial \xi^*} + \omega_i \sum_{\substack{j=1 \\ j \neq i}}^{n} \frac{j_j^* D_s \overline{M}}{M_j D_{ij}^e}
$$

$$
SB_1 = R_i \frac{\xi_{ref}^2}{\rho D_s} - \frac{j_i^*}{D_s} \frac{\partial D_s}{\partial \xi^*} - \frac{j_i^*}{c^*} \frac{\partial c^*}{\partial \xi^*} - \frac{j_i^*}{\overline{M}} \frac{\partial \overline{M}}{\partial \xi^*}
$$

C.3   Mole based model not including the continuity equation

The model equations for the steady state, non-convective mole based model not using the continuity equation to simplify the species balance will be derived.

C.3.1   The temperature balance

The general temperature balance derived earlier (A.63):

$$((1-\epsilon)\rho_p Cp_p + \epsilon c^* c_{ref} \sum_{i=1}^{n} x_i Cp_i')\frac{\partial T^*}{\partial t^*} =$$

$$-c^* c_{ref} v_r^* \sum_{i=1}^{n} x_i Cp_i' \frac{\partial T^*}{\partial \xi^*} - \frac{(\frac{2q^*}{\xi^*} + \frac{\partial q^*}{\partial \xi^*})\lambda}{D_{ref}} + \frac{\xi_{ref}^2(-\triangle H_R)R}{D_{ref}T_{ref}} \tag{C.33}$$

Steady state is assumed:

$$0 = -c^* c_{ref} v_r^* \sum_{i=1}^{n} x_i Cp_i' \frac{\partial T^*}{\partial \xi^*} - \frac{(\frac{2q^*}{\xi^*} + \frac{\partial q^*}{\partial \xi^*})\lambda}{D_{ref}} + \frac{\xi_{ref}^2(-\triangle H_R)R}{D_{ref}T_{ref}} \tag{C.34}$$

no convective transport is assumed:

$$0 = -\frac{(\frac{2q^*}{\xi^*} + \frac{\partial q^*}{\partial \xi^*})\lambda}{D_{ref}} + \frac{\xi_{ref}^2(-\triangle H_R)R}{D_{ref}T_{ref}} \tag{C.35}$$

The equation is rearranged and the used equation is given as:

$$\frac{2q^*}{\xi^*} + \frac{\partial q^*}{\partial \xi^*} = \frac{\xi_{ref}^2(-\triangle H_r)R}{T_{ref}\lambda} \tag{C.36}$$

C.3.2   Species mole balance

The mole based fluxes are obtained from the species mole balance. The general dimensionless equation is given as derived earlier (A.62):

$$\frac{\partial}{\partial t^*}(c^* x_i) + \frac{1}{\xi^{*2}}\frac{\partial}{\partial \xi^*}(\xi^{*2} c^* x_i u_\xi^*) = -\frac{1}{\xi^{*2}}\frac{\partial}{\partial \xi^*}(\xi^{*2} J_i^*) + R_i'\frac{\xi_{ref}^2}{D_{ref}c_{ref}} \tag{C.37}$$

Steady state is assumed.

$$\frac{1}{\xi^{*2}}\frac{\partial}{\partial \xi^*}(\xi^{*2} c^* x_i u_\xi^*) = -\frac{1}{\xi^{*2}}\frac{\partial}{\partial \xi^*}(\xi^{*2} J_i^*) + R_i'\frac{\xi_{ref}^2}{D_{ref}c_{ref}} \tag{C.38}$$

No convective transport is assumed and the equation is rearranged:

$$0 = -\frac{1}{\xi^{*2}}\frac{\partial}{\partial \xi^*}(\xi^{*2} J_i^*) + R_i'\frac{\xi_{ref}^2}{D_{ref}c_{ref}} \tag{C.39}$$

Expanding the first terms to reflect the equation used in the model:

$$\frac{2J_i^*}{\xi^{*2}} + \frac{\partial J_i^*}{\partial \xi^*} = R_i'\frac{\xi_{ref}^2}{D_{ref}c_{ref}} \tag{C.40}$$

C.3.3 Maxwell-Stefan diffusion model

The general Maxwell-Stefan model on mole basis as given in A.67:

$$j_i^* = \frac{-c^* \frac{\partial x_i}{\partial \xi^*} + \sum_{\substack{j=1 \\ j \neq i}}^{n} \frac{j_j^* x_i}{D_{ij}^e}}{\sum_{\substack{j=1 \\ j \neq i}}^{i} \frac{x_j}{D_{ij}^e}} \tag{C.41}$$

Rearranged to the implemented form:

$$\frac{j_i^* D_{ref}}{c^*} \sum_{\substack{j=1 \\ j \neq i}}^{i} \frac{x_j}{D_{ij}^e} + \frac{\partial x_i}{\partial \xi^*} = \frac{D_{ref}}{c^*} \sum_{\substack{j=1 \\ j \neq i}}^{n} \frac{j_j^* x_i}{D_{ij}^e} \tag{C.42}$$

C.3.4 Concentration equation

The concentration is obtained from the ideal gas law.

$$\frac{p}{RT} = c \tag{C.43}$$

C.4   Solution strategy

The different equations are first discussed in short and the main summary of the solution strategy is given in table C.2. In the table the used equations combined with boundary conditions are shown. The solution strategy is also visualized in the form on how it would be implemented by the use of orthogonal collocation, shown in figure C.2.

C.4.1   Temperature equation

The temperature equation combined with the Fourier's law is solved separately to obtain the temperature. Here the temperature is obtained from Fourier's law and the heat flux is obtained from the temperature equation. The temperature is specified at the surface of the pellet for the Fourier's law, while the heat flux is specified at the center for the temperature balance.

C.4.2   Species mole balance and Maxwell-Stefan diffusion

The species mole balance is solved for N-1 components to obtain the mole based transport fluxes. The mole based fluxes are then used to obtain the mole fractions throughout the catalyst particle by using the Maxwell-Stefan diffusion model also here for N-1 components. The last flux and mole fractions are solved using their respective constitutive law given in the solution strategy. The mole fraction is specified at the surface of the catalyst particle, while the flux is specified at the center for the species mole balance.

C.4.3   Concentration

The ideal gas law is solved outside the numerical problem and is solved using the previous iterative values.

Table C.2: Summary of the solution strategy

Equations, LHS represents terms in the problem matrix and the RHS represents the terms in the source vector:	Boundary conditions:
Fourier's law $$q^* + \frac{\partial T^*}{\partial \xi^*} = 0 \qquad (C.44)$$	Boundary condition at $\xi = \xi^p$ $$T = T^b \qquad (C.45)$$
Temperature equation: $$\frac{2q^*}{\xi^*} + \frac{\partial q^*}{\partial \xi^*} = \frac{\xi_{ref}^2(-\triangle H_R)R}{T_{ref}\lambda} \qquad (C.46)$$	Boundary condition at $\xi = 0$ $$q = 0 \qquad (C.47)$$
Species mole balance, used for N-1 components: $$\frac{2J_i^*}{\xi^{*2}} + \frac{\partial J_i^*}{\partial \xi^*} = R_i' \frac{\xi_{ref}^2}{D_{ref}c_{ref}} \qquad (C.48)$$	Boundary condition at $\xi = 0$ $$J_i = 0 \qquad (C.49)$$
Last flux(H2O) in the species balance is solved by: $$\sum_{i=1}^{n} J_i = 0 \qquad (C.50)$$	No boundary condition $-$
Maxwell-Stefan diffusion model for N-1 components: $$\frac{j_i^* D_{ref}}{c^*} \sum_{\substack{j=1 \\ j \neq i}}^{i} \frac{x_j}{D_{ij}^e} + \frac{\partial x_i}{\partial \xi^*} = \frac{D_{ref}}{c^*} \sum_{\substack{j=1 \\ j \neq i}}^{n} \frac{j_j^* x_i}{D_{ij}^e} \quad (C.51)$$	Boundary condition at $\xi = \xi^p$: $$x_i = x_i^b \qquad (C.52)$$
Last mass fraction(H2O) in the species balance is solved by: $$\sum_{i=1}^{n} x_i = 1 \qquad (C.53)$$	No boundary condition $-$
Ideal gas law modified for concentration*: $$\frac{p}{RT} = c \qquad (C.54)$$	No boundary condition $-$

*Solved outside of the numerical collocation system and calculated from previous iteration values

$$
\begin{bmatrix} q \\ T \\ J_{CH_4} \\ J_{CO} \\ J_{CO_2} \\ J_{H_2} \\ J_{N_2} \\ J_{H_2O} \\ x_{CH_4} \\ x_{CO} \\ x_{CO_2} \\ x_{H_2} \\ x_{N_2} \\ x_{H_2O} \end{bmatrix}
=
\begin{bmatrix} 0 \\ \dfrac{-\triangle H_r \xi^{*2} \lambda}{T_{ref}} \\ MS_2 \\ MS_2 \\ MS_2 \\ MS_2 \\ MS_2 \\ 0 \\ SB_1 \\ SB_1 \\ SB_1 \\ SB_1 \\ SB_1 \\ 1 \end{bmatrix}
$$

Figure C.2: Mole based collocation matrix using the Maxwell-Stefan diffusion model.

$$MS_1 = \frac{D_{ref}}{c^*} \sum_{\substack{j=1 \\ j\neq i}}^{i} \frac{x_j}{D_{ij}^e}$$

$$MS_2 = \frac{D_{ref}}{c^*} \sum_{\substack{j=1 \\ j\neq i}}^{n} \frac{j_j^* x_i}{D_{ij}^e}$$

$$SB_1 = R_i' \frac{\xi_{ref}^2}{D_{ref} c_{ref}}$$

C.5 Effect of continuity, rigorous models

Due to the small changes in the models and the results given by including the continuity equation in the more rigorous models the alternative species balance equations are only derived. These equations can be replaced in the rigorous model derived in chapter 5 for a complete walk-through and a solution strategy.

C.5.1 Species mass balance

The mass based fluxes are obtained from the species mass balance. The general dimensionless equation is given as derived earlier (A.55):

$$\frac{\partial}{\partial t^*}(\rho^* \omega_i) + \frac{1}{\xi^{*2}}\frac{\partial}{\partial \xi^*}(\xi^{*2}\rho^* \omega_i v_\xi^*) = -\frac{1}{\xi^{*2}}\frac{\partial}{\partial \xi^*}(\xi^{*2}j_i^*) + R_i \frac{\xi_{ref}^2}{D_{ref}\rho_{ref}} \qquad \text{(C.55)}$$

Steady state is assumed and the equation is rearranged.

$$\frac{1}{\xi^{*2}}\frac{\partial}{\partial \xi^*}(\xi^{*2}\rho^* \omega_i v_\xi^*) + \frac{1}{\xi^{*2}}\frac{\partial}{\partial \xi^*}(\xi^{*2}j_i^*) = R_i \frac{\xi_{ref}^2}{D_{ref}\rho_{ref}} \qquad \text{(C.56)}$$

The first and second term is written out:

$$\frac{2\rho^* \omega_i v_\xi^*}{\xi^*} + \frac{\partial \rho^*}{\partial \xi^*}\omega_i v_\xi^* + \frac{\partial \omega_i}{\partial \xi^*}\rho^* v_\xi^* + \frac{\partial v_\xi^*}{\partial \xi^*}\omega_i \rho^* + \frac{2j_i^*}{\xi^*} + \frac{\partial j_i^*}{\partial \xi^*} = R_i \frac{\xi_{ref}^2}{D_{ref}\rho_{ref}} \qquad \text{(C.57)}$$

The equation is rearranged to show how it is implemented. The LHS is implemented in the collocation matrix and the RHS in the source vector:

$$\frac{2\rho^* \omega_i v_\xi^*}{\xi^*} + \frac{\partial \omega_i}{\partial \xi^*}\rho^* v_\xi^* + \frac{\partial v_\xi^*}{\partial \xi^*}\omega_i \rho^* + \frac{2j_i^*}{\xi^*} + \frac{\partial j_i^*}{\partial \xi^*} = R_i \frac{\xi_{ref}^2}{D_{ref}\rho_{ref}} - \frac{\partial \rho^*}{\partial \xi^*}\omega_i v_\xi^* \qquad \text{(C.58)}$$

This equation can be swapped out for eq 115 in chapter 5 for a complete solution strategy.

C.5.2 Species mole balance

The mole based fluxes are obtained from the species mole balance. The general dimensionless equation is given as derived earlier (A.62):

$$\frac{\partial}{\partial t^*}(c^* x_i) + \frac{1}{\xi^{*2}}\frac{\partial}{\partial \xi^*}(\xi^{*2}c^* x_i u_\xi^*) = -\frac{1}{\xi^{*2}}\frac{\partial}{\partial \xi^*}(\xi^{*2}J_i^*) + R_i' \frac{\xi_{ref}^2}{D_{ref}c_{ref}} \qquad \text{(C.59)}$$

Steady state is assumed and the equation is rearranged.

$$\frac{1}{\xi^{*2}}\frac{\partial}{\partial \xi^*}(\xi^{*2}c^* x_i u_\xi^*) + \frac{1}{\xi^{*2}}\frac{\partial}{\partial \xi^*}(\xi^{*2}J_i^*) = R_i' \frac{\xi_{ref}^2}{D_{ref}c_{ref}} \qquad \text{(C.60)}$$

The first and second term is written out:

$$\frac{2c^* x_i u_\xi^*}{\xi^*} + \frac{\partial x_i}{\partial \xi^*}c^* u_\xi^* + \frac{\partial c^*}{\partial \xi^*}x_i u_\xi^* + \frac{\partial u_\xi^*}{\partial \xi^*}x_i c^* + \frac{2J_i^*}{\xi^*} + \frac{\partial J_i^*}{\partial \xi^*} = R_i' \frac{\xi_{ref}^2}{D_{ref}c_{ref}} \qquad \text{(C.61)}$$

This equation can be swapped out for eq 133 in chapter 5 for a complete solution strategy.

C.6   additional results - Effect of continuity equation
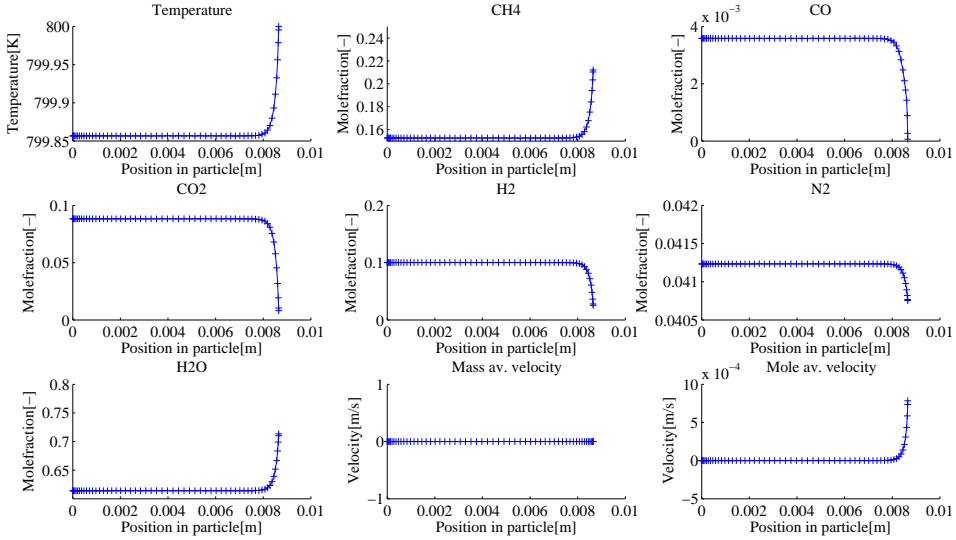
Figure C.3: Mass: Comparison of replacing the convective terms in the species mass balance with the LHS of the continuity equation or not. Replaced(—), not replaced(+++), basic boundary condtions are used, 60 collocation points.
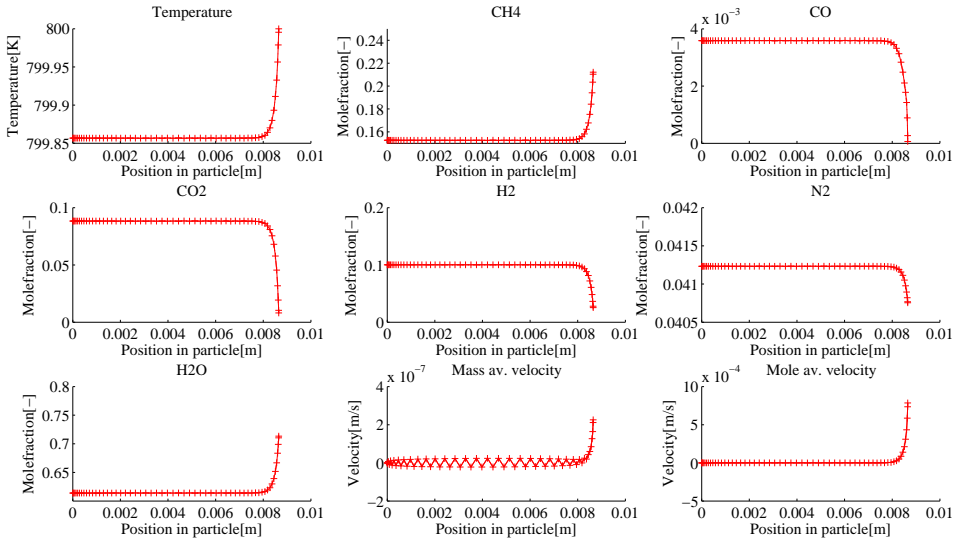
Figure C.4: Mole: Comparison of replacing the convective terms in the species mole balance with the LHS of the continuity equation or not. Replaced(—), not replaced(+++), basic boundary conditions are used, 60 collocation points.

D 5 Rigorous steady state models

D.1 Mass based model

D.1.1 The temperature balance

The general temperature balance derived earlier (A.56):

$$((1 - \epsilon)\rho_p C p_p + \epsilon^* \rho_{ref} \sum_{i=1}^{n} \omega_i C p_i)\frac{\partial T^*}{\partial t^*} =$$

$$-\rho^* \rho_{ref} v_\xi^* \sum_{i=1}^{n} \omega_i C p_i \frac{\partial T^*}{\partial \xi^*} - \frac{(\frac{2q^*}{\xi^*} + \frac{\partial q^*}{\partial \xi^*})\lambda}{D_{ref}} + \frac{\xi_{ref}^2(-\triangle H_R)R}{D_{ref}T_{ref}} \tag{D.1}$$

Steady state is assumed:

$$0 = -\rho^* \rho_{ref} v_\xi^* \sum_{i=1}^{n} \omega_i C p_i \frac{\partial T^*}{\partial \xi^*} - \frac{(\frac{2q^*}{\xi^*} + \frac{\partial q^*}{\partial \xi^*})\lambda}{D_{ref}} + \frac{\xi_{ref}^2(-\triangle H_R)R}{D_{ref}T_{ref}} \tag{D.2}$$

The equation is rearranged and the used equation is given as:

$$\frac{D_{ref}}{\lambda}\rho^* \rho_{ref} v_\xi^* \sum_{i=1}^{n} \omega_i C p_i \frac{\partial T^*}{\partial \xi^*} = -(\frac{2q^*}{\xi^*} + \frac{\partial q^*}{\partial \xi^*}) + \frac{\xi_{ref}^2(-\triangle H_R)R}{T_{ref}\lambda} \tag{D.3}$$

D.1.2 Species mass balance

The mass based fluxes are obtained from the species mass balance. The general dimensionless equation is given as derived earlier (A.55):

$$\frac{\partial}{\partial t^*}(\rho^* \omega_i) + \frac{1}{\xi^{*2}}\frac{\partial}{\partial \xi^*}(\xi^{*2}\rho^* \omega_i v_\xi^*) = -\frac{1}{\xi^{*2}}\frac{\partial}{\partial \xi^*}(\xi^{*2}j_i^*) + R_i \frac{\xi_{ref}^2}{D_{ref}\rho_{ref}} \tag{D.4}$$

Steady state is assumed.

$$\frac{1}{\xi^{*2}}\frac{\partial}{\partial \xi^*}(\xi^{*2}\rho^* \omega_i v_\xi^*) = -\frac{1}{\xi^{*2}}\frac{\partial}{\partial \xi^*}(\xi^{*2}j_i^*) + R_i \frac{\xi_{ref}^2}{D_{ref}\rho_{ref}} \tag{D.5}$$

The first term is written out to identify the continuity equation.

$$\frac{1}{\xi^{*2}}\frac{\partial \omega_i}{\partial \xi^*}(\xi^{*2}\rho^* v_\xi^*) + \omega_i \frac{1}{\xi^{*2}}\frac{\partial}{\partial \xi^*}(\xi^{*2}\rho^* v_\xi^*) = -\frac{1}{\xi^{*2}}\frac{\partial}{\partial \xi^*}(\xi^{*2}j_i^*) + R_i \frac{\xi_{ref}^2}{D_{ref}\rho_{ref}} \tag{D.6}$$

The second term is identified as the LHS of the mass based continuity equation (A.57) when steady state is assumed, swapped for the RHS of the mass based continuity equation gives:

$$\frac{1}{\xi^{*2}}\frac{\partial \omega_i}{\partial \xi^*}(\xi^{*2}\rho^* v_\xi^*) = -\frac{1}{\xi^{*2}}\frac{\partial}{\partial \xi^*}(\xi^{*2}j_i^*) + R_i \frac{\xi_{ref}^2}{D_{ref}\rho_{ref}} \tag{D.7}$$

The second term is expanded and the equation is rearranged to reflect the implemented equation:

$$\frac{\partial \omega_i}{\partial \xi^*}(\rho^* v_\xi^*) + (\frac{2j_i^*}{\xi^*} + \frac{\partial j_i^*}{\partial \xi^*}) = R_i \frac{\xi_{ref}^2}{D_{ref}\rho_{ref}} \tag{D.8}$$

D.1.3 Mass based continuity equation

Velocity is obtained from the mass based continuity equation, starting out from the general equation (A.57)

$$\frac{\partial \rho^*}{\partial t^*} + \frac{1}{\xi^{*2}} \frac{\partial}{\partial \xi^*} (\xi^{*2} \rho^* v^*) = 0 \tag{D.9}$$

Steady state is assumed:

$$\frac{1}{\xi^{*2}} \frac{\partial}{\partial \xi^*} (\xi^{*2} \rho^* v^*) = 0 \tag{D.10}$$

The derivative term is expanded to reflect the used equation:

$$\frac{2}{\xi^*} v^* \rho^* + \frac{\partial \rho^*}{\partial \xi^*} v^* + \frac{\partial v^*}{\partial \xi^*} \rho^* = 0 \tag{D.11}$$

D.1.4 Wilke diffusion model

The general Wilke diffusion model as given in (A.58):

$$j_i^* = -\rho^* \frac{D_{im}}{D_{ref}} \frac{\partial \omega_i}{\partial \xi^*} \qquad D_{im} = \frac{1 - \omega_i}{\overline{M} \sum_{\substack{j=1 \\ j \neq i}}^{n} \frac{\omega_j}{M_j D_{ij}^e}} \tag{D.12}$$

Rearranged to the implemented form:

$$j_i^* \frac{D_{ref}}{D_{im} \rho^*} + \frac{\partial \omega_i}{\partial \xi^*} = 0 \qquad D_{im} = \frac{1 - \omega_i}{\overline{M} \sum_{\substack{j=1 \\ j \neq i}}^{n} \frac{\omega_j}{M_j D_{ij}^e}} \tag{D.13}$$

D.1.5 Wilke-Bosanquet diffusion model

$$j_i^* = -\rho^* \frac{D_{i,eff}}{D_{ref}} \frac{\partial \omega_i}{\partial \xi^*} \qquad \frac{1}{D_{i,eff}} = \frac{1}{D_{im}} + \frac{1}{D_{iK}^e} \tag{D.14}$$

Rearranged to the implemented form:

$$j_i^* \frac{D_{ref}}{D'_{i,eff} \rho^*} + \frac{\partial \omega_i}{\partial \xi^*} = 0 \qquad \frac{1}{D'_{i,eff}} = \frac{1}{\frac{1 - \omega_i}{\overline{M} \sum_{\substack{j=1 \\ j \neq i}}^{n} \frac{\omega_j}{M_j D_{ij}^e}}} + \frac{1}{D_{iK}^e} \tag{D.15}$$

D.1.6 Maxwell-Stefan diffusion model

The general Maxwell-Stefan model as given in (A.60):

$$j_i^* = \frac{\frac{-\rho^* \omega_i}{D_{ref}} \frac{1}{\overline{M}} \frac{\partial}{\partial \xi^*} (\overline{M}) - \frac{\rho^*}{D_{ref}} \frac{\partial \omega_i}{\partial \xi^*} + \overline{M} \omega_i \sum_{\substack{j=1 \\ j \neq i}}^{n} \frac{j_j^*}{M_j D_{ij}^e}}{\overline{M} \sum_{\substack{j=1 \\ j \neq i}}^{i} \frac{\omega_j}{M_j D_{ij}^e}} \tag{D.16}$$

Rearranged to the implemented form:

$$j_i^* \frac{\overline{M} D_{ref}}{\rho^*} \sum_{\substack{j=1 \\ j \neq i}}^{i} \frac{\omega_j}{M_j D_{ij}^e} + \frac{\partial \omega_i}{\partial \xi^*} = \frac{-\omega_i}{\overline{M}} \frac{\partial \overline{M}}{\partial \xi^*} + \frac{\overline{M} D_{ref}}{\rho^*} \omega_i \sum_{\substack{j=1 \\ j \neq i}}^{n} \frac{j_j^*}{M_j D_{ij}^e} \tag{D.17}$$

113

D.1.7 Dusty gas diffusion model

The general Maxwell-Stefan model as given in (A.61):

$$
j_i^* = \frac{\overline{M}^2 \sum_{\substack{j=1 \\ j \neq i}}^{n} \frac{\omega_i j_j^*}{M_j D_{ij}^e} - \frac{v^* \omega_i \overline{M}}{D_{iK}^e} - \frac{\omega_i \rho^*}{D_{ref}} \frac{\partial \overline{M}}{\partial \xi^*} - \frac{\rho^* \overline{M}}{D_{ref}} \frac{\partial \omega_i}{\partial \xi^*}}{\overline{M}^2 \sum_{\substack{j=1 \\ j \neq i}}^{n} \frac{\omega_j}{M_j D_{ij}^e} + \frac{\overline{M}}{D_{iK}^e}}
\tag{D.18}
$$

Rearranged to the implemented form:

$$
j_i^* \frac{D_{ref}}{\rho^*} \left(\overline{M} \sum_{\substack{j=1 \\ j \neq i}}^{n} \frac{\omega_j}{M_j D_{ij}^e} + \frac{1}{D_{iK}^e} \right) + \frac{\partial \omega_i}{\partial \xi^*} = \frac{\overline{M} D_{ref}}{\rho^*} \sum_{\substack{j=1 \\ j \neq i}}^{n} \frac{\omega_i j_j^*}{M_j D_{ij}^e} - \frac{v^* \omega_i D_{ref}}{D_{iK}^e \rho^*} - \frac{\omega_i}{\overline{M}} \frac{\partial \overline{M}}{\partial \xi^*}
\tag{D.19}
$$

D.1.8 Darcy's law

Darcy's law is used to obtain the pressure(A.38).

$$
\frac{v^* \mu D_{ref}}{B p_{ref}} + \frac{\partial p^*}{\partial \xi^*} = 0
\tag{D.20}
$$

D.1.9 Density equation

The density is obtained from modified ideal gas law:

$$
\frac{p \overline{M}}{RT} = \rho
\tag{D.21}
$$

D.2 Mass based solution strategy

The different equations are first discussed in short and the main summary of the solution strategy is given in table D.1. In the table the used equations combined with rigorous boundary conditions are shown. The solution strategy is also visualized in the form on how it would be implemented by the use of orthogonal collocation, shown in figure D.1.

D.2.1 Temperature equation

The temperature equation is solved in combination with Fourier's law in order to obtain two first order partial differential equations. Here the heat flux is obtained from the temperature equation and the temperature is obtained from Fourier's law. The temperature is specified at the surface for the Fourier's law with the included transfer limitation, while the flux is specified at the center of the particle for the temperature equation.The temperature can also be specified directly at the surface for the simple version of the boundary condition.

D.2.2 Species Mass balance and diffusion models

The species mass balance is solved to obtain the mass based fluxes. The mass based fluxes are then used to obtain the mass fractions throughout the catalyst particle using the different diffusion models. This is done for N-1 components for both the transport fluxes and the mass fractions, the last components is solved with a fitting constitutive law as seen in the solution strategy table. As boundary conditions the mass fractions are specified at the surface for the diffusion model with transfer limitations, while the fluxes are specified at the center for the species mass balance. As for the Fourier's law the mass fractions can be specified directly at the surface for a simple version of the boundary condition.

D.2.3 Mass averaged velocity

The mass averaged velocity is obtained from the mass based continuity equation, and the velocity is specified as a boundary condition at the center of the particle.

D.2.4 Pressure

The pressure is obtained from Darcy's law by the use of mass averaged velocity, and here the pressure is specified at the surface as a boundary condition.

D.2.5 Density

The density is obtained by the ideal gas law multiplied with averaged molecular weight. These values are obtained using previous iterative values and is solved outside of the matrix system.

Table D.1: Summary of the solution strategy

Equations, LHS represents terms in the problem matrix and the RHS represents the terms in the source vector:	Boundary conditions:
Fourier's law $$q^* + \frac{\partial T^*}{\partial \xi^*} = 0 \qquad (D.22)$$	Boundary condition at $\xi = \xi^p$ $$hT^* = \frac{q^*\lambda}{\xi_{ref}} + \rho Cp_g T^* v^* \frac{D_{ref}}{\xi_r ef} + h \qquad (D.23)$$
Temperature equation: $$\frac{D_{ref}}{\lambda}\rho^*\rho_{ref}v_\xi^*\sum_{i=1}^n \omega_i Cp_i \frac{\partial T^*}{\partial \xi^*} + (\frac{2q^*}{\xi^*} + \frac{\partial q^*}{\partial \xi^*}) = \\ \frac{\xi_{ref}^2(-\triangle H_R)R}{T_{ref}\lambda} \qquad (D.24)$$	Boundary condition at $\xi = 0$ $$q = 0 \qquad (D.25)$$
Species mass balance, used for N-1 components: $$\frac{\partial \omega_i}{\partial \xi^*}(\rho^* v_\xi^*) + (\frac{2j_i^*}{\xi^*} + \frac{\partial j_i^*}{\partial \xi^*}) = R_i \frac{\xi_{ref}^2}{D_{ref}\rho_{ref}} \qquad (D.26)$$	Boundary condition at $\xi = 0$ $$j_i = 0 \qquad (D.27)$$
Last flux(H2O) in the species balance is solved by: $$\sum_{i=1}^n j_i^* = 0 \qquad (D.28)$$	No boundary condition —
Diffusion model: One of the four diffusion models in table D.2 is used	Boundary condition at $\xi = \xi^p$: $$\omega_i = \frac{(j_i^* \frac{D_{ref}}{\xi_{ref}} + v^* \frac{D_{ref}}{\xi_{ref}}\rho^*\omega_i)}{k_i\rho^*} + \frac{\omega_i}{\rho^*} \qquad (D.29)$$
Last fraction(H2O) in the diffusion model is solved by: $$\sum_{i=1}^n \omega_i = 1 \qquad (D.30)$$	No boundary condition —
Mass based continuity equation: $$\frac{2}{\xi^*}v^* + \frac{\partial v^*}{\partial \xi^*} = -\frac{\partial \rho^*}{\partial \xi^*}\frac{v^*}{\rho^*} \qquad (D.31)$$	Boundary condition at $\xi = 0$ $$v^* = 0 \qquad (D.32)$$
Darcy's law: $$\frac{v^*\mu}{Bp_{ref}} + \frac{\partial p^*}{\partial \xi^*} = 0 \qquad (D.33)$$	Boundary condition at $\xi = \xi^p$ $$p = p^b \qquad (D.34)$$
Ideal gas law modified for density*: $$\frac{p\overline{M}}{RT} = \rho \qquad (D.35)$$	No boundary condition —
Mole averaged velocity * ** $$u - v = \sum_{i=1}^N \frac{j_i \overline{M}}{\rho M_i} \qquad (D.36)$$	No boundary condition —

*solved outside of the collocation matrix, i.e. purely based on previous iterative values ** Solved for comparison with the mole based model.

Table D.2: Diffusion models on their implemented form

LHS is implemented in the collocation matrix, and the RHS is implemented in the source vector

Wilke:

$$j_i^* \frac{D_{ref}}{D_{im}\rho^*} + \frac{\partial \omega_i}{\partial \xi^*} = 0 \qquad D_{im} = \frac{1 - \omega_i}{\overline{M} \sum_{\substack{j=1 \\ j \neq i}}^{n} \frac{\omega_j}{M_j D_{ij}^e}} \tag{D.37}$$

Wilke-Bosanquet:

$$j_i^* \frac{D_{ref}}{D_{i,eff}\rho^*} + \frac{\partial \omega_i}{\partial \xi^*} = 0 \qquad \frac{1}{D_{i,eff}} = \frac{1}{\frac{1-\omega_i}{\overline{M} \sum_{\substack{j=1 \\ j \neq i}}^{n} \frac{\omega_j}{M_j D_{ij}^e}}} + \frac{1}{D_{iK}^e} \tag{D.38}$$

Maxwell-Stefan:

$$j_i^* \frac{\overline{M} D_{ref}}{\rho^*} \sum_{\substack{j=1 \\ j \neq i}}^{i} \frac{\omega_j}{M_j D_{ij}^e} + \frac{\partial \omega_i}{\partial \xi^*} = \frac{-\omega_i}{\overline{M}} \frac{\partial \overline{M}}{\partial \xi^*} + \frac{\overline{M} D_{ref}}{\rho^*} \omega_i \sum_{\substack{j=1 \\ j \neq i}}^{n} \frac{j_j^*}{M_j D_{ij}^e} \tag{D.39}$$

Dusty gas:

$$j_i^* \frac{D_{ref}}{\rho^*} (\overline{M} \sum_{\substack{j=1 \\ j \neq i}}^{n} \frac{\omega_j}{M_j D_{ij}^e} + \frac{1}{D_{iK}^e}) + \frac{\partial \omega_i}{\partial \xi^*} = \frac{\overline{M} D_{ref}}{\rho^*} \sum_{\substack{j=1 \\ j \neq i}}^{n} \frac{\omega_i j_j^*}{M_j D_{ij}^e} - \frac{\omega_i}{\overline{M}} \frac{\partial \overline{M}}{\partial \xi^*} \tag{D.40}$$

$$
\begin{bmatrix}
1\bullet & \frac{\partial}{\partial\xi^*} & 0 & 0 & 0 & 0 & 0 & 0 & 0 & 0 & 0 & 0 & 0 & 0 & 0 & 0 \\
X_1 & T_1 & 0 & 0 & 0 & 0 & 0 & 0 & 0 & 0 & 0 & 0 & 0 & 0 & 0 & 0 \\
0 & 0 & DM_1\bullet & 0 & 0 & 0 & 0 & 0 & \frac{\partial}{\partial\xi^*} & 0 & 0 & 0 & 0 & 0 & 0 & 0 \\
0 & 0 & 0 & DM_1\bullet & 0 & 0 & 0 & 0 & 0 & \frac{\partial}{\partial\xi^*} & 0 & 0 & 0 & 0 & 0 & 0 \\
0 & 0 & 0 & 0 & DM_1\bullet & 0 & 0 & 0 & 0 & 0 & \frac{\partial}{\partial\xi^*} & 0 & 0 & 0 & 0 & 0 \\
0 & 0 & 0 & 0 & 0 & DM_1\bullet & 0 & 0 & 0 & 0 & 0 & \frac{\partial}{\partial\xi^*} & 0 & 0 & 0 & 0 \\
0 & 0 & 0 & 0 & 0 & 0 & DM_1\bullet & 0 & 0 & 0 & 0 & 0 & \frac{\partial}{\partial\xi^*} & 0 & 0 & 0 \\
0 & 0 & 1\bullet & 1\bullet & 1\bullet & 1\bullet & 1\bullet & 1\bullet & 0 & 0 & 0 & 0 & 0 & 0 & 0 & 0 \\
0 & 0 & SB_1\bullet & 0 & 0 & 0 & 0 & 0 & 1\bullet & 0 & 0 & 0 & 0 & 0 & X_1 & 0 \\
0 & 0 & 0 & SB_1\bullet & 0 & 0 & 0 & 0 & 0 & 1\bullet & 0 & 0 & 0 & 0 & X_1 & 0 \\
0 & 0 & 0 & 0 & SB_1\bullet & 0 & 0 & 0 & 0 & 0 & 1\bullet & 0 & 0 & 0 & X_1 & 0 \\
0 & 0 & 0 & 0 & 0 & SB_1\bullet & 0 & 0 & 0 & 0 & 0 & 1\bullet & 0 & 0 & X_1 & 0 \\
0 & 0 & 0 & 0 & 0 & 0 & SB_1\bullet & 0 & 0 & 0 & 0 & 0 & 1\bullet & 0 & X_1 & 0 \\
0 & 0 & 0 & 0 & 0 & 0 & 0 & 0 & 1\bullet & 1\bullet & 1\bullet & 1\bullet & 1\bullet & 1\bullet & 0 & 0 \\
0 & 0 & 0 & 0 & 0 & 0 & 0 & 0 & 0 & 0 & 0 & 0 & 0 & 0 & X_1 & 0 \\
0 & 0 & 0 & 0 & 0 & 0 & 0 & 0 & 0 & 0 & 0 & 0 & 0 & 0 & Dl_1\bullet & \frac{\partial}{\partial\xi^*}
\end{bmatrix}
\begin{bmatrix}
q^* \\ T^* \\ j_{CH_4} \\ j_{CO} \\ j_{CO_2} \\ j_{H_2} \\ j_{N_2} \\ j_{H_2O} \\ \omega_{CH_4} \\ \omega_{CO} \\ \omega_{CO_2} \\ \omega_{H_2} \\ \omega_{N_2} \\ \omega_{H_2O} \\ v^* \\ p^*
\end{bmatrix}
=
\begin{bmatrix}
0 \\ T_2 \\ DM_2 \\ DM_2 \\ DM_2 \\ DM_2 \\ DM_2 \\ 0 \\ SB_2 \\ SB_2 \\ SB_2 \\ SB_2 \\ SB_2 \\ 1 \\ MC_1 \\ 0
\end{bmatrix}
$$

Figure D.1: Collocation matrix, mass based. Explanation on the labeled terms for the problem matrix can be seen in table D.3 while the explanation for the source vector term is found in table D.4

Table D.3: Terms in the collocation matrix

Label in matrix	Collocation matrix terms:	multiplied with:
X_1	$$\frac{2}{\xi^*} + \frac{\partial}{\partial \xi^*}$$	q^*, ω_i, v^*
T_1	$$\frac{D_{ref}}{\lambda} \rho^* \rho_{ref} v_\xi^* \sum_{i=1}^{n} \omega_i Cp_i \frac{\partial}{\partial \xi^*}$$	T^*
DM_1	Wilke: $$\frac{D_{ref}}{D_{im}\rho^*}$$	j_i^*
DM_1	Wilke-Bosanquet: $$\frac{D_{ref}}{D_{i,eff}\rho^*}$$	j_i^*
DM_1	Maxwell-Stefan: $$\frac{\overline{M} D_{ref}}{\rho^*} \sum_{\substack{j=1 \\ j \neq i}}^{i} \frac{\omega_j}{M_j D_{ij}^e}$$	j_i^*
DM_1	Dusty gas: $$\frac{D_{ref}}{\rho^*}\left(\overline{M} \sum_{\substack{j=1 \\ j \neq i}}^{n} \frac{\omega_j}{M_j D_{ij}^e} + \frac{1}{D_{iK}^e}\right)$$	j_i^*
SB_1	$$\rho^* v_\xi^* \frac{\partial}{\partial \xi^*}$$	ω_i
Dl_1	$$\frac{\mu}{B p_{ref}}$$	v^*

Table D.4: Terms in the source vector

Label in source vector	Source vector
T_2	Source term temperature equation: $$\frac{-\triangle H_r \xi_{ref}^2}{T_{ref}\lambda}$$
DM_2	Wilke: $$0$$
DM_2	Wilke-Bosanquet: $$0$$
DM_2	Maxwell-Stefan: $$\frac{-\omega_i}{\overline{M}}\frac{\partial \overline{M}}{\partial \xi^*} + \frac{\overline{M}D_{ref}}{\rho^*}\omega_i \sum_{\substack{j=1 \\ j\neq i}}^{n} \frac{j_j^*}{M_j D_{ij}^e}$$
DM_2	Dusty gas: $$\frac{\overline{M}D_{ref}}{\rho^*}\sum_{\substack{j=1 \\ j\neq i}}^{n}\frac{\omega_i j_j^*}{M_j D_{ij}^e} - \frac{\omega_i}{\overline{M}}\frac{\partial \overline{M}}{\partial \xi^*}$$
SB_2	Source term species balance: $$R_i\frac{\xi_{ref}^2}{D_{ref}\rho_{ref}}$$
MC_1	Source term continuity equation: $$-\frac{\partial \rho^*}{\partial \xi^*}\frac{v^*}{\rho^*}$$

D.3   Mole based model

D.3.1   The temperature balance

The general temperature balance derived earlier (A.63):

$$((1-\epsilon)\rho_p Cp_p + \epsilon c^* c_{ref} \sum_{i=1}^{n} x_i Cp_i') \frac{\partial T^*}{\partial t^*} =$$

$$-c^* c_{ref} v_\xi^* \sum_{i=1}^{n} x_i Cp_i' \frac{\partial T^*}{\partial \xi^*} - \frac{(\frac{2q^*}{\xi^*} + \frac{\partial q^*}{\partial \xi^*})\lambda}{D_{ref}} + \frac{\xi_{ref}^2 (-\triangle H_R) R}{D_{ref} T_{ref}}$$

(D.41)

Steady state is assumed:

$$0 = -c^* c_{ref} v_\xi^* \sum_{i=1}^{n} x_i Cp_i' \frac{\partial T^*}{\partial \xi^*} - \frac{(\frac{2q^*}{\xi^*} + \frac{\partial q^*}{\partial \xi^*})\lambda}{D_{ref}} + \frac{\xi_{ref}^2 (-\triangle H_R) R}{D_{ref} T_{ref}}$$

(D.42)

The equation is rearranged and the used equation is given as:

$$\frac{D_{ref}}{\lambda} c^* c_{ref} v_\xi^* \sum_{i=1}^{n} x_i Cp_i' \frac{\partial T^*}{\partial \xi^*} + (\frac{2q^*}{\xi^*} + \frac{\partial q^*}{\partial \xi^*}) = \frac{\xi_{ref}^2 (-\triangle H_R) R}{T_{ref}\lambda}$$

(D.43)

D.3.2   Species mole balance

The mole based fluxes are obtained from the species mole balance. The general dimensionless equation is given as derived earlier (A.62):

$$\frac{\partial}{\partial t^*}(c^* x_i) + \frac{1}{\xi^{*2}} \frac{\partial}{\partial \xi^*}(\xi^{*2} c^* x_i u_\xi^*) = -\frac{1}{\xi^{*2}} \frac{\partial}{\partial \xi^*}(\xi^{*2} J_i^*) + R_i' \frac{\xi_{ref}^2}{D_{ref} c_{ref}}$$

(D.44)

Steady state is assumed.

$$\frac{1}{\xi^{*2}} \frac{\partial}{\partial \xi^*}(\xi^{*2} c^* x_i u_\xi^*) = -\frac{1}{\xi^{*2}} \frac{\partial}{\partial \xi^*}(\xi^{*2} J_i^*) + R_i' \frac{\xi_{ref}^2}{D_{ref} c_{ref}}$$

(D.45)

The first term is written out to identify the continuity equation.

$$\frac{1}{\xi^{*2}} \frac{\partial x_i}{\partial \xi^*}(\xi^{*2} c^* u_\xi^*) + x_i \frac{1}{\xi^{*2}} \frac{\partial}{\partial \xi^*}(\xi^{*2} c^* u_\xi^*) = -\frac{1}{\xi^{*2}} \frac{\partial}{\partial \xi^*}(\xi^{*2} J_i^*) + R_i' \frac{\xi_{ref}^2}{D_{ref} c_{ref}}$$

(D.46)

The second term is identified as the LHS of the mole based continuity equation (A.64) when steady state is assumed, swapped for the RHS of the mole based continuity equation gives:

$$\frac{1}{\xi^{*2}} \frac{\partial x_i}{\partial \xi^*}(\xi^{*2} c^* u_\xi^*) + x_i (\frac{\xi_{ref}^2}{c_{ref} D_{ref}}) \sum_{i=1}^{n} R_i' = -\frac{1}{\xi^{*2}} \frac{\partial}{\partial \xi^*}(\xi^{*2} J_i^*) + R_i' \frac{\xi_{ref}^2}{D_{ref} c_{ref}}$$

(D.47)

Expanding the third term and rearranging the equation to reflect the equation used in the model:

$$\frac{\partial x_i}{\partial \xi^*}(c^* u_\xi^*) + (\frac{2J_i^*}{\xi^*} + \frac{\partial J_i^*}{\partial \xi^*}) = (R_i' - x_i \sum_{i=1}^{n} R_i') \frac{\xi_{ref}^2}{D_{ref} c_{ref}}$$

(D.48)

D.3.3   Continuity equation - Mole based

$$\frac{\partial c^*}{\partial t^*} + \frac{1}{\xi^{*2}}\frac{\partial}{\partial \xi^*}(\xi^{*2}c^*u_\xi^*) = \left(\frac{\xi_{ref}^2}{c_{ref}D_{ref}}\right)\sum_{i=1}^{n}R_i' \tag{D.49}$$

Steady state is assumed:

$$\frac{1}{\xi^{*2}}\frac{\partial}{\partial \xi^*}(\xi^{*2}c^*u_\xi^*) = \left(\frac{\xi_{ref}^2}{c_{ref}D_{ref}}\right)\sum_{i=1}^{n}R_i' \tag{D.50}$$

The derivative is expanded which gives the used equation:

$$\frac{2}{\xi^*}c^*u^* + \frac{\partial c^*}{\partial \xi^*}u^* + \frac{\partial u^*}{\partial \xi^*}c^* = \left(\frac{\xi_{ref}^2}{c_{ref}D_{ref}}\right)\sum_{i=1}^{n}R_i' \tag{D.51}$$

D.3.4   Darcy's law

Darcy's law is used to obtain the pressure(A.38).

$$\frac{v^*\mu D_{ref}}{Bp_{ref}} + \frac{\partial p^*}{\partial \xi^*} = 0 \tag{D.52}$$

D.3.5   Wilke diffusion model

The general Wilke diffusion model on mole basis as given in A.65:

$$J_i^* = -c^*D_{im}'\frac{\partial x_i}{\partial \xi^*} \qquad D_{im}' = \frac{1-x_i}{\sum_{\substack{j=1\\j\neq i}}^{n}\frac{x_j}{D_{ij}^e}} \tag{D.53}$$

Rearranged to the implemented form:

$$J_i^*\frac{D_{ref}}{c^*D_{im}'} + \frac{\partial x_i}{\partial \xi^*} = 0 \qquad D_{im}' = \frac{1-x_i}{\sum_{\substack{j=1\\j\neq i}}^{n}\frac{x_j}{D_{ij}^e}} \tag{D.54}$$

D.3.6   Wilke-Bosanquet diffusion model

$$J_i^* = -c^*\frac{D_{i,eff}'}{D_{ref}}\frac{\partial x_i}{\partial \xi^*} \qquad \frac{1}{D_{i,eff}'} = \frac{1}{D_{im}'} + \frac{1}{D_{iK}^e} \tag{D.55}$$

Rearranged to the implemented form:

$$J_i^*\frac{D_{ref}}{D_{i,eff}'c^*} + \frac{\partial x_i}{\partial \xi^*} = 0 \qquad \frac{1}{D_{i,eff}'} = \frac{1}{\frac{1-x_i}{\sum_{\substack{j=1\\j\neq i}}^{n}\frac{x_j}{D_{ij}^e}}} + \frac{1}{D_{iK}^e} \tag{D.56}$$

D.3.7 Maxwell-Stefan diffusion model

The general Maxwell-Stefan model on mole basis as given in A.67:

$$j_i^* = \frac{-c^* \frac{\partial x_i}{\partial \xi^*} + \sum_{\substack{j=1 \\ j \neq i}}^{n} \frac{j_j^* x_i}{D_{ij}^e}}{\sum_{\substack{j=1 \\ j \neq i}}^{i} \frac{x_j}{D_{ij}^e}} \tag{D.57}$$

Rearranged to the implemented form:

$$\frac{j_i^* D_{ref}}{c^*} \sum_{\substack{j=1 \\ j \neq i}}^{i} \frac{x_j}{D_{ij}^e} + \frac{\partial x_i}{\partial \xi^*} = \frac{D_{ref}}{c^*} \sum_{\substack{j=1 \\ j \neq i}}^{n} \frac{j_j^* x_i}{D_{ij}^e} \tag{D.58}$$

D.3.8 Dusty gas diffusion model

The general dusty gas model on mole basis as given in A.68:

$$J_i^* = \frac{-\frac{c^*}{D_{ref}} \frac{\partial x_i}{\partial \xi^*} + \sum_{\substack{j=1 \\ j \neq i}}^{n} \frac{J_j^* x_i}{D_{ij}^e} - \frac{c^* x_i u^*}{D_{iK}^e}}{\sum_{\substack{j=1 \\ j \neq i}}^{i} \frac{x_j}{D_{ij}^e} + \frac{1}{D_{iK}^e}} \tag{D.59}$$

Rearranged to the implemented form:

$$J_i^* \frac{D_{ref}}{c^*} \left(\sum_{\substack{j=1 \\ j \neq i}}^{i} \frac{x_j}{D_{ij}^e} + \frac{1}{D_{iK}^e} \right) = -\frac{\partial x_i}{\partial \xi^*} + \frac{D_{ref}}{c^*} \sum_{\substack{j=1 \\ j \neq i}}^{n} \frac{J_j^* x_i}{D_{ij}^e} - \frac{D_{ref} x_i u^*}{D_{iK}^e} \tag{D.60}$$

D.3.9 Concentration equation

The concentration is obtained from the ideal gas law.

$$\frac{p}{RT} = c \tag{D.61}$$

D.4   Mole based solution strategy

The different equations are first discussed in short and the main summary of the solution strategy is given in table D.5. In the table the used equations combined with rigorous boundary conditions are shown. The solution strategy is also visualized in the form on how it would be implemented by the use of orthogonal collocation, shown in figure D.2.

D.4.1   Temperature equation

The temperature equation is solved in combination with Fourier's law in order to obtain two first order partial differential equations. Here the heat flux is obtained from the temperature equation and the temperature is obtained from Fourier's law. The temperature is specified at the surface for the Fourier's law with the included transfer limitation, while the flux is specified at the center of the particle for the temperature equation.The temperature can also be specified directly at the surface for the simple version of the boundary condition.

D.4.2   Species Mole balance and diffusion models

The species mole balance is solved to obtain the mole based fluxes. The mole based fluxes are then used to obtain the mole fractions throughout the catalyst particle using the different diffusion models. This is done for N-1 components for both the transport fluxes and the mole fractions, the last components is solved with a fitting constitutive law as seen in the solution strategy table. As boundary conditions the mole fractions are specified at the surface for the diffusion model with transfer limitations, while the fluxes are specified at the center for the species mole balance. As for the Fourier's law the mole fractions can be specified directly at the surface for a simple version of the boundary condition.

D.4.3   Mole and mass averaged velocity

The mole averaged velocity is obtained from the mole based continuity equation, and the velocity is specified as a boundary condition at the center of the particle. The averaged mass based velocity needed for the temperature and pressure equation is obtained from the mole based transport fluxes.

D.4.4   Pressure

The pressure is obtained from Darcy's law by the use of mass averaged velocity, and here the pressure is specified at the surface as a boundary condition.

D.4.5   Concentration

The total concentration is obtained from the ideal gas law.

Table D.5: Summary of the solution strategy

Equations, LHS represents terms in the problem matrix and the RHS represents the terms in the source vector:	Boundary conditions:
Fourier's law $$q^* + \frac{\partial T^*}{\partial \xi^*} = 0 \qquad (D.62)$$	Boundary condtion at $\xi = \xi^p$ $$hT^* = \frac{q^*\lambda}{\xi_{ref}} + cCp'_g T^* v^* \frac{D_{ref}}{\xi_{ref}} + h \qquad (D.63)$$
Temperature equation: $$\frac{D_{ref}}{\lambda} c^* c_{ref} v^*_\xi \sum_{i=1}^{n} x_i Cp'_i \frac{\partial T^*}{\partial \xi^*} + (\frac{2q^*}{\xi^*} + \frac{\partial q^*}{\partial \xi^*}) = \frac{\xi^2_{ref}(-\triangle H_R)R}{T_{ref}\lambda} \qquad (D.64)$$	Boundary condtition at $\xi = 0$ $$q = 0 \qquad (D.65)$$
Species mole balance, solved for N-1 components: $$\frac{\partial x_i}{\partial \xi^*}(c^* u^*_\xi) + (\frac{2J^*_i}{\xi^*} + \frac{\partial J^*_i}{\partial \xi^*}) = (R'_i - x_i \sum_{i=1}^{n} R'_i)\frac{\xi^2_{ref}}{D_{ref}c_{ref}} \qquad (D.66)$$	Boundary condition at $\xi = 0$ $$J_i = 0 \qquad (D.67)$$
Last flux(H2O) in the species balance is solved by: $$\sum_{i=1}^{n} J^*_i = 0 \qquad (D.68)$$	No boundary condition $$-$$
Diffusion mode, solved for N-1 componentsl: One of the four diffusion models in table D.6 is used	Boundary condition at $\xi = \xi^p$: $$x_i = \frac{(J^*_i \frac{D_{ref}}{\xi_{ref}} + u^* \frac{D_{ref}}{\xi_{ref}} c^* x_i)}{k_i c^*} + \frac{\omega_i}{c^*} \qquad (D.69)$$
Last fraction(H2O) in the diffusion model is solved by: $$\sum_{i=1}^{n} x_i = 1 \qquad (D.70)$$	No boundary condition $$-$$
Continuity equation mole based: $$\frac{2}{\xi^*} c^* u^* + \frac{\partial c^*}{\partial \xi^*} u^* + \frac{\partial u^*}{\partial \xi^*} c^* = (\frac{\xi^2_{ref}}{c_{ref}D_{ref}}) \sum_{i=1}^{n} R'_i \quad (D.71)$$	Boundary condition at $\xi = 0$ $$u = 0 \qquad (D.72)$$
Mass averaged velocity*: $$v^* = \sum_{i=1}^{N} \frac{J^*_i M_i}{c^*_i \overline{M}} + u^* \qquad (D.73)$$	No boundary condition $$-$$
Ideal gas law , algebraic: $$c = \frac{p}{RT} \qquad (D.74)$$	No boundary condition $$-$$
Pressure, Darcy's law $$\frac{\partial p^*}{\partial \xi^*} = -\frac{v^*\mu D_{ref}}{Bp_{ref}} \qquad (D.75)$$	Boundary condition at $\xi = \xi^p$: $$p = p^b \qquad (D.76)$$

*Solved outside of the collocation matrix

Table D.6: Diffusion models on their implemented form

LHS is implemented in the collocation matrix, and the RHS is implemented in the source vector

Wilke:

$$J_i^* \frac{D_{ref}}{c^* D_{im}'} + \frac{\partial x_i}{\partial \xi^*} = 0 \qquad D_{im}' = \frac{1 - x_i}{\sum_{\substack{j=1 \\ j \neq i}}^{n} \frac{x_j}{D_{ij}^e}} \qquad (D.77)$$

Wilke-Bosanquet:

$$j_i^* \frac{D_{ref}}{D_{i,eff}' c^*} + \frac{\partial x_i}{\partial \xi^*} = 0 \qquad \frac{1}{D_{i,eff}'} = \frac{1}{\frac{1 - x_i}{\sum_{\substack{j=1 \\ j \neq i}}^{n} \frac{x_j}{D_{ij}^e}}} + \frac{1}{D_{iK}^e} \qquad (D.78)$$

Maxwell-Stefan:

$$\frac{j_i^* D_{ref}}{c^*} \sum_{\substack{j=1 \\ j \neq i}}^{i} \frac{x_j}{D_{ij}^e} + \frac{\partial x_i}{\partial \xi^*} = \frac{D_{ref}}{c^*} \sum_{\substack{j=1 \\ j \neq i}}^{n} \frac{j_j^* x_i}{D_{ij}^e} \qquad (D.79)$$

Dusty gas:

$$J_i^* \frac{D_{ref}}{c^*} (\sum_{\substack{j=1 \\ j \neq i}}^{i} \frac{x_j}{D_{ij}^e} + \frac{1}{D_{iK}^e}) + \frac{\partial x_i}{\partial \xi^*} = \frac{D_{ref}}{c^*} \sum_{\substack{j=1 \\ j \neq i}}^{n} \frac{J_j^* x_i}{D_{ij}^e} - \frac{D_{ref} x_i u^*}{D_{iK}^e} \qquad (D.80)$$

Figure D.2: Collocation matrix, mole based. Explanation on the labeled terms for the problem matrix can be seen in table D.7 while the explanation for the source vector term is found in table D.8

Table D.7: Terms in the collocation matrix

Label in matrix	Collocation matrix terms:	multiplied with:
X_1	$\dfrac{2}{\xi^*} + \dfrac{\partial}{\partial \xi^*}$	q^*, x_i, u^*
T_1	$\dfrac{D_{ref}}{\lambda} \rho^* \rho_{ref} v_\xi^* \sum\limits_{i=1}^{n} \omega_i Cp_i \dfrac{\partial}{\partial \xi^*}$	T^*
DM_1	Wilke: $\dfrac{D_{ref}}{D'_{im} c^*}, \quad D_{im} = \dfrac{1 - x_i}{\sum\limits_{\substack{j=1 \\ j \neq i}}^{n} \frac{x_j}{D_{ij}^e}}$	J_i^*
DM_1	Wilke-Bosanquet: $\dfrac{D_{ref}}{D'_{i,eff} c^*}, \quad \dfrac{1}{D'_{i,eff}} = \dfrac{1}{\frac{1 - x_i}{\sum\limits_{\substack{j=1 \\ j \neq i}}^{n} \frac{x_j}{D_{ij}^e}}} + \dfrac{1}{D_{iK}^e}$	J_i^*
DM_1	Maxwell-Stefan: $\dfrac{D_{ref}}{c^*} \sum\limits_{\substack{j=1 \\ j \neq i}}^{i} \dfrac{x_j}{D_{ij}^e}$	J_i^*
DM_1	Dusty gas: $\dfrac{D_{ref}}{c^*} \left(\sum\limits_{\substack{j=1 \\ j \neq i}}^{i} \dfrac{x_j}{D_{ij}^e} + \dfrac{1}{D_{iK}^e} \right)$	J_i^*
SB_1	$c^* u_\xi^* \dfrac{\partial}{\partial \xi^*}$	x_i
MC_1	$u^* \dfrac{\partial}{\partial \xi^*}$	c^*

Table D.8: Terms in the source vector

Label in source vector	Source vector
T_2	Source term temperature equation: $$\frac{-\triangle H_r \xi_{ref}^2}{T_{ref}\lambda}$$
DM_2	Wilke: $$0$$
DM_2	Wilke-Bosanquet: $$0$$
DM_2	Maxwell-Stefan: $$\frac{D_{ref}}{c^*}\sum_{\substack{j=1 \\ j\neq i}}^{n}\frac{J_j^* x_i}{D_{ij}^e}$$
DM_2	Dusty gas: $$\frac{D_{ref}}{c^*}\sum_{\substack{j=1 \\ j\neq i}}^{n}\frac{J_j^* x_i}{D_{ij}^e} - \frac{D_{ref}x_i u^*}{D_{iK}^e}$$
SB_2	Source term species balance: $$(R_i' - x_i\sum_{i=1}^{n}R_i')\frac{\xi_{ref}^2}{D_{ref}c_{ref}}$$
MC_2	Source term continuity equation: $$(\frac{\xi_{ref}^2}{c_{ref}D_{ref}})\sum_{i=1}^{n}R_i'$$
Dl_1	Source term Darcy's law: $$-\frac{v^*\mu D_{ref}}{Bp_{ref}}$$

D.5   Additional results

D.5.1   Wilke - No transfer limitations
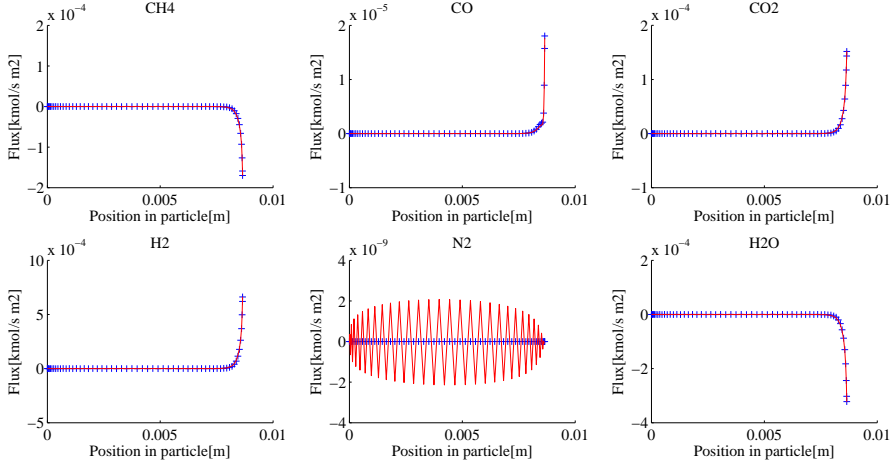
Figure D.3:   Comparison of the transport fluxes, mole based(—) and mass based(+++).

D.5.2   Wilke - Rigorous
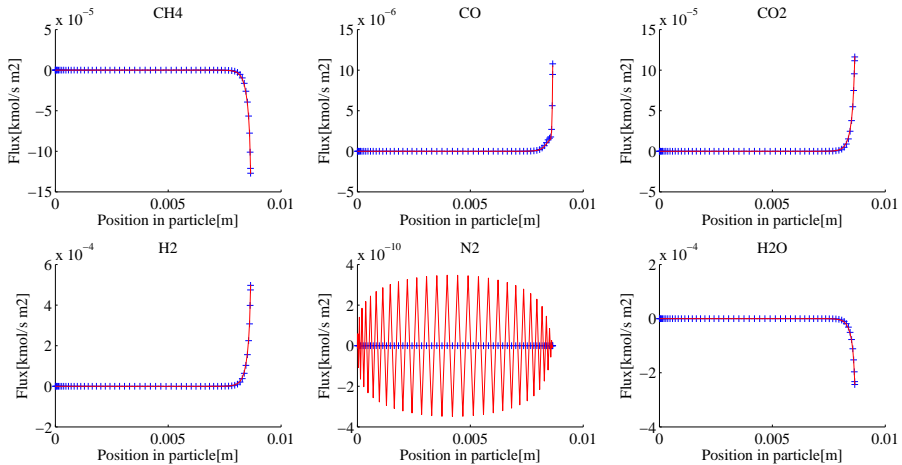
Figure D.4:   Comparison of the transport fluxes, mole based(—) and mass based(+++).

D.5.3 Wilke-Bosanquet - No transfer limitations
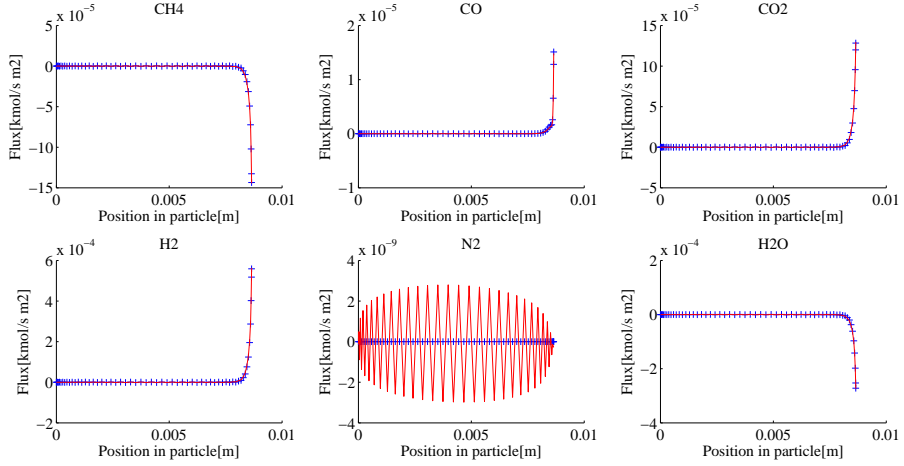
Figure D.5: Comparison of the transport fluxes, mole based(—) and mass based(+++).

D.5.4 Wilke-Bosanquet - Rigorous
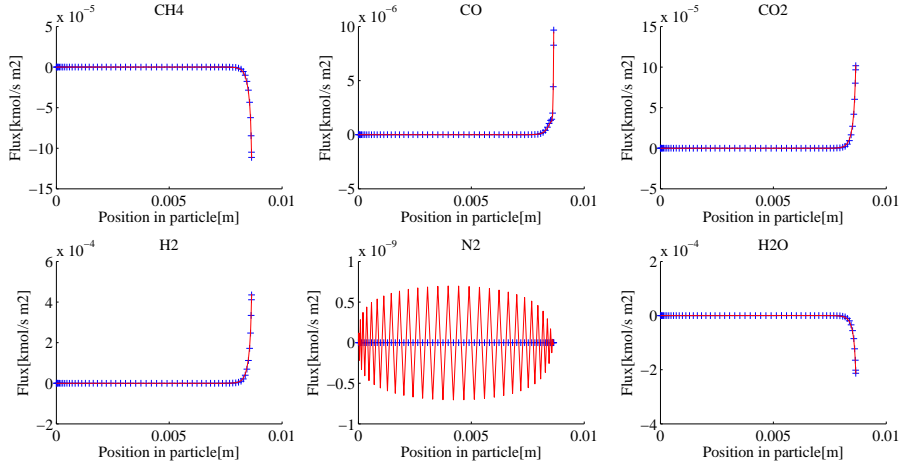
Figure D.6: Comparison of the transport fluxes, mole based(—) and mass based(+++).

D.5.5 Maxwell-Stefan - No transfer limitations
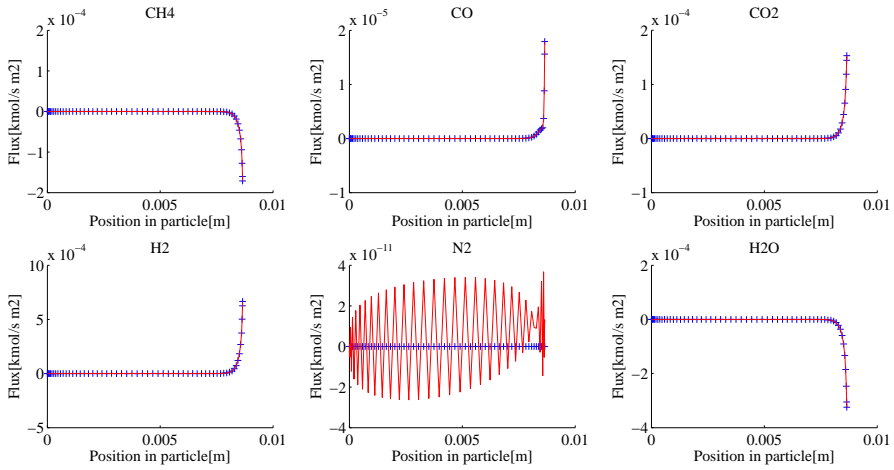
Figure D.7: Comparison of the transport fluxes, mole based(—) and mass based(+++).

D.5.6 Maxwell-Stefan - Rigorous
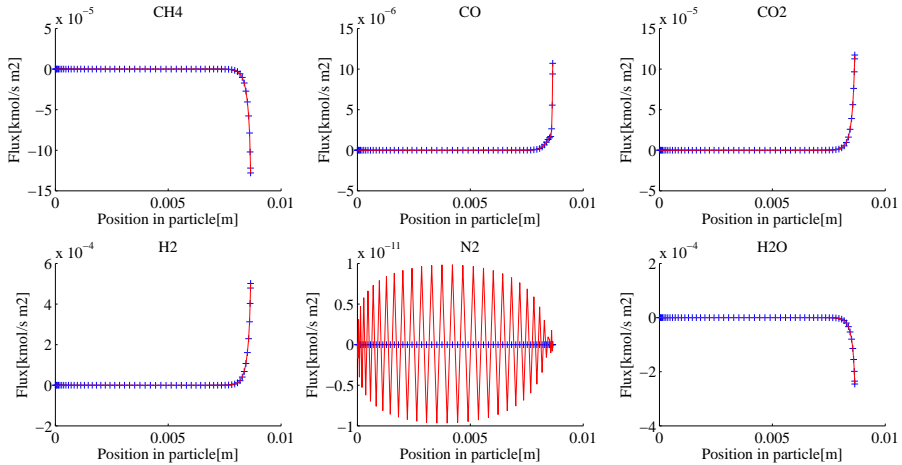
Figure D.8: Comparison of the transport fluxes, mole based(—) and mass based(+++).

D.5.7 Dusty gas - No transfer limitations
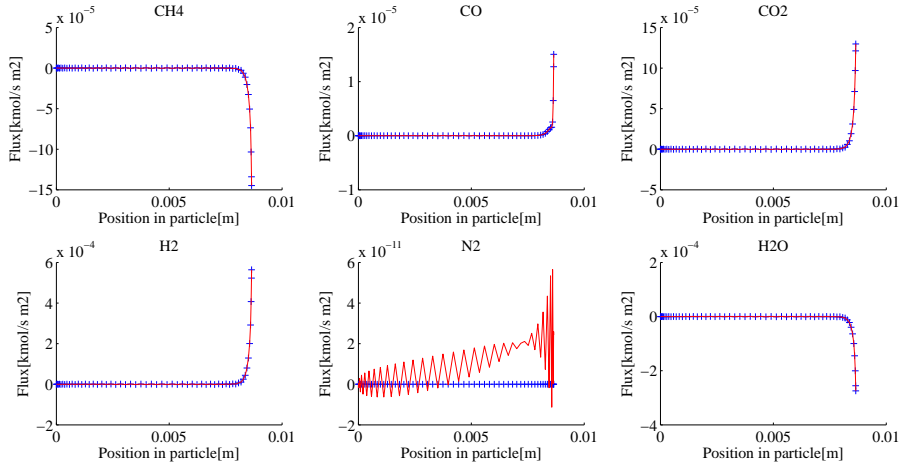
Figure D.9: Comparison of the transport fluxes, mole based(—) and mass based(+++).

D.5.8 Dusty gas - Rigorous
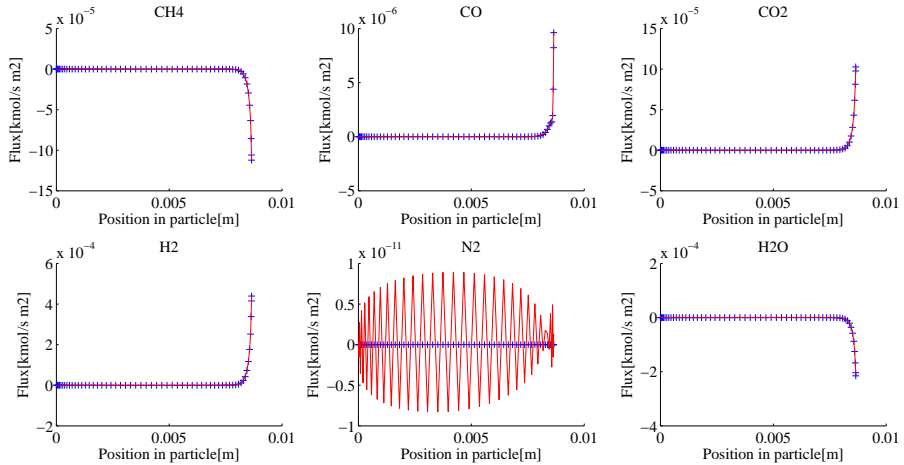
Figure D.10: Comparison of the transport fluxes, mole based(—) and mass based(+++).

D.5.9   Pressure plots - No transfer limitations
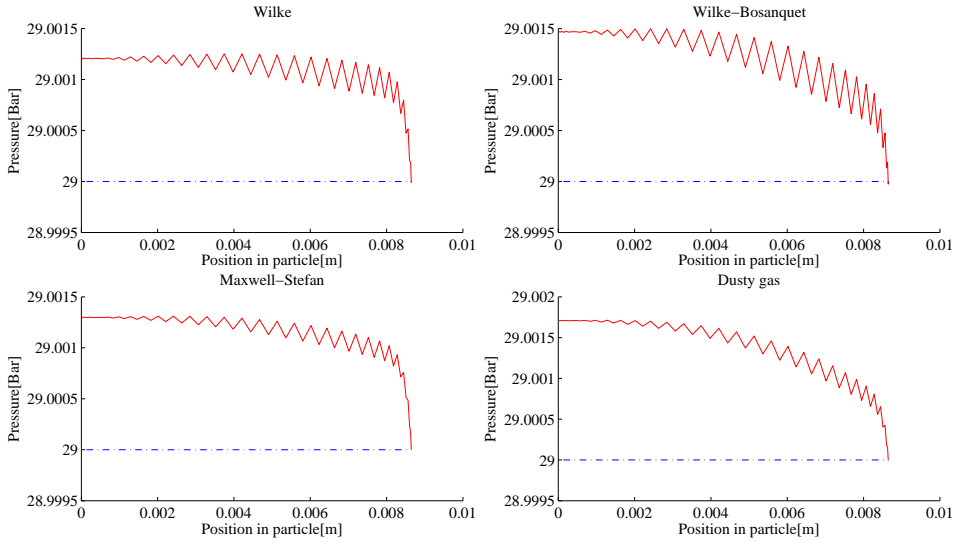
Figure D.11: Comparison of the pressure development for the different diffusion models, mole based(—) and mass based(-.-.-).

D.5.10   Pressure plots - Rigorous
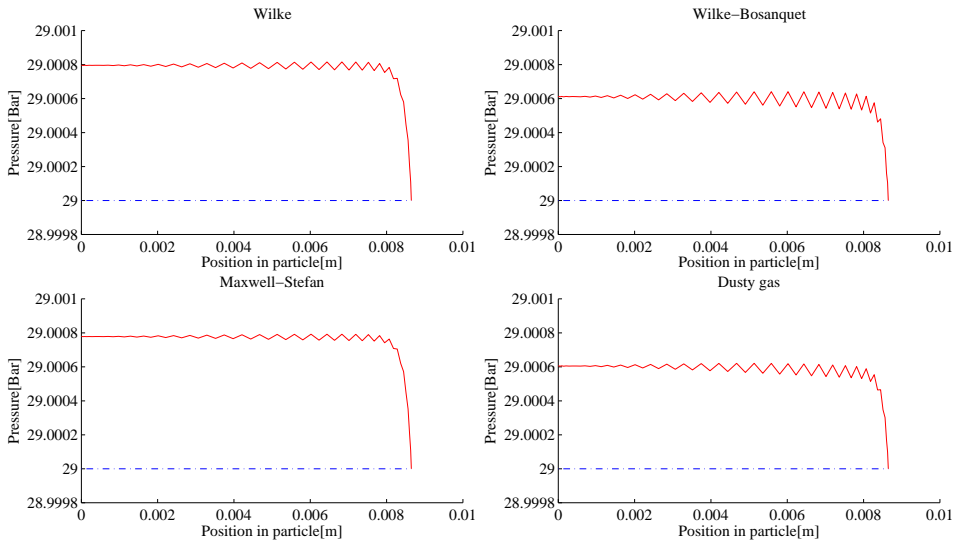
Figure D.12: Comparison of the pressure development for the different diffusion models, mole based(—) and mass based(-.-.-).

E   6 Alternative rigorous steady state Wilke model

Here the alternative species balance equations used in the alternative Wilke models be derived. The model is quite similar to the rigorous steady state cases. However the affected equations are derived and a swappable solution strategy is presented. The mass and mole based rigorous steady state solution strategy in table D.1 and D.5 can be swapped with the model considering corrective fluxes in table E.2 and E.1 respectively.

E.1   Mass based alternative Wilke model using corrective velocities

E.1.1   The species mass balance

The difference from the already used equation is that the species balance is to be corrected an additional corrective convective term v_c. with:

$$v_c = \sum_i D_{im} \nabla \omega_i \tag{E.1}$$

Introducing the new term, $v_{cor} = v_\xi + v_c$ and inserting the correction gives the same species balance and continuity equation as obtained in the model derivation for the rigorous models in appendix D, but now with a corrected velocity instead:

Species balance with corrected velocity:

$$\frac{\partial \omega_i}{\partial \xi^*}(\rho^* v_{cor}^*) + \left(\frac{2j_i^*}{\xi^*} + \frac{\partial j_i^*}{\partial \xi^*}\right) = R_i \frac{\xi_{ref}^2}{D_{ref}\rho_{ref}} \tag{E.2}$$

E.1.2   Continuity eqution with corrected velocity

As for the species mass balance, the velocity term is replaced with the new corrected velocity term:

$$\frac{2}{\xi^*} v_{cor}^* \rho^* + \frac{\partial \rho^*}{\partial \xi^*} v_{cor}^* + \frac{\partial v_{cor}^*}{\partial \xi^*} \rho^* = 0 \tag{E.3}$$

E.1.3   Temperature equation and Darcy's law

In order to only include the correction for the species balance and the continuity equation, it is needed to subtract the corrective term for the temperature equation and Darcy's law. The used velocity in the temperature equation and Darcy's law will be defined as $v^* = v_{cor}^* - v_c^*$.

Temperature equation:

$$\frac{D_{ref}}{\lambda} \rho^* \rho_{ref} (v_{cor}^* - v_c^*) \sum_{i=1}^{n} \omega_i Cp_i \frac{\partial T^*}{\partial \xi^*} = -\left(\frac{2q^*}{\xi^*} + \frac{\partial q^*}{\partial \xi^*}\right) + \frac{\xi_{ref}^2(-\triangle H_R)R}{T_{ref}\lambda} \tag{E.4}$$

Darcy's law:

$$\frac{(v_{cor}^* - v_c^*)\mu D_{ref}}{Bp_{ref}} + \frac{\partial p^*}{\partial \xi^*} = 0 \tag{E.5}$$

Table E.1: Summary of the mass based solution strategy

Equations, LHS represents terms in the problem matrix and the RHS represents the terms in the source vector:	Boundary conditions:
Fourier's law $$q^* + \frac{\partial T^*}{\partial \xi^*} = 0 \qquad (E.6)$$	Boundary condition at $\xi = \xi^p$ $$T = T^b \qquad (E.7)$$
Temperature equation: $$\frac{D_{ref}}{\lambda} \rho^* \rho_{ref} (v^*_{cor} - v^*_c) \sum_{i=1}^{n} \omega_i Cp_i \frac{\partial T^*}{\partial \xi^*} + (\frac{2q^*}{\xi^*} + \frac{\partial q^*}{\partial \xi^*}) =$$ $$\frac{\xi^2_{ref}(-\triangle H_R)R}{T_{ref}\lambda} \qquad (E.8)$$	Boundary condition at $\xi = 0$ $$q = 0 \qquad (E.9)$$
Species mass balance, used for N components: $$\frac{\partial \omega_i}{\partial \xi^*}(\rho^* v^*_{cor}) + (\frac{2j^*_i}{\xi^*} + \frac{\partial j^*_i}{\partial \xi^*}) = R_i \frac{\xi^2_{ref}}{D_{ref}\rho_{ref}} \qquad (E.10)$$	Boundary condition at $\xi = 0$ $$j_i = 0 \qquad (E.11)$$
Diffusion model, solved for N components: Wilke diffusion in table D.2 is used	Boundary condition at $\xi = \xi^p$: $$\omega_i = \omega^b_i \qquad (E.12)$$
Mass based continuity equation: $$\frac{2}{\xi^*} v^*_{cor} + \frac{\partial v^*_{cor}}{\partial \xi^*} = -\frac{\partial \rho^*}{\partial \xi^*} \frac{v^*_{cor}}{\rho^*} \qquad (E.13)$$	Boundary condition at $\xi = 0$ $$v^*_{cor} = 0 \qquad (E.14)$$
Darcy's law: $$\frac{(v^*_{cor} - v^*_c)\mu}{Bp_{ref}} + \frac{\partial p^*}{\partial \xi^*} = 0 \qquad (E.15)$$	Boundary condition at $\xi = \xi^p$ $$p = p^b \qquad (E.16)$$
Ideal gas law modified for density*: $$\frac{p\overline{M}}{RT} = \rho \qquad (E.17)$$	No boundary condition $$-$$
Mole averaged velocity * ** $$u - v = \sum_{i=1}^{N} \frac{j_i \overline{M}}{\rho M_i} \qquad (E.18)$$	No boundary condition $$-$$

*solved outside of the collocation matrix, i.e. purely based on previous iterative values ** Solved for comparison with the mole based model.

E.2 Mole based alternative Wilke model using corrective velocities

E.2.1 The species mass balance

The difference from the already used equation is that the species balance is to be corrected with an additional corrective velocity term u_c:

$$u_c = \sum_i D'_{im} \nabla \omega_i \qquad (E.19)$$

Introducing the new term, $u_{cor} = u_\xi + u_c$ and inserting the correction gives the same species balance and continuity equation as obtained in the model derivation for the rigorous models in appendix D, but now with a corrected velocity instead:

Species balance with corrected velocity:

$$\frac{\partial x_i}{\partial \xi^*}(c^* u^*_{cor}) + \left(\frac{2J_i^*}{\xi^*} + \frac{\partial J_i^*}{\partial \xi^*}\right) = \left(R'_i - x_i \sum_{i=1}^{n} R'_i\right)\frac{\xi_{ref}^2}{D_{ref}c_{ref}} \qquad (E.20)$$

E.2.2 Continuity equation with corrected velocity

As for the species mass balance, the velocity term is replaced with the new corrected velocity term:

$$\frac{2}{\xi^*}c^* u^*_{cor} + \frac{\partial c^*}{\partial \xi^*}u^*_{cor} + \frac{\partial u^*_{cor}}{\partial \xi^*}c^* = \left(\frac{\xi_{ref}^2}{c_{ref}D_{ref}}\right)\sum_{i=1}^{n} R'_i \qquad (E.21)$$

E.2.3 Temperature equation and Darcy's law

The temperature and Darcy's law are calculated in the same manner as before. However the mass based velocity is now obtained from the modified equation:

$$v^* = \sum_{i=1}^{N} \frac{J_i^* M_i}{c_i^* \overline{M}} + (u^*_{cor} - u^*_c) \qquad (E.22)$$

Table E.2: Summary of the mole based solution strategy

Equations, LHS represents terms in the problem matrix and the RHS represents the terms in the source vector:	Boundary conditions:
Fourier's law $$q^* + \frac{\partial T^*}{\partial \xi^*} = 0 \qquad \text{(E.23)}$$	Boundary condition at $\xi = \xi^p$ $$T = T^b \qquad \text{(E.24)}$$
Temperature equation: $$\frac{D_{ref}}{\lambda} c^* c_{ref} v_\xi^* \sum_{i=1}^n x_i Cp_i' \frac{\partial T^*}{\partial \xi^*} + \left(\frac{2q^*}{\xi^*} + \frac{\partial q^*}{\partial \xi^*}\right) =$$ $$\frac{\xi_{ref}^2 (-\triangle H_R) R}{T_{ref}\lambda} \qquad \text{(E.25)}$$	Boundary condition at $\xi = 0$ $$q = 0 \qquad \text{(E.26)}$$
Species mole balance, solved for N components: $$\frac{\partial x_i}{\partial \xi^*}(c^* u_{cor}^*) + \left(\frac{2J_i^*}{\xi^*} + \frac{\partial J_i^*}{\partial \xi^*}\right) = (R_i' - x_i \sum_{i=1}^n R_i') \frac{\xi_{ref}^2}{D_{ref}c_{ref}} \qquad \text{(E.27)}$$	Boundary condition at $\xi = 0$ $$J_i = 0 \qquad \text{(E.28)}$$
Last flux(H2O) in the species balance is solved by: $$\sum_{i=1}^n J_i = 0 \qquad \text{(E.29)}$$	No boundary condition $$-$$
Diffusion mode, solved for N componentsl: Wilke diffusion from table D.6 is used	Boundary condition at $\xi = \xi^p$: $$x_i = x_i^b \qquad \text{(E.30)}$$
Last fraction(H2O) in the diffusion model is solved by: $$\sum_{i=1}^n x_i = 1 \qquad \text{(E.31)}$$	No boundary condition $$-$$
Continuity equation mole based: $$\frac{2}{\xi^*}c^* u_{cor}^* + \frac{\partial c^*}{\partial \xi^*}u_{cor}^* + \frac{\partial u_{cor}^*}{\partial \xi^*}c^* = \left(\frac{\xi_{ref}^2}{c_{ref}D_{ref}}\right)\sum_{i=1}^n R_i' \qquad \text{(E.32)}$$	Boundary condition at $\xi = 0$ $$u = 0 \qquad \text{(E.33)}$$
Mass averaged velocity*: $$v^* = \sum_{i=1}^N \frac{J_i^* M_i}{c_i^* \overline{M}} + (u_{cor}^* - u_c^*) \qquad \text{(E.34)}$$	No boundary condition $$-$$
Ideal gas law , algebraic: $$c = \frac{p}{RT} \qquad \text{(E.35)}$$	No boundary condition $$-$$
Pressure, Darcy's law $$\frac{\partial p^*}{\partial \xi^*} = -\frac{v^* \mu D_{ref}}{B p_{ref}} \qquad \text{(E.36)}$$	Boundary condtition at $\xi = \xi^p$: $$p = p^b \qquad \text{(E.37)}$$

*Solved outside of the collocation matrix

F 7 Alternative numerical methods for solving the rigorous steady state models

To solve the presented problem using the least squares method rather than orthogonal collocation, some small changes needs to be introduced: In the solution method the variable T and q has changed places also the ω_i, x_i and J_i, j_i. This was needed in order to obtain a stable matrix.

F.1 Mass based model

$$
\mathbf{A}
\begin{bmatrix}
T^* \\
q^* \\
\omega_{CH_4} \\
\omega_{CO} \\
\omega_{CO_2} \\
\omega_{H_2} \\
\omega_{N_2} \\
\omega_{H_2O} \\
j_{CH_4} \\
j_{CO} \\
j_{CO_2} \\
j_{H_2} \\
j_{N_2} \\
j_{H_2O} \\
v^* \\
p^*
\end{bmatrix}
=
\begin{bmatrix}
0 \\
T_2 \\
DM_2 \\
DM_2 \\
DM_2 \\
DM_2 \\
DM_2 \\
1 \\
SB_2 \\
SB_2 \\
SB_2 \\
SB_2 \\
SB_2 \\
0 \\
MC_1 \\
0
\end{bmatrix}
$$

Figure F.1: Collocation matrix, mass based. Explanation on the labeled terms can be seen in table H.2

Table F.1: Terms in the collocation matrix

Label in matrix	Collocation matrix terms:	multiplied with:
X_1	$$\frac{2}{\xi^*} + \frac{\partial}{\partial \xi^*}$$	q^*, ω_i, v^*
T_1	$$\frac{D_{ref}}{\lambda} \rho^* \rho_{ref} v_r^* \sum_{i=1}^{n} \omega_i Cp_i \frac{\partial}{\partial \xi^*}$$	T^*
DM_1	Wilke: $$\frac{D_{ref}}{D_{im}\rho^*}$$	j_i^*
DM_1	Wilke-Bosanquet: $$\frac{D_{ref}}{D_{i,eff}\rho^*}$$	j_i^*
DM_1	Maxwell-Stefan: $$\frac{\overline{M} D_{ref}}{\rho^*} \sum_{\substack{j=1 \\ j \neq i}}^{i} \frac{\omega_j}{M_j D_{ij}^e}$$	j_i^*
DM_1	Dusty gas: $$\frac{D_{ref}}{\rho^*}(\overline{M} \sum_{\substack{j=1 \\ j \neq i}}^{n} \frac{\omega_j}{M_j D_{ij}^e} + \frac{1}{D_{iK}^e})$$	j_i^*
SB_1	$$\rho^* v_\xi^* \frac{\partial}{\partial \xi^*}$$	ω_i
Dl_1	$$\frac{\mu}{B p_{ref}}$$	v^*

Table F.2: Terms in the source vector

Label in source vector	Source vector
T_2	Source term temperature equation: $$\frac{-\triangle H_r \xi_{ref}^2}{T_{ref}\lambda}$$
DM_2	Wilke: $$0$$
DM_2	Wilke-Bosanquet: $$0$$
DM_2	Maxwell-Stefan: $$\frac{-\omega_i}{\overline{M}}\frac{\partial \overline{M}}{\partial \xi^*} + \frac{\overline{M}D_{ref}}{\rho^*}\omega_i \sum_{\substack{j=1 \\ j\neq i}}^{n}\frac{j_j^*}{M_j D_{ij}^e}$$
DM_2	Dusty gas: $$\frac{\overline{M}D_{ref}}{\rho^*}\sum_{\substack{j=1 \\ j\neq i}}^{n}\frac{\omega_i j_j^*}{M_j D_{ij}^e} - \frac{\omega_i}{\overline{M}}\frac{\partial \overline{M}}{\partial \xi^*}$$
SB_2	Source term species balance: $$R_i \frac{\xi_{ref}^2}{D_{ref}\rho_{ref}}$$
MC_1	Source term continuity equation: $$-\frac{\partial \rho^*}{\partial \xi^*}\frac{v^*}{\rho^*}$$

F.2 Mole based model

Figure F.2: Collocation matrix - Maxwell-Stefan, mole based

Table F.3: Terms in the collocation matrix

Label in matrix	Collocation matrix terms:	multiplied with:
X_1	$\dfrac{2}{\xi^*} + \dfrac{\partial}{\partial \xi^*}$	q^*, x_i, u^*
T_1	$\dfrac{D_{ref}}{\lambda} \rho^* \rho_{ref} v_r^* \sum\limits_{i=1}^{n} \omega_i C p_i \dfrac{\partial}{\partial \xi^*}$	T^*
DM_1	Wilke: $\dfrac{D_{ref}}{D'_{im} c^*}, \quad D'_{im} = \dfrac{1 - x_i}{\sum\limits_{\substack{j=1 \\ j \neq i}}^{n} \frac{x_j}{D^e_{ij}}}$	J_i^*
DM_1	Wilke-Bosanquet: $\dfrac{D_{ref}}{D'_{i,eff} c^*}, \qquad \dfrac{1}{D'_{i,eff}} = \dfrac{1}{\frac{1 - x_i}{\sum\limits_{\substack{j=1 \\ j \neq i}}^{n} \frac{x_j}{D_{ij}}}} + \dfrac{1}{D^e_{i,K}}$	J_i^*
DM_1	Maxwell-Stefan: $\dfrac{D_{ref}}{c^*} \sum\limits_{\substack{j=1 \\ j \neq i}}^{i} \dfrac{x_j}{D^e_{ij}}$	J_i^*
DM_1	Dusty gas: $\dfrac{D_{ref}}{c^*} (\sum\limits_{\substack{j=1 \\ j \neq i}}^{i} \dfrac{x_j}{D^e_{ij}}$	J_i^*
SB_1	$c^* u_\xi^* \dfrac{\partial}{\partial \xi^*}$	x_i
MC_1	$u^* \dfrac{\partial}{\partial \xi^*}$	c^*

Table F.4: Terms in the source vector

Label in source vector	Source vector
T_2	Source term temperature equation: $$\frac{-\triangle H_r \xi_{ref}^2}{T_{ref}\lambda}$$
DM_2	Wilke: $$0$$
DM_2	Wilke-Bosanquet: $$0$$
DM_2	Maxwell-Stefan: $$\frac{D_{ref}}{c^*}\sum_{\substack{j=1\\j\neq i}}^{n}\frac{J_j^* x_i}{D_{ij}^e}$$
DM_2	Dusty gas: $$\frac{D_{ref}}{c^*}\sum_{\substack{j=1\\j\neq i}}^{n}\frac{J_j^* x_i}{D_{ij}^e} - \frac{D_{ref}x_i u^*}{D_{iK}^e}$$
SB_2	Source term species balance: $$(R_i' - x_i\sum_{i=1}^{n}R_i')\frac{\xi_{ref}^2}{D_{ref}c_{ref}}$$
MC_2	Source term continuity equation: $$(\frac{\xi_{ref}^2}{c_{ref}D_{ref}})\sum_{i=1}^{n}R_i'$$
Dl_1	Source term Darcy's law: $$-\frac{v^*\mu D_{ref}}{Bp_{ref}}$$

G   8 Rigorous transient models

This appendix consists of the model derivations for the transient models on both mass and mole basis. Some additional results using the dusty gas diffusion method is also presented here.

The fully rigorous one dimensional model for simulating the SMR reaction in a catalyst particle will be derived. The derivation consists mainly of discretisizing the transient term and rearranging the equations to the implemented form.

The transient terms are discretisized using the theta method derived in the theory chapter 2.5, the equation 70, that is rearranged to the implementing form is represented here for convinience:

$$f^{t+1} + \Delta t \theta \mathcal{L} f^{t+1} = \Delta t \theta g^{t+1} + \Delta t (1 - \theta)(g^t - \mathcal{L} f^t) + f^t \tag{G.1}$$

G.1   Mass based model derivation

G.1.1   Temperature equation

The temperature equation are derived from the general dimensionless temperature equation A.56 derived in the theory:

$$((1 - \epsilon)\rho_p C p_p + \epsilon \rho^* \rho_{ref} \sum_{i=1}^{n} \omega_i C p_i) \frac{D_{ref}}{\lambda} \frac{\partial T^*}{\partial t^*} =$$
$$-\rho^* \rho_{ref} v_r^* \frac{D_{ref}}{\lambda} \sum_{i=1}^{n} \omega_i C p_i \frac{\partial T^*}{\partial \xi^*} - \left(\frac{2q^*}{\xi^*} + \frac{\partial q^*}{\partial \xi^*}\right) + \frac{\xi_{ref}^2 (-\triangle H_R) R}{\lambda T_{ref}} \tag{G.2}$$

Rearrange to free the transient term:

$$\frac{\partial T^*}{\partial t^*} + \frac{\rho^* \rho_{ref} v_r^* \sum_{i=1}^{n} \omega_i C p_i \frac{\partial T^*}{\partial \xi^*} + \frac{\lambda}{D_{ref}} \left(\frac{2q^*}{\xi^*} + \frac{\partial q^*}{\partial \xi^*}\right)}{((1 - \epsilon)\rho_p C p_p + \epsilon \rho^* \rho_{ref} \sum_{i=1}^{n} \omega_i C p_i)} =$$
$$\frac{\xi_{ref}^2 (-\triangle H_R) R}{D_{ref} T_{ref}} \frac{1}{((1 - \epsilon)\rho_p C p_p + \epsilon \rho^* \rho_{ref} \sum_{i=1}^{n} \omega_i C p_i)} \tag{G.3}$$

Inserted in transient discretizing equation G.1 and reflecting the implemented form:

$$T^{*(t+1)} + \Delta t \theta \frac{\rho^{*(t+1)} \rho_{ref} v_r^{*(t+1)} \sum_{i=1}^{n} \omega_i C p_i \frac{\partial T^{*(t+1)}}{\partial \xi^*} + \frac{\lambda}{D_{ref}} \left(\frac{2q^{*(t+1)}}{\xi^*} + \frac{\partial q^{*(t+1)}}{\partial \xi^*}\right)}{((1 - \epsilon)\rho_p C p_p + \epsilon \rho^{*(t+1)} \rho_{ref} \sum_{i=1}^{n} \omega_i^{(t+1)} C p_i)} =$$
$$\Delta t \theta \frac{\xi_{ref}^2 (-\triangle H_R) R^{(t+1)}}{D_{ref} T_{ref}} \frac{1}{((1 - \epsilon)\rho_p C p_p + \epsilon \rho^{*(t+1)} \rho_{ref} \sum_{i=1}^{n} \omega_i^{(t+1)} C p_i)}$$
$$+\Delta t (1 - \theta) \frac{\left(\frac{\xi_{ref}^2 (-\triangle H_R) R^{(t)}}{D_{ref} T_{ref}} - (\rho^{*(t)} \rho_{ref} v_r^{*(t+1)} \sum_{i=1}^{n} \omega_i C p_i \frac{\partial T^{*(t)}}{\partial \xi^*} + \frac{\lambda}{D_{ref}} \left(\frac{2q^{*(t)}}{\xi^*} + \frac{\partial q^{*(t)}}{\partial \xi^*}\right))\right)}{((1 - \epsilon)\rho_p C p_p + \epsilon \rho^{*(t)} \rho_{ref} \sum_{i=1}^{n} \omega_i^{(t)} C p_i)}$$
$$+ T^{*(t)}) \tag{G.4}$$

G.1.2 continuity

The general dimensionless continuity equation A.57 derived in the theory:

$$\frac{\partial \rho^*}{\partial t^*} + \frac{1}{\xi^{*2}} \frac{\partial}{\partial \xi^*}(\xi^{*2}\rho^* v^*) = 0 \tag{G.5}$$

Expand the terms:

$$\frac{\partial \rho^*}{\partial t^*} + \frac{2\rho^* v^*}{\xi^*} + \frac{\partial \rho^*}{\partial \xi^*}v^* + \frac{\partial v^*}{\partial \xi^*}\rho^* = 0 \tag{G.6}$$

Discretisizing the transient term with the theta method equation G.1:

$$\rho^{*(t+1)} + \Delta t\theta\Big(\frac{2\rho^{*(t+1)}v^{*(t+1)}}{\xi^*} + \frac{\partial v^{*(t+1)}}{\partial \xi^*}\rho^{*(t+1)} + \frac{\partial \rho^{*(t+1)}}{\partial \xi^*}v^{*(t+1)}\Big) =$$
$$+\Delta t(1-\theta)\Big(-\frac{2\rho^{*(t)}v^{*(t)}}{\xi^*} - \frac{\partial v^{*(t)}}{\partial \xi^*}\rho^{*(t)} - \frac{\partial \rho^{*(t)}}{\partial \xi^*}v^{*(t)}\Big) + \rho^{*(t)} \tag{G.7}$$

G.1.3 Species balance

The general dimensionless species mass balance equation A.55 derived in the theory:

$$\frac{\partial}{\partial t^*}(\rho^* \omega_i) + \frac{1}{\xi^{*2}}\frac{\partial}{\partial \xi^*}(\xi^{*2}\rho^* \omega_i v_\xi^*) = -\frac{1}{\xi^{*2}}\frac{\partial}{\partial \xi^*}(\xi^{*2}j_i^*) + R_i\frac{\xi_{ref}^2}{D_{ref}\rho_{ref}} \tag{G.8}$$

Expanding the terms to identify continuity equation:

$$\frac{\partial \rho^*}{\partial t^*}\omega_i + \frac{\partial \omega_i}{\partial t^*}\rho + \frac{\partial \omega_i}{\partial \xi^*}\rho^* v_\xi^* + \omega_i\frac{1}{\xi^{*2}}\frac{\partial}{\partial \xi^*}(\xi^{*2}\rho^* v_\xi^*) = -\frac{1}{\xi^{*2}}\frac{\partial}{\partial \xi^*}(\xi^{*2}j_i^*) + R_i\frac{\xi_{ref}^2}{D_{ref}\rho_{ref}} \tag{G.9}$$

The first and the fourth term identified as the RHS of the continuity equation multiplied with ω_i, swapping with the LHS gives:

$$\frac{\partial \omega_i}{\partial t^*}\rho^* + \frac{\partial \omega_i}{\partial \xi^*}\rho^* v_\xi^* = -\Big(\frac{2j_i^*}{\xi^*} + \frac{\partial j_i^*}{\partial \xi^*}\Big) + R_i\frac{\xi_{ref}^2}{D_{ref}\rho_{ref}} \tag{G.10}$$

Rearranging to free the transient term from other variables:

$$\frac{\partial \omega_i}{\partial t^*} + \frac{\partial \omega_i}{\partial \xi^*}v_\xi^* + \Big(\frac{2j_i^*}{\rho^*\xi^*} + \frac{1}{\rho^*}\frac{\partial j_i^*}{\partial \xi^*}\Big) = R_i\frac{\xi_{ref}^2}{D_{ref}\rho_{ref}\rho^*} \tag{G.11}$$

Discretisizing the transient term with the theta method equation G.1:

$$\omega_i^{(t+1)} + \Delta t\theta\Big(\frac{\partial \omega_i^{(t+1)}}{\partial \xi^*}v_\xi^* + \frac{2j_i^{*(t+1)}}{\rho^{*(t+1)}\xi^*} + \frac{1}{\rho^{*(t+1)}}\frac{\partial j_i^{*(t+1)}}{\partial \xi^*}\Big) =$$
$$\Delta t\theta R_i^{(t+1)}\frac{\xi_{ref}^2}{D_{ref}\rho_{ref}\rho^{*(t+1)}}\Delta t(1-\theta)\Big(R_i^{(t)}\frac{\xi_{ref}^2}{D_{ref}\rho_{ref}\rho^{*(t)}}$$
$$-\Big(\frac{\partial \omega_i^{(t)}}{\partial \xi^*}v_\xi^* + \frac{2j_i^{*(t)}}{\rho^{*(t)}\xi^*} + \frac{1}{\rho^{*(t)}}\frac{\partial j_i^{*(t)}}{\partial \xi^*}\Big)\Big) + \omega_i^t \tag{G.12}$$

G.1.4 Diffusion models

The diffusion models used are identical to the ones used in the rigorous steady state model, the derivation can be found in appendix D. Only the Maxwell-Stefan and the dusty gas diffusion models are considered in the transient models.

G.1.5 Supportive equations

The remaining equations needed to simulate the problem does not require any changes from the given form in the theory. However they are included in the solution strategy.

G.2 Solution strategy

The different equations are discussed in short and the main summary of the solution strategy is given in table G.1. In the table the used equations combined with a fitting boundary condition are shown. The solution strategy is also visualized in the form on how it would be implemented by the use of orthogonal collocation, shown in figure G.1.

G.2.1 Temperature equation

The transient temperature equation is used to calculate the change of temperature with time and the heat flux. The already solved heat flux are then used to calculate the temperature from Fourier's law.

G.2.2 Species Mass balance and diffusion model

From the species mass balance, the change in mass fractions with time and the mass based fluxes for N-1 components are obtained. The last component is obtained from the constitutive law A.39. The mass based fluxes are used with the diffusion models to obtain the mass fractions again for N-1 components with the last being solved from the constitutive law A.40.

G.2.3 Continuity equation

From the continuity equation, the mass averaged velocity and the change of density with time are obtained.

G.2.4 Darcy's Law

The pressure is obtained from Darcy's Law.

G.2.5 Density

The density is obtained from the modified version of the ideal gas law. This equation are now implemented in the problem matrix in order to stabilize the iteration process.

Table G.1: Summary of the solution strategy

Equations, LHS represents terms in the problem matrix and the RHS represents the terms in the source vector:	Boundary conditions:
Fourier's law $$q^* + \frac{\partial T^*}{\partial \xi^*} = 0 \qquad (G.13)$$	Boundary condition at $\xi = \xi^p$ $$hT^* = \frac{q^* \lambda}{\xi_{ref}} + \rho C p_g T^* v^* \frac{D_{ref}}{\xi_r ef} + h$$ $$(G.14)$$
Temperature equation: Equation G.4	Boundary condition at $\xi = 0$ $$q = 0 \qquad (G.15)$$
Species mass balance, used for N-1 components: Equation G.12	Boundary condition at $\xi = 0$ $$j_i = 0 \qquad (G.16)$$
Last flux(H2O) in the species balance is solved by: $$\sum_{i=1}^{n} j_i^* = 0 \qquad (G.17)$$	No boundary condition —
Diffusion model: One of the four diffusion models in table D.2 is used	Boundary condition at $\xi = \xi^p$: $$\omega_i = \frac{(j_i^* \frac{D_{ref}}{\xi_{ref}} + v^* \frac{D_{ref}}{\xi_{ref}} \rho^* \omega_i)}{k_i \rho^*} + \frac{\omega_i}{\rho^*}$$ $$(G.18)$$
Last mass fraction(H2O) in the species balance is solved by: $$\sum_{i=1}^{n} \omega_i = 1 \qquad (G.19)$$	No boundary condition —
Mass based continuity equation: Equation G.7	Boundary condition at $\xi = 0$ $$v^* = 0 \qquad (G.20)$$
Darcy's law: $$\frac{v^* \mu}{B p_{ref}} + \frac{\partial p^*}{\partial \xi^*} = 0 \qquad (G.21)$$	Boundary condition at $\xi = \xi^p$ $$p = p^b \qquad (G.22)$$
Density, dimensionless: $$\frac{p p_{ref} \overline{M}}{R T \rho_{ref}} = \rho^* \qquad (G.23)$$	No boundary condition —
Mole averaged velocity* $$u - v = \sum_{i=1}^{N} \frac{j_i \overline{M}}{\rho M_i} \qquad (G.24)$$	No boundary condition —

*Solved outside of the solver system, based on previous iteration values.

$$
\mathbf{A}\,
\begin{bmatrix}
q^* \\ T^* \\ j_{CH_4} \\ j_{CO} \\ j_{CO_2} \\ j_{H_2} \\ j_{N_2} \\ j_{H_2O} \\ \omega_{CH_4} \\ \omega_{CO} \\ \omega_{CO_2} \\ \omega_{H_2} \\ \omega_{N_2} \\ \omega_{H_2O} \\ v^* \\ p^* \\ \rho^*
\end{bmatrix}
=
\begin{bmatrix}
0 \\ T_2 \\ DM_2 \\ DM_2 \\ DM_2 \\ DM_2 \\ DM_2 \\ 0 \\ SB_2 \\ SB_2 \\ SB_2 \\ SB_2 \\ SB_2 \\ 1 \\ MC_1 \\ 0 \\ 0
\end{bmatrix}
$$

Figure G.1: Collocation matrix for a mass based fully rigorous transient pellet model. Explanation on the labeled terms can be seen in table G.2 for the problem matrix and in table G.3 for the source vector

Table G.2: Labeled terms in the collocation matrix

Label in matrix	Collocation matrix terms:	multiplied with:
X_1	$$\dfrac{\Delta t\theta\frac{\lambda}{D_{ref}}\left(\frac{2}{\xi^*}+\frac{\partial}{\partial\xi^*}\right)}{\left((1-\epsilon)\rho_p Cp_p+\epsilon\rho^{*(t+1)}\rho_{ref}\sum_{i=1}^n\omega_i^{(t+1)}Cp_i\right)}$$	q^*
T_1	$$1\bullet+\dfrac{\Delta t\theta\rho^{*(t+1)}\rho_{ref}v_r^{*(t+1)}\sum_{i=1}^n\omega_i Cp_i\frac{\partial}{\partial\xi^*}}{\left((1-\epsilon)\rho_p Cp_p+\epsilon\rho^{*(t+1)}\rho_{ref}\sum_{i=1}^n\omega_i^{(t+1)}Cp_i\right)}$$	T^*
DM_1	Maxwell-Stefan: $$\dfrac{\overline{M}D_{ref}}{\rho^*}\sum_{\substack{j=1\\j\neq i}}^{i}\frac{\omega_j}{M_j D_{ij}^e}$$	j_i^*
DM_1	Dusty gas: $$\dfrac{D_{ref}}{\rho^*}\left(\overline{M}\sum_{\substack{j=1\\j\neq i}}^{n}\frac{\omega_j}{M_j D_{ij}^e}+\frac{1}{D_{iK}^e}\right)$$	j_i^*
X_2	$$\Delta t\theta\frac{1}{\rho^{*(t+1)}}\left(\frac{2}{\xi^*}+\frac{\partial}{\partial\xi^*}\right)$$	j_i^*
SB_1	$$1\bullet+\Delta t\theta v_\xi^*\frac{\partial}{\partial\xi^*}$$	ω_i,ρ^*
X_3	$$\Delta t\theta\rho^{*(t+1)}\left(\frac{2}{\xi^*}+\frac{\partial}{\partial\xi^*}\right)$$	v_ξ^*
Dl_1	$$\dfrac{\mu}{Bp_{ref}}$$	v_ξ^*

Table G.3: Labeled terms in the source vector

Label in source vector	Source vector
T_2	Source term temperature equation: LHS of equation G.4
DM_2	Maxwell-Stefan: $$\frac{-\omega_i}{\overline{M}}\frac{\partial \overline{M}}{\partial \xi^*} + \frac{\overline{M}D_{ref}}{\rho^*}\omega_i \sum_{\substack{j=1 \\ j\neq i}}^{n} \frac{j_j^*}{M_j D_{ij}^e}$$
DM_2	Dusty gas: $$\frac{\overline{M}D_{ref}}{\rho^*}\sum_{\substack{j=1 \\ j\neq i}}^{n} \frac{\omega_i j_j^*}{M_j D_{ij}^e} - \frac{\omega_i}{\overline{M}}\frac{\partial \overline{M}}{\partial \xi^*}$$
SB_2	Source term species balance: LHS of equation G.12
MC_1	Source term continuity equation: LHS of equation G.7

G.3 Mole based transient model

G.3.1 Temperature equation

The temperature equation are derived from the general dimensionless temperature equation A.63 derived in the theory:

$$
((1-\epsilon)\rho_p Cp_p + \epsilon\rho^* c_{ref}\sum_{i=1}^{n}\omega_i Cp_i)\frac{D_{ref}}{\lambda}\frac{\partial T^*}{\partial t^*} =
$$
$$
-c^* c_{ref}v_r^*\frac{D_{ref}}{\lambda}\sum_{i=1}^{n}x_i Cp_i'\frac{\partial T^*}{\partial \xi^*} - (\frac{2q^*}{\xi^*}+\frac{\partial q^*}{\partial \xi^*}) + \frac{\xi_{ref}^2(-\triangle H_R)R}{\lambda T_{ref}}
$$
(G.25)

Rearrange to free the transient term:

$$
\frac{\partial T^*}{\partial t^*} + \frac{c^* c_{ref}v_r^*\sum_{i=1}^{n}x_i Cp_i'\frac{\partial T^*}{\partial \xi^*} + \frac{\lambda}{D_{ref}}(\frac{2q^*}{\xi^*}+\frac{\partial q^*}{\partial \xi^*})}{((1-\epsilon)\rho_p Cp_p + \epsilon c^* c_{ref}\sum_{i=1}^{n}x_i Cp_i')} =
$$
$$
\frac{\xi_{ref}^2(-\triangle H_R)R}{D_{ref}T_{ref}}\frac{1}{((1-\epsilon)\rho_p Cp_p + \epsilon c^* c_{ref}\sum_{i=1}^{n}\omega_i Cp_i)}
$$
(G.26)

Inserted in transient discretized equation G.1 and reflecting the implemented form:

$$
T^{*(t+1)} + \Delta t\theta\frac{c^{*(t+1)}c_{ref}v_r^{*(t+1)}\sum_{i=1}^{n}x_i Cp_i'\frac{\partial T^{*(t+1)}}{\partial \xi^*} + \frac{\lambda}{D_{ref}}(\frac{2q^{*(t+1)}}{\xi^*}+\frac{\partial q^{*(t+1)}}{\partial \xi^*})}{((1-\epsilon)\rho_p Cp_p + \epsilon c^{*(t+1)}c_{ref}\sum_{i=1}^{n}x_i^{(t+1)}Cp_i')} =
$$
$$
\Delta t\theta\frac{\xi_{ref}^2(-\triangle H_R)R^{(t+1)}}{D_{ref}T_{ref}}\frac{1}{((1-\epsilon)\rho_p Cp_p + \epsilon c^{*(t+1)}c_{ref}\sum_{i=1}^{n}x_i^{(t+1)}Cp_i')}
$$
$$
+\Delta t(1-\theta)\frac{(\frac{\xi_{ref}^2(-\triangle H_R)R^{(t)}}{D_{ref}T_{ref}} - (c^{*(t)}c_{ref}v_r^{*(t+1)}\sum_{i=1}^{n}x_i Cp_i'\frac{\partial T^{*(t)}}{\partial \xi^*} + \frac{\lambda}{D_{ref}}(\frac{2q^{*(t)}}{\xi^*}+\frac{\partial q^{*(t)}}{\partial \xi^*})))}{((1-\epsilon)\rho_p Cp_p + \epsilon\rho^{*(t)}\rho_{ref}\sum_{i=1}^{n}x_i^{(t)}Cp_i')}
$$
$$
+T^{*(t)})
$$
(G.27)

G.3.2 continuity

The general dimensionless continuity equation A.64 derived in the theory:

$$
\frac{\partial c^*}{\partial t^*} + \frac{1}{\xi^{*2}}\frac{\partial}{\partial \xi^*}(\xi^{*2}c^* u_\xi^*) = \frac{\xi_{ref}^2}{c_{ref}D_{ref}}\sum_{i=1}^{n}R_i'
$$
(G.28)

Expand the terms:

$$
\frac{\partial c^*}{\partial t^*} + \frac{2c^* u_\xi^*}{\xi^*} + \frac{\partial c^*}{\partial \xi^*}u_{\xi^*}^* + \frac{\partial u_{\xi^*}}{\partial \xi^*}c^* = \frac{\xi_{ref}^2}{c_{ref}D_{ref}}\sum_{i=1}^{n}R_i'
$$
(G.29)

153

Discretising the transient term with the theta method equation G.1:

$$c^{*(t+1)} + \Delta t \theta \left(\frac{2c^{*(t+1)} u_\xi^{*(t+1)}}{\xi^*} + \frac{\partial c^{*(t+1)}}{\partial \xi^*} u_\xi^{*(t+1)} + \frac{\partial u_\xi^{*(t+1)}}{\partial \xi^*} c^{*(t+1)} \right) =$$

$$\Delta t \theta \frac{\xi_{ref}^2}{c_{ref} D_{ref}} \sum_{i=1}^n R_i^{'*(t+1)} + \Delta t (1-\theta) \left(\frac{\xi_{ref}^2}{c_{ref} D_{ref}} \sum_{i=1}^n R_i^{'*(t)} - \right. \qquad \text{(G.30)}$$

$$\left. \left(\frac{2c^{*(t)} u_\xi^{*(t)}}{\xi^*} + \frac{\partial c^{*(t)}}{\partial \xi^*} u_\xi^{*(t)} + \frac{\partial u_\xi^{*(t)}}{\partial \xi^*} c^{*(t)} \right) \right) + c^{*(t)}$$

G.3.3 Species balance

The general dimensionless species mass balance equation A.62 derived in the theory:

$$\frac{\partial}{\partial t^*}(c^* x_i) + \frac{1}{\xi^{*2}} \frac{\partial}{\partial \xi^*}(\xi^{*2} c^* x_i u_\xi^*) = -\frac{1}{\xi^{*2}} \frac{\partial}{\partial \xi^*}(\xi^{*2} J_i^*) + R_i' \frac{\xi_{ref}^2}{D_{ref} c_{ref}} \qquad \text{(G.31)}$$

Expanding the terms to identify continuity equation:

$$\frac{\partial c^*}{\partial t^*} x_i + \frac{\partial x_i}{\partial t} c^* + \frac{\partial x_i}{\partial \xi^*} c^* u_\xi^* + x_i \frac{1}{\xi^{*2}} \frac{\partial}{\partial \xi^*}(\xi^{*2} c^* u_\xi^*) + \frac{2 J_i^*}{\xi^*} + \frac{\partial J_i^*}{\partial \xi^*} = R_i' \frac{\xi_{ref}^2}{D_{ref} c_{ref}}$$

$$\text{(G.32)}$$

The first and the fourth term identified as the RHS of the continuity equation multiplied with x_i, swapping with the LHS gives:

$$\frac{\partial x_i}{\partial t^*} c^* + \frac{\partial x_i}{\partial \xi^*} c^* u_\xi^* + \frac{2 J_i^*}{\xi^*} + \frac{\partial J_i^*}{\partial \xi^*} = \left(R_i' - x_i \sum_{i=1}^n R_i' \right) \frac{\xi_{ref}^2}{D_{ref} c_{ref}} \qquad \text{(G.33)}$$

Rearranging to free the transient term from other variables:

$$\frac{\partial x_i}{\partial t^*} + \frac{\partial x_i}{\partial \xi^*} u_\xi^* + \frac{2 J_i^*}{c^* \xi^*} + \frac{1}{c^*} \frac{\partial J_i^*}{\partial \xi^*} = \left(R_i' - x_i \sum_{i=1}^n R_i' \right) \frac{\xi_{ref}^2}{D_{ref} c_{ref} c^*} \qquad \text{(G.34)}$$

Discretisizing the transient term with the theta method equation G.1:

$$x_i^{(t+1)} + \Delta t \theta \left(\frac{\partial x_i^{(t+1)}}{\partial \xi^*} u_\xi^{*(t+1)} + \frac{2 J_i^{*(t+1)}}{c^{*(t+1)} \xi^*} + \frac{1}{c^{*(t+1)}} \frac{\partial J_i^{*(t+1)}}{\partial \xi^*} \right) =$$

$$\Delta t \theta \left(R_i^{'(t+1)} - x_i \sum_{i=1}^n R_i^{'(t+1)} \right) \frac{\xi_{ref}^2}{D_{ref} c_{ref} c^{*(t+1)}} \Delta t (1-\theta)$$

$$\left(\left(R_i^{'(t)} - x_i \sum_{i=1}^n R_i^{'(t)} \right) \frac{\xi_{ref}^2}{D_{ref} c_{ref} c^{*(t)}} - \left(\frac{\partial x_i^{(t)}}{\partial \xi^*} u_\xi^{*(t)} + \frac{2 J_i^{*(t)}}{c^{*(t)} \xi^*} + \frac{1}{c^{*(t)}} \frac{\partial J_i^{*(t)}}{\partial \xi^*} \right) \right) + x_i^t$$

$$\text{(G.35)}$$

G.3.4 Diffusion models

The diffusion models used are identical to the ones used in the rigorous steady state model, the derivation can be found in appendix D. Only the Maxwell-Stefan and the dusty gas diffusion models are considered in the transient models.

G.3.5 Supportive equations

The remaining equations needed to simulate the problem does not require any changes from the given form in the theory. However they are included in the solution strategy.

G.4 Solution strategy

The different equations are first discussed in short and the main summary of the solution strategy is given in table G.4. In the table the used equations combined with a fitting boundary condition are shown. The solution strategy is also visualized in the form on how it would be implemented by the use of orthogonal collocation, shown in figure G.2.

G.4.1 Temperature equation

The transient temperature equation is used to calculate the change of temperature with time and the heat flux. The already solved heat flux are then used to calculate the temperature from Fourier's law.

G.4.2 Species mole balance and diffusion model

From the species mole balance, the change in mole fractions with time and the mole based fluxes for N-1 components are obtained. The last component is obtained from the constitutive law A.41. The mole based fluxes are used with the diffusion models to obtain the mole fractions again for N-1 components with the last being solved from the constitutive law A.42.

G.4.3 Continuity equation

From the continuity equation, the mole averaged velocity and the change of concentration with time are obtained.

G.4.4 Darcy's Law

The pressure is obtained from Darcy's Law. Here the needed mass averaged velocity is obtained from the mole based fluxes.

G.4.5 Concentration

The concentration is obtained from the ideal gas law. This equation is now convenient to have in the problem matrix as it stabilizes the iteration.

Table G.4: Summary of the solution strategy

Equations, LHS represents terms in the problem matrix and the RHS represents the terms in the source vector:	Boundary conditions:
Fourier's law $$q^* + \frac{\partial T^*}{\partial \xi^*} = 0 \qquad (G.36)$$	Boundary condition at $\xi = \xi^p$ $$hT^* = \frac{q^*\lambda}{\xi_{ref}} + cCp'_g T^* v^* \frac{D_{ref}}{\xi_{ref}} + h \qquad (G.37)$$
Temperature equation: Equation G.27	Boundary condition at $\xi = 0$ $$q = 0 \qquad (G.38)$$
Species mass balance, solved for N-1 components: Equation G.35	Boundary condition at $\xi = 0$ $$J_i = 0 \qquad (G.39)$$
Last flux(H2O) in the species balance is solved by: $$\sum_{i=1}^{n} J_i^* = 0 \qquad (G.40)$$	No boundary condition —
Diffusion model, solved for N-1 components: One of the four diffusion models in table D.2 is used	Boundary condition at $\xi = \xi^p$: $$x_i = \frac{(J_i^* \frac{D_{ref}}{\xi_{ref}} + u^* \frac{D_{ref}}{\xi_{ref}} c^* x_i)}{k_i c^*} + \frac{\omega_i}{c^*} \qquad (G.41)$$
Last mole fraction(H2O) in the species balance is solved by: $$\sum_{i=1}^{n} x_i = 1 \qquad (G.42)$$	No boundary condition —
Mass based continuity equation: Equation G.30	Boundary condition at $\xi = 0$ $$u_\xi^* = 0 \qquad (G.43)$$
Darcy's law: $$\frac{v^*\mu}{Bp_{ref}} + \frac{\partial p^*}{\partial \xi^*} = 0 \qquad (G.44)$$	Boundary condition at $\xi = \xi^p$ $$p = p^b \qquad (G.45)$$
Concentration, dimensionless: $$\frac{pp_{ref}}{RTc_{ref}} = c^* \qquad (G.46)$$	No boundary condition —
Mass averaged velocity*: $$v^* = \sum_{i=1}^{N} \frac{J_i^* M_i}{c_i^* \overline{M}} + u^* \qquad (G.47)$$	No boundary condition —

*solved outside of the collocation matrix, i.e. purely based on previous iterative values.

Figure G.2: Collocation matrix for a mass based fully rigorous transient pellet model. Explanation on the labeled terms can be seen in table G.5 for the problem matrix and in table G.6 for the source vector.

Table G.5: Terms in the collocation matrix

Label in matrix	Collocation matrix terms:	multiplied with:
X_1	$$\frac{\Delta t \theta \frac{\lambda}{D_{ref}}(\frac{2}{\xi^*} + \frac{\partial}{\partial \xi^*})}{((1-\epsilon)\rho_p Cp_p + \epsilon c^{*(t+1)} c_{ref} \sum_{i=1}^{n} x_i^{(t+1)} Cp_i')}$$	q^*
T_1	$$1 \bullet + \frac{\Delta t \theta \rho^{*(t+1)} c_{ref} v_r^{*(t+1)} \sum_{i=1}^{n} x_i Cp_i' \frac{\partial}{\partial \xi^*}}{((1-\epsilon)\rho_p Cp_p + \epsilon c^{*(t+1)} c_{ref} \sum_{i=1}^{n} x_i^{(t+1)} Cp_i')}$$	T^*
DM_1	Maxwell-Stefan: $$\frac{D_{ref}}{c^*} \sum_{\substack{j=1 \\ j \neq i}}^{i} \frac{x_j}{D_{ij}^e}$$	J_i^*
DM_1	Dusty gas: $$\frac{D_{ref}}{c^*}(\sum_{\substack{j=1 \\ j \neq i}}^{i} \frac{x_j}{D_{ij}^e}$$	J_i^*
X_2	$$\Delta t \theta \frac{1}{c^{*(t+1)}}(\frac{2}{\xi^*} + \frac{\partial}{\partial \xi^*})$$	J_i^*
SB_1	$$1 \bullet + \Delta t \theta u_\xi^* \frac{\partial}{\partial \xi^*}$$	x_i, c^*
X_3	$$\Delta t \theta c^{*(t+1)}(\frac{2}{\xi^*} + \frac{\partial}{\partial \xi^*})$$	u_ξ^*

Table G.6: Terms in the source vector

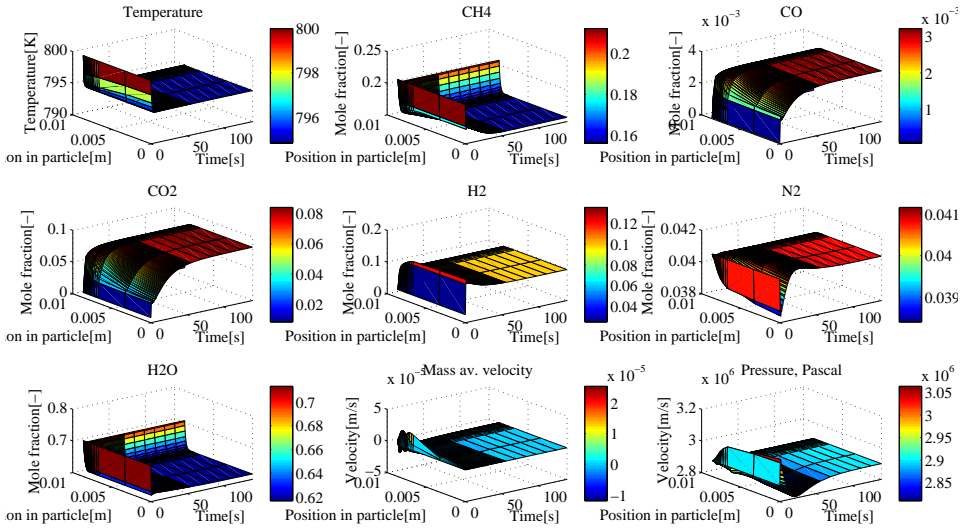| Label in source vector	Source vector
T_2	Source term temperature equation: LHS of equation G.27
DM_2	Maxwell-Stefan: $$\frac{D_{ref}}{c^*} \sum_{\substack{j=1 \\ j\neq i}}^{n} \frac{J_j^* x_i}{D_{ij}^e}$$
DM_2	Dusty gas: $$\frac{D_{ref}}{c^*} \sum_{\substack{j=1 \\ j\neq i}}^{n} \frac{J_j^* x_i}{D_{ij}^e} - \frac{D_{ref} x_i u^*}{D_{iK}^e}$$
SB_2	Source term species balance: LHS of equation G.35
MC_1	Source term continuity equation: LHS of equation G.30
Dl_1	Source term Darcy's law: $$-\frac{v^* \mu D_{ref}}{B p_{ref}}$$

G.5   Additional results

Figure G.3: Rigorous Transient mass based model using the dusty gas diffusion model simulated with the orhogonal collocation method.
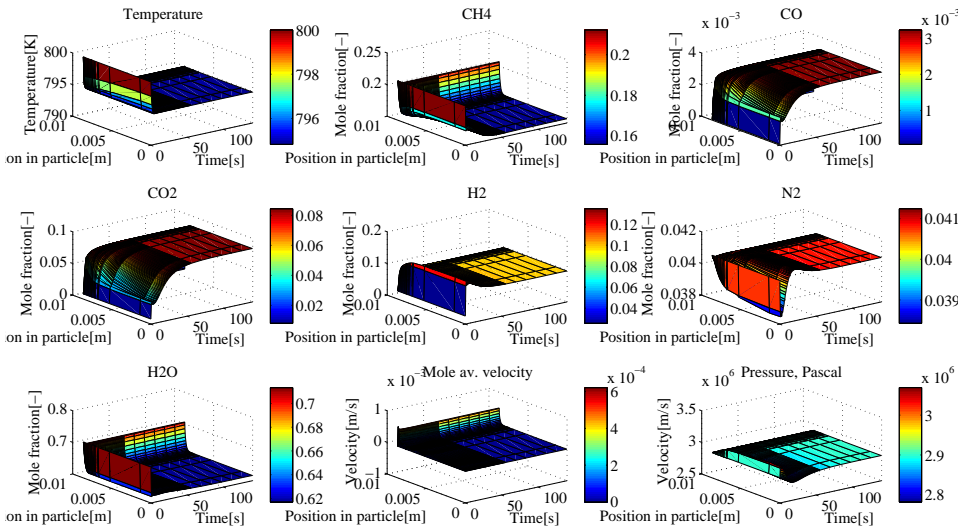

Figure G.4: Rigorous Transient mole based model using the dusty gas diffusion model simulated with the orhogonal collocation method.
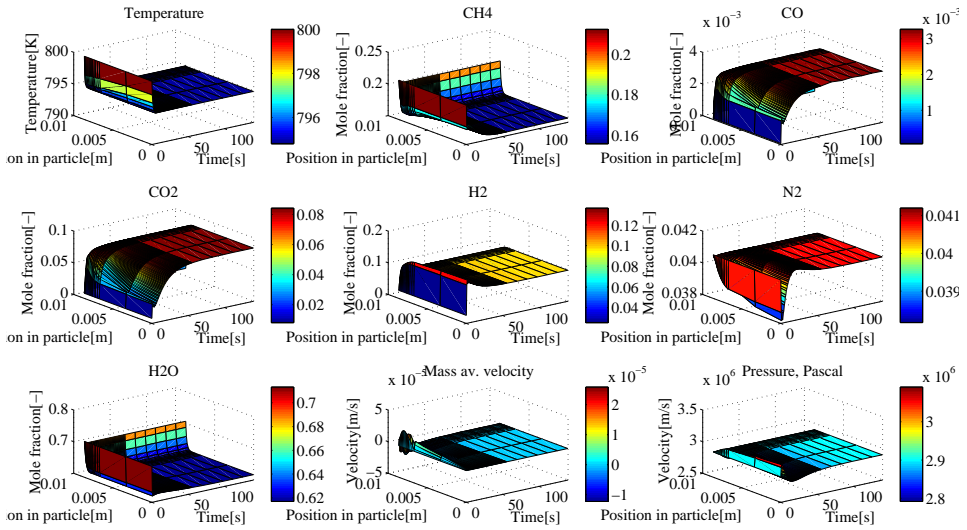
Figure G.5: Rigorous Transient mass based model using the dusty gas diffusion model simulated with the least squares method.
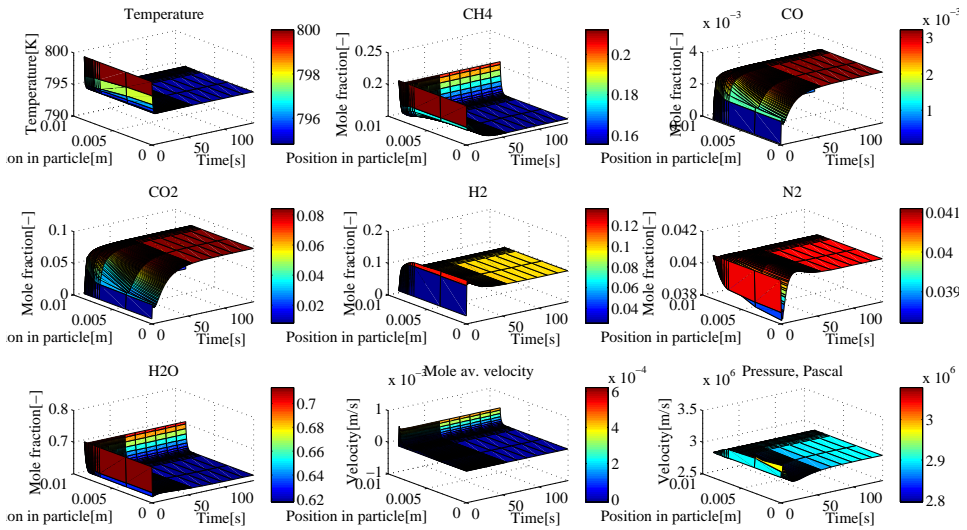

Figure G.6: Rigorous Transient mole based model using the dusty gas diffusion model simulated with the least squares method.
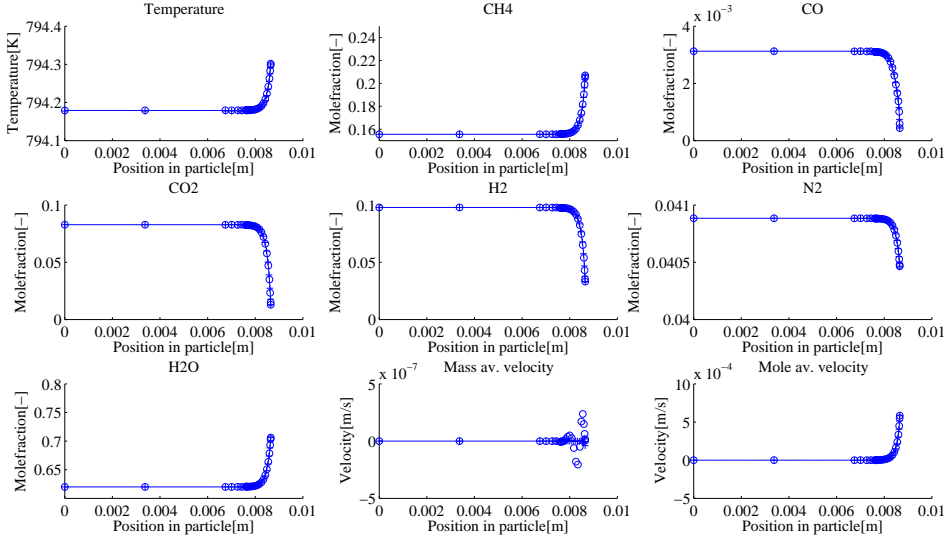
Figure G.7: Steady state comparison of the transient mass based Maxwell-Stefan models. Orthogonal collocation(ooo), least squares (+++) and the original steady state orthogonal non-element results(—).
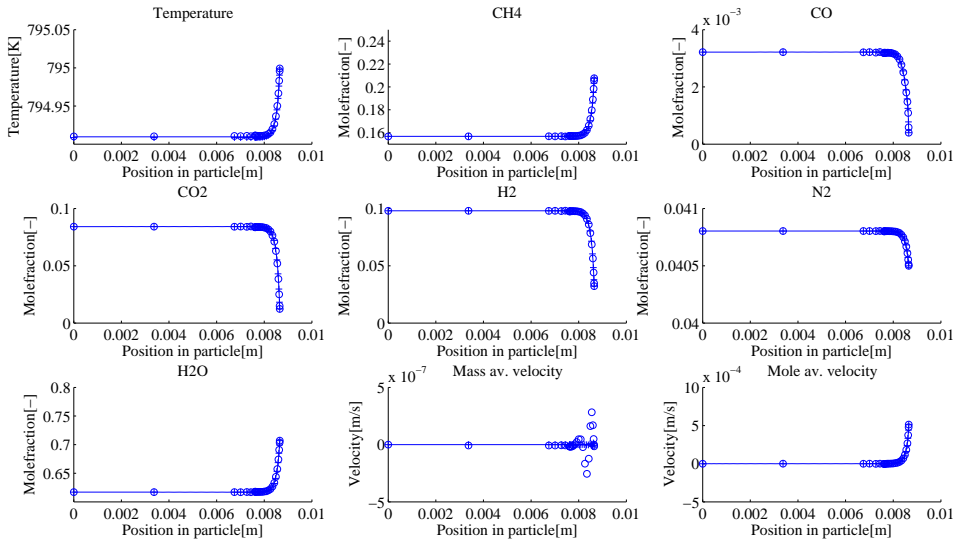

Figure G.8: Steady state comparison of the transient mass based dusty gas models. Orthogonal collocation(ooo), least squares (+++) and the original steady state orthogonal non-element results(—).

H   9 Comparing the numerical methods - Reactor model

The temperature equation will be derived for the reactor model in one dimension. Starting out from the general equation 4, considering cylindrical coordinates and applying a cross sectional average:

$$((1-\epsilon)\rho_p Cp_p + \epsilon\rho\sum_{i=1}^{n}\omega_i Cp_i)\frac{\partial T}{\partial t} + \rho\sum_{i=1}^{n}\omega_i Cp_i v\frac{\partial T}{\partial z} = -\frac{\partial q}{\partial z} + (-\triangle H_R)R + Q$$

(H.1)

Transforming the equation to the dimensionless form using the correlations given in table A.9 and inserting for the external heat $Q = \frac{4U}{d_t}(T_w - T)$ from the walls of the reactor:

$$((1-\epsilon)\rho_p Cp_p + \epsilon\rho\sum_{i=1}^{n}\omega_i Cp_i)\frac{\partial T^*}{\partial t^*}\frac{T_{ref}v_{ref}}{z_{ref}} + \rho\sum_{i=1}^{n}\omega_i Cp_i v^*\frac{\partial T^*}{\partial z^*}\frac{T_{ref}v_{ref}}{z_{ref}} =$$
$$-\frac{\partial q^*}{\partial z^*}\frac{\lambda T_{ref}}{z_{ref}^2} + (-\triangle H_R)R + \frac{4U}{d_t}(T_w - T)$$

(H.2)

Rearranging the equation:

$$\frac{\partial T^*}{\partial t^*} + \frac{\rho\sum_{i=1}^{n}\omega_i Cp_i v^*\frac{\partial T^*}{\partial z^*} + \frac{\partial q^*}{\partial z^*}\frac{\lambda}{v_{ref}z_{ref}}}{((1-\epsilon)\rho_p Cp_p + \epsilon\rho\sum_{i=1}^{n}\omega_i Cp_i)} = \frac{((-\triangle H_R)R + \frac{4U}{d_t}(T_w - T))\frac{z_{ref}}{T_{ref}v_{ref}}}{((1-\epsilon)\rho_p Cp_p + \epsilon\rho\sum_{i=1}^{n}\omega_i Cp_i)}$$

(H.3)

Using the theta method described in chapter 2.5 to discretize the transient term gives:

$$T^{*(t+1)} + \Delta t^*\theta(\frac{\rho\sum_{i=1}^{n}\omega_i^{*(t+1)}Cp_i v^*\frac{\partial T^{*(t+1)}}{\partial z^*} + \frac{\partial q^{*(t+1)}}{\partial z^*}\frac{\lambda^{*(t+1)}}{v_{ref}z_{ref}}}{((1-\epsilon)\rho_p Cp_p + \epsilon\rho^{*(t+1)}\sum_{i=1}^{n}\omega_i^{*(t+1)}Cp_i)}) =$$
$$\Delta t^*\theta(\frac{((-\triangle H_R^{*(t+1)})R + \frac{4U}{d_t}(T_w - T^{*(t+1)}))\frac{z_{ref}}{T_{ref}v_{ref}}}{((1-\epsilon)\rho_p Cp_p + \epsilon\rho^{*(t+1)}\sum_{i=1}^{n}\omega_i^{*(t+1)}Cp_i)})+$$
$$\Delta t^*(1-\theta)(\frac{((-\triangle H_R)R^{*(t)} + \frac{4U}{d_t}(T_w - T^{*(t)}))\frac{z_{ref}}{T_{ref}v_{ref}}}{((1-\epsilon)\rho_p Cp_p + \epsilon\rho^{*(t)}\sum_{i=1}^{n}\omega_i^{*(t)}Cp_i)} -$$
$$\frac{\rho^{*(t)}\sum_{i=1}^{n}\omega_i^{*(t)}Cp_i v^*\frac{\partial T^{*(t)}}{\partial z^*} + \frac{\partial q^{*(t)}}{\partial z^*}\frac{\lambda^{*(t)}}{v_{ref}z_{ref}}}{((1-\epsilon)\rho_p Cp_p + \epsilon\rho\sum_{i=1}^{n}\omega_i^{*(t)}Cp_i)}) + T^{*(t)}$$

(H.4)

H.1 Continuity equation

Starting out from the general continuity equation 30, cylindrical coordinates are assumed and a cross sectional average is applied:

$$\frac{\partial \rho}{\partial t} + \frac{\partial}{\partial z}(\rho v) = 0 \tag{H.5}$$

Using the correlations given in A.9 to transform the equation to a dimensionless form:

$$\frac{\partial \rho^*}{\partial t^*} + \frac{\partial}{\partial z^*}(\rho^* v^*) = 0 \tag{H.6}$$

Expanding the terms:

$$\frac{\partial \rho^*}{\partial t^*} + \frac{\partial \rho^*}{\partial z^*}v^* + \frac{\partial v^*}{\partial z^*}\rho^* = 0 \tag{H.7}$$

Using the theta method described in chapter 2.5 to discretize the transient term:

$$\rho^{*(t+1)} + \Delta t\theta(\frac{\partial \rho^{*(t+1)}}{\partial z^*}v^{*(t+1)} + \frac{\partial v^{*(t+1)}}{\partial z^*}\rho^{*(t+1)}) =$$
$$\Delta t(1-\theta)(-(\frac{\partial \rho^{*(t)}}{\partial z^*}v^{*(t)} + \frac{\partial v^{*(t)}}{\partial z^*}\rho^{*(t)})) + \rho^{*(t)} \tag{H.8}$$

H.2 Species balance equation

Starting out from the general species mass balance equation 8, cylindrical coordinates are assumed, a cross sectional average is applied and the equation is transformed to a dimensionless form using the correlations in table A.9:

$$\frac{\partial}{\partial t^*}(\rho^* \omega_i) + \frac{\partial}{\partial z^*}(\rho^* \omega_i v_z^*) = -\frac{\partial}{\partial z^*}(j_i^*) + R_i\frac{z_{ref}^2}{D_{ref}\rho_{ref}} \tag{H.9}$$

Expanding the equation to identify continuity equation:

$$\frac{\partial \rho^*}{\partial t^*}\omega_i + \frac{\partial \omega_i}{\partial t^*}\rho + \frac{\partial \omega_i}{\partial z^*}\rho^* v_\xi^* + \omega_i\frac{\partial}{\partial z^*}(\rho^* v_\xi^*) = -\frac{\partial}{\partial z^*}(j_i^*) + R_i\frac{z_{ref}^2}{D_{ref}\rho_{ref}} \tag{H.10}$$

The first and fourth term is identified as the RHS of the continuity equation H.6 multiplied with ω_i, swapping for the LHS:

$$\frac{\partial \omega_i}{\partial t^*}\rho^* + \frac{\partial \omega_i}{\partial z^*}\rho^* v_\xi^* = -\frac{\partial j_i^*}{\partial z^*} + R_i\frac{z_{ref}^2}{D_{ref}\rho_{ref}} \tag{H.11}$$

Rearranging to the implemented form:

$$\frac{\partial \omega_i}{\partial t^*} + \frac{\partial \omega_i}{\partial z^*}v_\xi^* + \frac{1}{\rho^*}\frac{\partial j_i^*}{\partial z^*} = R_i\frac{z_{ref}^2}{D_{ref}\rho_{ref}\rho^*} \tag{H.12}$$

Using the theta method described in chapter 2.5 to discretize the transient term:

$$\omega_i^{(t+1)} + \Delta t\theta(\frac{\partial \omega_i^{(t+1)}}{\partial \xi^*}v_z^* + \frac{1}{\rho^{*(t+1)}}\frac{\partial j_i^{*(t+1)}}{\partial z^*}) = \Delta t\theta R_i^{(t+1)}\frac{z_{ref}^2}{D_{ref}\rho_{ref}\rho^{*(t+1)}}$$
$$\Delta t(1-\theta)(R_i^{(t)}\frac{z_{ref}^2}{D_{ref}\rho_{ref}\rho^{*(t)}} - (\frac{\partial \omega_i^{(t)}}{\partial \xi^*}v_z^* + \frac{1}{\rho^{*(t)}}\frac{\partial j_i^{*(t)}}{\partial z^*})) + \omega_i^t \tag{H.13}$$

H.3   Additional equations

The mass fractions are calculated from the dispersion equation:

$$j^* = -\frac{D_{disp}}{v_{ref}z_{ref}}\rho^*\frac{\partial \omega_i}{\partial z^*} \tag{H.14}$$

The pressure is calculated from the Ergun's equation:

$$\frac{\partial p^*}{\partial z^*} = -\frac{f\rho^* v_z^{*2}}{d_p}\frac{\rho_{ref}v_{ref}^{*2}z_{ref}}{p_{ref}} \tag{H.15}$$

where:

$$f = \frac{1-\epsilon}{\epsilon^3}(a + b\frac{1-\epsilon}{Re_p}) \tag{H.16}$$

$$a = 1.75 \tag{H.17}$$

$$b = 4.2Re_p^{\frac{5}{6}} \tag{H.18}$$

$$Re_p = \frac{\rho_g v_z d_p}{\mu} \tag{H.19}$$

H.4   Solution strategy

The solution strategy used to obtain the results are presented here. The main summary of the solution strategy can be seen in table H.1, where the used equations are combined with a fitting boundary condition. The solution strategy is also visualized in figure H.1. The same setup was used for both of the numerical methods.

H.4.1   Temperature equation

As for the pellet models the temperature equation is used to calculate the heat flux and the change of temperature with time. The heat flux is then used in combination with Fourier's law to obtain the temperature. The temperature is specified at the inlet as a boundary condition for the Fourier's law, while we set that there are no change in the heat flux for the temperature equation at the outlet of the reactor.

H.4.2   Species mass balance and dispersion

The species mass balance is solved to obtain the mass based fluxes and the change of mass fractions with time. The mass fractions is obtained from the dispersion equation with the mass based fluxes. As for the temperature equation we set the boundary condition for the species balance to have no change in flux at the outlet, while we specify the mass fractions at the inlet for the dispersion equation.

H.4.3   Continuity and Ergun's equation

The continuity equation is used to obtain the mass averaged velocity and specify the velocity at the inlet. The velocity can then be used to calculate the pressure change throughout the reactor with the Ergun's equation. The pressure is specified at the outlet for the Ergun's equation.

H.4.4   Density equation

As this is a transient model it is convenient to include the algebraic version of the modified ideal gas law in the problem matrix as this stabilizes the system. Since it is a algebraic equation no boundary condition is needed.

Table H.1: Summary of the solution strategy

Equations, LHS represents terms in the problem matrix and the RHS represents the terms in the source vector:	Boundary conditions:
Fourier's law $$q^* + \frac{\partial T^*}{\partial \xi^*} = 0 \qquad \text{(H.20)}$$	Boundary condition at $z = 0$ $$T = T^b \qquad \text{(H.21)}$$
Temperature equation: $$\text{Equation H.4 is used} \qquad \text{(H.22)}$$	Boundary condition at $z = z_{end}$ $$q = 0 \qquad \text{(H.23)}$$
Species mole balance, used for N-1 components: $$\text{Equation H.13 is used} \qquad \text{(H.24)}$$	Boundary condition at $z = z_{end}$ $$j_i = 0 \qquad \text{(H.25)}$$
Last flux(H2O) in the species balance is solved by: $$\sum_{i=1}^{n} j_i = 0 \qquad \text{(H.26)}$$	No boundary condition $-$
Dispersion equation: $$j^* \frac{v_{ref} z_{ref}}{D_{disp}\rho^*} + \frac{\partial \omega_i}{\partial z^*} = 0 \qquad \text{(H.27)}$$	Boundary condition at $z = 0$ $$\omega_i = \omega_i^b \qquad \text{(H.28)}$$
Last molefraction(H2O) in the species balance is solved by: $$\sum_{i=1}^{n} \omega_i = 1 \qquad \text{(H.29)}$$	No boundary condition $-$
Continuity equation mass based: $$\text{Equation H.8 is used} \qquad \text{(H.30)}$$	Boundary condition at $z = 0$ $$v = v_{in} \qquad \text{(H.31)}$$
Modified ideal gas law , algebraic: $$\rho^* - \frac{p\overline{M}}{RT\rho_{ref}} = 0 \qquad \text{(H.32)}$$	No boundary condition $-$
Ergun's equation $$\frac{\partial p^*}{\partial z^*} + \frac{f\rho^* v_z^{*2}}{d_p} \frac{\rho_{ref} v_{ref}^{*2} z_{ref}}{p_{ref}} = 0 \qquad \text{(H.33)}$$	Boundary condition at $z = z_{end}$ $$p = p^b \qquad \text{(H.34)}$$

Figure H.1: Collocation matrix, mass based. Explanation on the labeled terms can be seen in table H.2

Table H.2: Terms in the collocation matrix

Label in matrix	Collocation matrix terms:	multiplied with:
X_1	$$\dfrac{\Delta t\theta\frac{\lambda}{D_{ref}}\frac{\partial}{\partial z^*}}{((1-\epsilon)\rho_p Cp_p + \epsilon\rho^{*(t+1)}\rho_{ref}\sum_{i=1}^{n}\omega_i^{(t+1)}Cp_i)}$$	q^*
T_1	$$1\bullet + \dfrac{\Delta t\theta\rho^{*(t+1)}\rho_{ref}v_r^{*(t+1)}\sum_{i=1}^{n}\omega_i Cp_i\frac{\partial}{\partial z^*}}{((1-\epsilon)\rho_p Cp_p + \epsilon\rho^{*(t+1)}\rho_{ref}\sum_{i=1}^{n}\omega_i^{(t+1)}Cp_i)}$$	T^*
Dp_1	$$\dfrac{v_{ref}z_{ref}}{D_{disp}\rho^*}$$	j_i^*
X_2	$$\Delta t\theta\frac{1}{\rho^{*(t+1)}}\frac{\partial}{\partial z^*}$$	j_i^*
SB_1	$$1\bullet + \Delta t\theta v_\xi^*\frac{\partial}{\partial z^*}$$	ω_i, ρ^*
X_3	$$\Delta t\theta\rho^{*(t+1)}\frac{\partial}{\partial z^*}$$	v_z^*
E_1	$$\frac{f\rho^* v_z^*}{d_p}\frac{\rho_{ref}v_{ref}^{*2}z_{ref}}{p_{ref}}$$	v_z^*

Label in source vector	Source vector
T_2	Source term temperature equation: LHS of equation H.4
SB_2	Source term species balance: LHS of equation H.13
MC_1	Source term continuity equation: LHS of equation H.8

I Pulse iteration

During the thesis a method was developed to reduce the simulation times. The method seems to work very well for heavy under-relaxed models, but the method has not been fully investigated as it was not the purpose of the thesis. The method is a modification to the basic under-relaxation method used:

$$f = \alpha f_{new} + (1 - \alpha) f_{old} \tag{I.1}$$

Here the purpose is to only introduce a fraction of the new solution for each iteration during the Picard iteration, with α being the under relaxation parameter.

Since this is a very basic under-relaxation method it is a high probability of different convergence rates for short and long wavelength components of the residual. The method presented here increases the under-relaxation parameter in pulses in order to speed up the convergence of the long wavelength components in the simulation system, as seen in figure I.1.

The improvements by using this method will be examined for the fully rigorous pellet model using Maxwell-Stefan diffusion. Here a heavy under-relaxation parameter of $2 * 10^{-4}$ is needed for the mass fractions to obtain a solution, by increasing this parameter to 0.02 for every 100th iteration a significant reduction in the amount of iterations and simulation time is obtained. This can be seen in figure I.1 where each time a pulse in the under relaxation parameter is introduced, a drastic reduction the residual happens at the same time. However setting the amplitude of the pulse too high or the interval between the pulses to short will result in the system going unstable. This will require some trial and error, but good results have been seen when setting the pulse interval between 80-100 and the pulse amplitude approximately 100 times the original under relaxation parameter.
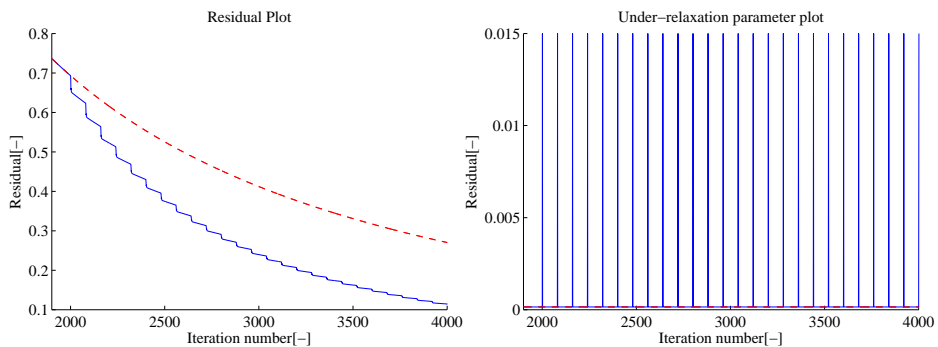

Figure I.1: Comparison the regular iteration(- - -) method versus the pulse iteration method(—).

The use of this method resulted in a reduction in simulation times of approximately 75% for the pellet equations as seen in table 13. This was acquired for a rigorous steady state Maxwell-Stefan model with the use of elements. A suggested code is presented in the following chapter.

I.1 Suggested implementation code for the pulse iteration method

```
itcount=itcount+1
Pulse=Pulse+1;
if Pulse>100 && itcount>2000
alpha=0.02;
Pulse=1;
else
alpha=0.0002;
end
```